

UNCLASSIFIED

AD NUMBER
ADB241076
NEW LIMITATION CHANGE
TO Approved for public release, distribution unlimited
FROM Distribution authorized to U.S. Gov't. agencies only; Proprietary Info.; Oct 98. Other requests shall be referred to US Army Medical Research and Materiel Command, Fort Detrick, MD 21702-5012.
AUTHORITY
USAMRMC ltr, 2 Feb 2001.

THIS PAGE IS UNCLASSIFIED

AD_____

AWARD NUMBER DAMD17-94-J-4113

TITLE: Addition of Olfactory Stimuli Reality for Medical Training Applications

PRINCIPAL INVESTIGATOR: Myron W. Krueger

CONTRACTING ORGANIZATION: Artificial Reality Corporation
Vernon CT 06066

REPORT DATE: November 1998

TYPE OF REPORT: Annual

PREPARED FOR: U.S. Army Medical Research and Materiel Command
Fort Detrick, Maryland 21702-5012

DISTRIBUTION STATEMENT: Distribution authorized to U.S. Government agencies only (proprietary information, Oct 98). Other requests for this document shall be referred to U.S. Army Medical Research and Materiel Command, 504 Scott Street, Fort Detrick, Maryland 21702-5012.

The views, opinions and/or findings contained in this report are those of the author(s) and should not be construed as an official Department of the Army position, policy or decision unless so designated by other documentation.

**Reproduced From
Best Available Copy**

DTIC QUALITY INSPECTED 3

NOTICE

USING GOVERNMENT DRAWINGS, SPECIFICATIONS, OR OTHER DATA INCLUDED IN THIS DOCUMENT FOR ANY PURPOSE OTHER THAN GOVERNMENT PROCUREMENT DOES NOT IN ANY WAY OBLIGATE THE U.S. GOVERNMENT. THE FACT THAT THE GOVERNMENT FORMULATED OR SUPPLIED THE DRAWINGS, SPECIFICATIONS, OR OTHER DATA DOES NOT LICENSE THE HOLDER OR ANY OTHER PERSON OR CORPORATION; OR CONVEY ANY RIGHTS OR PERMISSION TO MANUFACTURE, USE, OR SELL ANY PATENTED INVENTION THAT MAY RELATE TO THEM.

LIMITED RIGHTS LEGEND

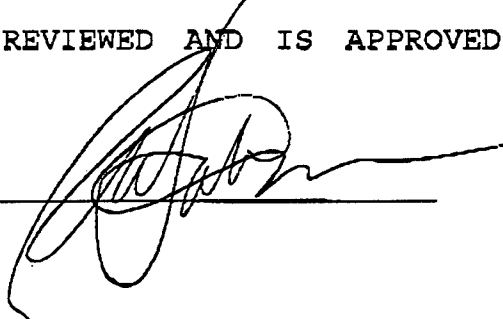
Award Number: DAMD17-94-J-4113

Organization: Artificial Reality Corporation

Location of Limited Rights Data (Pages):

Those portions of the technical data contained in this report marked as limited rights data shall not, without the written permission of the above contractor, be (a) released or disclosed outside the government, (b) used by the Government for manufacture or, in the case of computer software documentation, for preparing the same or similar computer software, or (c) used by a party other than the Government, except that the Government may release or disclose technical data to persons outside the Government, or permit the use of technical data by such persons, if (i) such release, disclosure, or use is necessary for emergency repair or overhaul or (ii) is a release or disclosure of technical data (other than detailed manufacturing or process data) to, or use of such data by, a foreign government that is in the interest of the Government and is required for evaluational or informational purposes, provided in either case that such release, disclosure or use is made subject to a prohibition that the person to whom the data is released or disclosed may not further use, release or disclose such data, and the contractor or subcontractor or subcontractor asserting the restriction is notified of such release, disclosure or use. This legend, together with the indications of the portions of this data which are subject to such limitations, shall be included on any reproduction hereof which includes any part of the portions subject to such limitations.

THIS TECHNICAL REPORT HAS BEEN REVIEWED AND IS APPROVED FOR PUBLICATION.

A handwritten signature in black ink, appearing to be 'A. J. ...', is written over a horizontal line. Below this line is another horizontal line, creating a space for a second signature or stamp.

REPORT DOCUMENTATION PAGE

Form Approved
OMB No. 0704-0188

Public reporting burden for this collection of information is estimated to average 1 hour per response, including the time for reviewing instructions, searching existing data sources, gathering and maintaining the data needed, and completing and reviewing the collection of information. Send comments regarding this burden estimate or any other aspect of this collection of information, including suggestions for reducing this burden, to Washington Headquarters Services, Directorate for Information Operations and Reports, 1215 Jefferson Davis Highway, Suite 1204, Arlington, VA 22202-4302, and to the Office of Management and Budget, Paperwork Reduction Project (0704-0188), Washington, DC 20503.

1. AGENCY USE ONLY (Leave blank)		2. REPORT DATE November 1998		3. REPORT TYPE AND DATES COVERED Annual (30 Sep 97 - 29 Sep 98)	
4. TITLE AND SUBTITLE Addition of Olfactory Stimuli to Virtual Reality for Medical Training Applications				5. FUNDING NUMBERS DAMD17-94-J-4113	
6. AUTHOR(S) Myron W. Krueger					
7. PERFORMING ORGANIZATION NAME(S) AND ADDRESS(ES) Artificial Reality Corporation Vernon, CT 06066				8. PERFORMING ORGANIZATION REPORT NUMBER	
9. SPONSORING / MONITORING AGENCY NAME(S) AND ADDRESS(ES) U.S. Army Medical Research and Materiel Command Fort Detrick, Maryland 21702-5012				10. SPONSORING / MONITORING AGENCY REPORT NUMBER	
11. SUPPLEMENTARY NOTES					
12a. DISTRIBUTION / AVAILABILITY STATEMENT Distribution authorized to U.S. Government agencies only (proprietary information, Oct 98). Other requests for this document shall be referred to U.S. Army Medical Research and Materiel Command, 504 Scott Street, Fort Detrick, Maryland 21702-5012.				12b. DISTRIBUTION CODE	
13. ABSTRACT (Maximum 200 words)					
14. SUBJECT TERMS Olfactory Stimuli, Virtual Reality, Training Applications				15. NUMBER OF PAGES 152	
				16. PRICE CODE	
17. SECURITY CLASSIFICATION OF REPORT Unclassified	18. SECURITY CLASSIFICATION OF THIS PAGE Unclassified	19. SECURITY CLASSIFICATION OF ABSTRACT Unclassified	20. LIMITATION OF ABSTRACT Limited		

19990125 040

FOREWORD

Opinions, interpretations, conclusions and recommendations are those of the author and are not necessarily endorsed by the U.S. Army.

_____ Where copyrighted material is quoted, permission has been obtained to use such material.

_____ Where material from documents designated for limited distribution is quoted, permission has been obtained to use the material.

_____ Citations of commercial organizations and trade names in this report do not constitute an official Department of Army endorsement or approval of the products or services of these organizations.

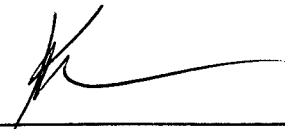
_____ In conducting research using animals, the investigator(s) adhered to the "Guide for the Care and Use of Laboratory Animals," prepared by the Committee on Care and use of Laboratory Animals of the Institute of Laboratory Resources, national Research Council (NIH Publication No. 86-23, Revised 1985).

_____ For the protection of human subjects, the investigator(s) adhered to policies of applicable Federal Law 45 CFR 46.

_____ In conducting research utilizing recombinant DNA technology, the investigator(s) adhered to current guidelines promulgated by the National Institutes of Health.

_____ In the conduct of research utilizing recombinant DNA, the investigator(s) adhered to the NIH Guidelines for Research Involving Recombinant DNA Molecules.

_____ In the conduct of research involving hazardous organisms, the investigator(s) adhered to the CDC-NIH Guide for Biosafety in Microbiological and Biomedical Laboratories.



PI - Signature

Date

Olfactory Stimuli for Medical Training in Virtual Reality
Second Annual Report
Myron W Krueger
Artificial Reality Corporation

CONTENTS

Executive Summary

Report Body

Appendix A. Dr. Thomas Avedisian, "Vibration-Induced Atomization of a Droplet"

Appendix B. Dr. Terry Acree, "Possibilities to Consider in Promoting the Concept of Aroma Enhanced Virtual Reality"

Appendix C. Dr. Amos Turk, "Simulated Odors: Methods and Possibilities"

Appendix D. Dr. Jannick Rolland, "Design of an Optical Orientation Sensor"

Appendix E. Dr. Jannick Rolland, "Design of an Anamorphic Fisheye Lens"

Appendix F. New England Automated Machine Design, "Drawings for Advanced Delivery System"

Second Annual Report
Olfactory Stimuli for Medical Training in Virtual Reality
Myron W Krueger
Artificial Reality Corporation

Executive Summary

The second year of the program focussed on the following activities:

1. system integration
2. odor delivery technology
3. odorant acquisition
4. tracking technology
5. odor studies

System Integration

Odor display capability was integrated into an immersive virtual reality system with a head-mounted display. This system featured wireless display of the virtual environment as well as wireless control of the odor presentation. Demonstration experiences permitting the user to move his head around to sniff the virtual objects were developed. A more elaborate scenario for an urban accident scenario has also been modelled.

Odor Delivery Systems

Two preliminary designs of advanced delivery systems have been developed. One of these was specified early in the year and could have been constructed immediately. However, given what we have learned, we were prudent to study the behavior of the actual odorants in more detail before committing to a design. A second family of advanced designs is now being prototyped and a very advanced approach not contemplated in the original proposal has been considered.

Odorant Acquisition

The odors required for medical simulations have been surveyed and proved to be much more poorly understood than expected, and certainly not available commercially as our original odor experts at Monell Chemical Senses Center in Philadelphia had believed. We have sought assistance from the companies in the fragrance industry, a free lance perfumer, a chemistry consultant, and environmental air quality monitoring firms.

We were surprised at how disappointing some of the industry's best efforts were. As noted earlier, the experience of the industry and perfumers is in developing aesthetically pleasing odors while many of the

odors needed by this project are either unpleasant or neutral. Of the few examples of such odors that we were able to find, only those that have been developed over many years are really convincing.

From the air quality firms, we have acquired formulations that have been used for testing some of the emergency scenario odors that we will need in battlefield casualty scenarios, e.g. formulations for gasoline and diesel fuel and exhaust. Burning fuels, explosives, and electrical fires are still needed. We are procuring basic odorant materials try mixing these for ourselves.

Wireless Tracking

Wireless operation is required to allow the participant to experience odors as part of the normal exploration of a virtual environment. While the tracking is still tethered, progress has been made on the development of a wireless technology. Seven alternative approaches have been analyzed. One was implemented in the first year, and two others are under development. Both are fast and accurate. One hinges on some difficult optics which are being designed by Dr. Jannick Rolland of CREOL (The Center for Research and Education in Optics Laboratory at the University of Central Florida). The initial optical designs were far too expensive to fabricate but several novel compromises have been considered and one has been fabricated.

Odor Psychophysical Studies

We focussed on technology during the second year and postponed the studies that will examine the value of odors in simulations and other human interface applications. To this end, we have had ongoing discussions with Joel Warm and William Dembers at the University of Cincinnati who have performed odor studies relating to military applications in the past. The PI's immediate interest is in assessing the value of odors as alarms. A related question of the use of odors to provide cues as to the state of useful but not critical information during surgery.

Third Year

In the final year, we will complete the wireless tracking system with an advanced portable odor display system. We will continue to do our best to acquire and develop the chemicals needed to support interesting training scenarios, although this is a difficult process. We will simulate one environment that chosen because the odors needed are easy to obtain. We will also do a battlefield mass casualty scenario and one for elective surgery.

Report

I. Project Summary

The activity in second year of the project emphasized the technology development and postponed some of the behavioral issues while we sought to increase our repertoire of odorant materials to the point where we could support meaningful training scenarios.

The main areas of activity were as follows:

1. System integration
2. Delivery system development
3. Odorant acquisition
4. Wireless tracking technology
5. Odor studies

II. System Integration

The most significant step has been the integration of the various components of the virtual reality system to create a system in which odor display is incorporated with head movement.

The participant can stand in a simple virtual environment and experience the odors that are associated with a number of objects that are depicted in that environment. As the person moves about the scene, they smell the odor of each object that they approach. The strength of the odor depends on the distance of their head from the odor stimulus.

We have found that coupling the strength of the odor to the head movement makes the experience of smelling it much more compelling. In situations where an odor simply permeates a scene, we find that odors are not as convincing. We also found that when an unpleasant odor is displayed, if the person cannot reduce the sensation by moving their head away from it, they feel that they are trapped in the head mount and want to take it off. One possible explanation for this is that odors in the real world may not be homogeneously distributed around the environment as odor research usually assumes, but there is some texture to the odor experience making it seem real and an odorized mask seem less so.

Making the odor display respond to head movement requires more abrupt switching from one odor to another and rapid variation of the

concentration of the selected odor as the head is moved. This feat is accomplished by using high speed valves in the current prototype. However, it also depends on the fact that current delivery schemes have a dedicated evaporation chamber for each odorant, so we are not flash evaporating the odorant on demand. Finally, concentration is being controlled by varying the duty cycle of solenoid valves rather than by using proportional valves to vary the concentration of the odorant or the air flow.

II.A. Wireless Operation

Since one goal is to allow participants to walk naturally around the virtual world and encounter odors as a natural consequence of their movement, the odor delivery system was made wireless. While more rapid switching between odors is ultimately required, we initially used an off-the-shelf wireless transmission module for this communication.

Again, since a completely wireless system is the ultimate goal, it was also desirable to transmit the video image by wireless means as well. This function was a little more difficult, because while the first demonstration system we used worked fine with a stationary receiver in a benign laboratory setting, it failed miserably when the participant walked around in a trade show environment with lots of other electronic equipment around.

The issue that we had naively stumbled on was well known to television engineers and even to the consumer of broadcast as opposed to cable-transmitted television. In the early days of television, it was common for ghost images to appear on the screen. These were the result of the signal reflecting off of buildings and other objects in the neighborhood. Since the reflected signal travelled a greater distance than the main signal, it was delayed and appeared as an electronic echo on the screen--the so-called "multipath" problem. By adjusting direction that the antenna was facing, it was often possible to aim it at the original signal and ignore the reflections.

We moved from low cost consumer transmitter/receiver pairs up to the systems used by network cameramen. These systems operate at a 2 Ghz frequency as opposed to the 900 Mhz of the units that we started with, thereby reducing the sensitivity to other equipment. However, while at first glance, it would seem that our task is the same as that faced by a

cameraman—to transmit a video image, there are two major differences. First, wireless cameras are often used outdoors and are known to have problems indoors. Second, the camera which is the transmitter is mobile and the receiver is stationary--usually in a nearby van. Virtual reality presents the reverse situation. The transmitter is stationary and the receiver--worn by the participant--is not only mobile, but it is also rotating with respect to the transmitter. Thus, we had severe multipath problems even with the high frequency system.

The solution is called a diversity receiver. Instead of a single receiver listening to the signal, this technique uses multiple antennas and continually chooses the one receiving the strongest signal. As the participant turns, the signal strength entering each antenna varies. The first such system we used was much better than the single antenna systems, but still had pronounced glitches as the person turned around. However, by moving to a much more powerful system, we were able to reduce the glitches to an acceptable faint one once each complete revolution. Why we should benefit from a transmitter which can send for miles when we are only going a few yards is a puzzle, but one which we became incurious about as soon as the performance was deemed adequate.

One consequence of our current solution is that we are doomed to video resolution for the moment and perhaps for the foreseeable future. We are not aware of any portable commercial product that will transmit VGA or greater resolution with or without diversity receivers. We have explored the possibility of designing such a capability with the manufacturer of the current system, but could not argue that there is an immediate commercial opportunity for such a system. Indeed, it is not obvious what application other than virtual reality would feel the need and unlikely that the virtual reality community—or what is left of it—would embark on the development of such a capability until the video resolution device had proven itself in the marketplace.

II.B. Odor Scenario

To test the odors that we are acquiring and the delivery capability we are developing, we have modelled an urban auto accident scenario into which we can insert our odors as they become available. At a downtown intersection, one car runs a traffic light and collides with another vehicle which is entering the intersection legally and then strikes a pedestrian

who is crossing the street.

The scene chosen was civilian rather than military primarily because we had more of the odors we would need to depict this scene. (The odors on hand vary greatly in their effectiveness.) Also, the graphics modelling required to illustrate a street intersection is easier to because the scene consists mainly of rectangular surfaces which are fairly close to the viewer and can be rendered quickly.

The scene that results from the accident contains a considerable number of opportunities for odors to be displayed. The offending car bursts into flame and the guilty driver staggers out of it and falls on the ground. Since his leg has been penetrated, he is suffering from arterial bleeding. Blood spurts from his wound and pools alongside his body. The large surface area of the blood makes the smell perceptible although near the individual's face, its rather subtle odor is eclipsed by the alcohol on his breath. Nearby trash cans that were knocked over by the accident add to the potpourri of odors.

The pedestrian's abdomen has been penetrated by some part of the car and smells of stool from a punctured bowel as well as from blood. The driver of the second car has suffered from a bloody but superficial head trauma. However, since he is on his way back from jogging in the park, he smells of sweat. Behind his car, fuel from a ruptured gas tank is puddling on the ground. As time passes after the accident, it seems unlikely to ignite.

Shortly after the accident, a squad car and an ambulance arrive and their engines are left running. Anyone moving near the rear of these vehicles will smell their exhausts. The squad car, however, does not smell of donuts—yet.

The participant is cast in the role of a single paramedic working alone (We acknowledge that they usually work in pairs.) faced with a classic triage situation because of the multiple casualties. He approaches the scene from the direction of the second car. A quick conversation with its driver confirms that this individual is not hurt seriously and can be skipped for the moment.

He then approaches the injured pedestrian who is lying on the ground.

Along the way, he is subjected to the smell of pizza wafting from a nearby restaurant. As he bends over this individual, he smells the fecal odor coming from the wound, but a quick check of this person's vitals indicates that his wounds while serious will not kill him in the next few minutes.

As the participant reaches the drunken driver, he notes the odor of the trash spilled around him and the alcohol on the victim's breath. He then attends to the serious bleeding from the leg. Once this bleeding is stopped, this victim has been stabilized and the paramedic returns to the abdominal injury.

During this scenario, it is assumed that the paramedic trainee would be in verbal communication with a remote trainer or with a remote physician who can monitor his actions through a simulated head-mounted video camera. Such teleconsulting could improve the level of care administered at the accident site and could allow ER personnel to have a better idea of what to expect.

II.C. Odor Behavior

In the development of this scenario, it became evident that each odor might behave differently, both because of differing physical properties and because of one's sensitivity to it. For instance, blood, gasoline, diesel fuel, etc will only be smelled if the person is close to the source or if the surface area is large. Sweat, alcohol, and trash smells will also probably only be perceptible near their sources. However, the smell of the fire will be affected by the wind and travel through the scene in gusts. The pizza odor, on the other hand, comes from a very large source and may be perceptible through a large part of the scene, although it could also be affected by the wind.

It is necessary to consider these influences when displaying odors. However, the behavior of the different odors in the real world in different atmospheric conditions has not been observed upon let alone recorded. Until instrumentation as good as the human nose can analyze real world environments to tell us what we have available to smell, we will have to rely on artistry based on personal observation and experience. However, while we do not know exactly how any given odor behaves, we can identify the types of behavior that might be possible and build the ability to simulate these behaviors into our simulations even if we do know exactly how to assign the parameters to any given odor.

In general, we can predict the need to model atmospheric conditions and circulation in virtual reality. We need to know how quickly each odorant—and each of its components—will evaporate under any set of conditions of temperature, barometric pressure, humidity, etc. We need to know how long each substance will remain airborne and in what concentrations people can detect it.

We will then need to model the circulation of the air, the influence of the local terrain and buildings on the wind, heat from the sun and fires, and even precipitation if we are to complete the virtual reality experience. While detailed air circulation models are beyond the scope of this project, the PI's experience of doing 5 years of gas flow visualization under contract with Pratt and Whitney give him a clear idea of what is involved in such simulation. He can even imagine robotic mobile fans and heaters surrounding the participant that would move in concert with him and provide the appropriate sensations moment by moment.

For the moment, we are content to do what the graphics community has done for depicting smoke and flames. They have simulated the appearance but not the detailed physics of these phenomena (which are not completely understood). In the inner city accident scenario, we had a graphic mode for explicitly showing the odor fields. The odors from the humans were shown as static plumes rising from the sources. These fields did not reach far from the sources because such odors are not strong and would dissipate quickly. In addition, there was enough of a breeze depicted to dilute these odors down below detectable levels.

III. Delivery System Development

In the first year, odor delivery systems for three different virtual reality formats were developed: the head-mounted display, a surgical training booth, and a CAVE. As a result of this experience, the CAVE format was abandoned because the CAVE space is very difficult and very expensive to odorize uniformly and to change rapidly. In addition, no means of selectively odorizing the space within the CAVE itself was conceived. This meant that while the environment surrounding the CAVE could have an odor, perversely objects which seemed to be in the CAVE could not have odors localized to them. The decision was made to recommend the same delivery system used with the HMD to be worn in the CAVE.

Currently, it is seen as desirable if the delivery system being developed for the HMD can also be for the surgical training booth. It is expected that the preliminary versions of that device which are not yet miniaturized can be used in that format. Only the volume of air odorized and the amount of odorant used will differ. However, the dilution of the odorized air by the ambient air in the booth reduces its strength by a factor of ten compared to breathing it through a mask.

One change has been made in the architecture of the surgical training booth. Originally, it was thought that we could introduce the odors by blowing them gently in the user's face and that the positive pressure would guarantee that he smelled only the newly introduced air and not any odors that had been introduced earlier. A ceiling exhaust system then evacuated the odors on a continual basis. While this approach works, we were concerned that the forced air in the face might bother some people and that residual air which collected at the bottom of the booth would never be evacuated causing the booth to absorb the odor. The only way to assure its elimination would be to exhaust air at the bottom of the booth as well as the top. While the above system had the benefit of requiring minimal changes to a standard library carrel, we decided to consider a different approach.

The new technique is to release the odors in front of the user's face as before, but not under pressure. Instead, a panel of exhaust holes is mounted behind his head. A suction greater than the capacity of the holes assures a uniform evacuation of odors across its surface. The result is a laminar flow from in front of the user's face to behind his head. Since the exhaust panel is not very thick, it can be mounted in an existing carrel and vented out the ceiling as before.

III.A. Advanced Delivery System Options

In the first year, a variety of odor delivery schemes were considered. In the second year, a number of these were evaluated and a main path chosen. Prototyping along that path has progressed and a twelve odor wireless system has been fabricated and is being tested.

III.A.1. General Delivery Architecture

An odor delivery system can consist of the following elements:

1. an odor storage technique

2. a means of converting the stored odor to a vapor
3. a means of introducing that vapor into a breathable air stream
4. a means of delivering the odorized air to the nose

III.A.2. Odor Storage

Several odor storage techniques have been examined including the following:

1. liquids
2. waxes
3. impregnated polymers
4. microencapsulation

In examining the virtues and disadvantages of each of these storage approaches, we discovered that the storage technique was not so important in and of itself as what it implied about the operation of the rest of the system and the cost of preparation.

For instance, odorants are most often distributed as liquids. The odorants that are incorporated into other storage media are sold in liquid form. Therefore, basing a delivery system on liquids would eliminate a processing step.

In addition, odorants which are encapsulated or impregnated in other materials must be released from those carrier substances before they can be vaporized. When they are released, there are two problems. One is assuring that all of the odorant ingredients are released simultaneously. The second is the residue of the carrier material that remains after the odorant has been released.

In the case of microencapsulation, each microcapsul has to be broken if its odor is to be released. This rupturing can be accomplished by heat or by mechanical pressure. In either case, the microcapsul cannot release its odor instantaneously. It will continue to smell until all of its odor has evaporated. Also, while microcapsuls are quite stable, they do leak, i.e. given a large number of unbroken capsuls, one can smell the odorant they contain. The release of odor before and after it is actually desired implies that microcapsuls would have to be broken and their odor released in a chamber apart from the air flow and valves would select which evaporation chamber would be selected.

The alternative is to live with the leakage or to permit the user to actually inhale the ruptured microcapsuls which are extremely small and made of benign materials. While this practice is probably safe given the short exposures, it seems to be cavalier to ask users to take anything into their bodies that they do not absolutely have to. Another problem with microencapsulation, of course, is the expense (about \$5K per odorant) of the process which has to be tailored to each material. In addition, the leakage implies that these materials cannot be stored indefinitely.

III.B. Odor Delivery Designs

III.B.1. Micro-Hotplates

In the case that each odorant has its own evaporation chamber, it is likely that the different components of each smell will be released differentially. In an approach which Lawrence Livermore Laboratories assured us they could realize, each odorant would be stored as a single droplet deposited on a micro-hotplate. In the case where the storage and evaporation chambers are identical, valves are required to release the vapor from each of these chambers. One problem with these micro-hotplates is that it is not clear how well they will work for the complex mixtures of materials which are typical of real world odors. In this case, the most volatile materials will evaporate first, cooling the heater. Over time, the odor released from the droplet will change character until only the least volatile component remains.

The way to counteract this is to store the odorant in a second chamber and to deposit a much smaller droplet on the hotplate which can be evaporated completely before the next droplet is deposited. One problem with this approach is that it is more complex, because individual valves must be provided for each hotplate as well as a means for depositing the droplets on it. In addition, there is a dilemma in getting the vapor from the hotplate to the main air stream. If the hotplate is in a separate chamber, valves are again required to release the vapor. If the hotplate is in or near the main air stream, there is the danger that that air will cool the hotplate. The hotplates would work if they could perform the valving function as well, releasing the vapor they create into the main air stream. However, it is likely that residue from the evaporation process would foul the hot plates over time.

III.B.2. Piezo-Electric Vaporization

Another approach that we investigated was the use of piezo-electric crystals to accelerate evaporation. Dr Thomas Avedisian of the Mechanical Engineering Department at Cornell performed a study of this approach for us on a consulting basis. His report is included as Appendix A. He was able to use the vibration of a piezo crystal to rupture a droplet so that it would create much smaller droplets. While this approach worked, it could not be very finely tuned. It also required a means of depositing droplets on the crystal and then a means of getting the droplets into the airstream. Once in the airstream, it would be necessary to guarantee that they would be completely evaporated before they reached the nose.

III.B.3. Piezo-Electric Films

Another small study was performed using piezo-electric films instead of crystals by Dr. Martin Fox of the Electrical Engineering Department of the University of Connecticut who has long experience with fabricating ultrasonic transducers for biomedical applications. In this case, higher frequencies could be used and vapors as opposed to droplets were created. As with the crystals, there was a problem with how to deposit droplets onto the film. Initially, the hope was that we could wick material onto the film from a reservoir. Piezo films could then be used to fabricate pumps, fans, and valves out of the same technology. The advantage would be that such a system would potentially be very inexpensive—even disposable. While such an approach could probably have been made to work, it would have required much more support than we were able to get from the manufacturers of these materials. As usual, there would be a significant tooling cost in order to achieve low cost production.

III.B.4. Ultrasonic Nozzle

Another approach we tried was to repurpose an ultrasonic nozzle typically used in spray painting manufactured by Sono-Tek Corporation of Milton, New York. This is similar to the vibrating piezo films except that it is done at a much higher frequency. In this case, cylindrical piezoelectric actuators vibrate a titanium tube at 120 Khz causing a very fine mist of tiny droplets to be released from its end. While this approach might have been ideal for odorizing a room, the quantity of material released was too large to be of interest for either a surgical simulation booth or a wearable odor display. It is quite possible that the approach could have been scaled down, but the product we tested was addressing a specific market and the manufacturer did not have the skills required to miniaturize it. Also,

while the mist produced was exceedingly fine, it still comprised individual droplets which we would be reluctant to feed directly into someone's nose without converting it into a vapor first. Thus, even with miniaturization, this approach would require another stage after it. Also, we were not able to turn it on and off instantly.

III.B.5. Air Stream Vaporization

The last idea is an example of a design approach that has informed our recent development. This approach is based on the following conclusions.

1. it is preferable to store the odors as liquids
2. it is advantageous to somehow convert the liquid odorant into a vapor at the point where it is introduced into the main air stream.
3. It would also be attractive if the liquid could be released into the air stream and vaporized there or released as a vapor rather than as droplets.

III.B.6. Micro-Droplet Formation

Microencapsulated materials have a discrete quality in that it is not possible to crush half a capsule. Similarly, droplet based systems have the droplet itself as their quantum. We have focussed on individual droplet formation, because it is quantifiable. If we know the concentration of the liquid, the size of the droplet, and the volume of air that it is vaporized into, we know the concentration of the odorant in the air that the participant is breathing.

While it might be possible to vary the dilution of the liquid as it is dispensed or to vary the volume of the air that it is mixed with, doing such precision mixing on the fly seems to be an undesirable complexity. Therefore, we are working with a fixed dilution and a fixed droplet size. We can vary the concentration of the odorant in the air by controlling the number of droplets released per unit time.

We have tried a number of methods for creating single droplets. One is to feed odorants through a very small glass, stainless steel, or teflon pipette. The pipette is attached to a piezo-electric crystal. When the crystal is oscillated at its resonant frequency, it shakes loose a steady stream of tiny (100 nl) droplets.

Our hope was that shaking loose one droplet would cause its volume to be replaced in the pipette by capillary action. This did not prove to be the case. A small positive pressure was required to keep the pipette filled. We

also hoped that we could give the crystal a single pulse and shake loose a single droplet. Because the pipette/crystal/odorant system has a fixed resonant frequency, several droplets are typically released.

However, we have found that if we keep the pipette oscillating, no droplets will be released unless we force them out. By providing very precise control of the flow into the pipette, we gain greater control of the number of droplets that are released. Initially, we controlled of the flow by using a linear actuator to advance the plunger of a syringe filled with odorant. Since the actuator was geared way down, very small numbers of droplets could be dispensed.

Two methods of vaporizing the odorant have been examined. The first is to simply let the droplets fall onto a hotplate which will cause them to evaporate. Since it takes a little time for the odorant to evaporate and there is the possibility of a residue building up, we thought about making the hotplate rotate to assure that droplets were always falling on a clean surface.

III.B.7. Micro-Venturi Vaporization

The other technique is to put the droplets into a micro-venturi system. This device is a carefully formed tube whose inside diameter is rapidly constricted and then gradually expanded. The result is that turbulence is maximized and therefore the droplet mixes uniformly with the air stream. Actually, the droplet is dispersed rather than evaporated. The venturi requires a minimum flow rate to operate (5 liters per minute) and a source of pressurized air (5-10 psi). Originally, we have had the participant wear a compressed air bottle strapped to his thigh. Recently, we have started to use a pump to provide the pressure, because it is lighter. Initially, the noise of the pump was communicated through the air flow to the participant's nose and through the eustachian tube to his ears where it was perceived as sound. Since then, quieter pumps have been found which operate from batteries.

The system as described only delivers a single odor. However, we found that we could drill up to 6 ports into the output of the venturi. Each of these operates as described. In addition, the output of several venturis can be fed into the input of yet another venturi for further mixing. We have currently done this for two venturis with six odors each for a total of

twelve odors.[Appendix F]

We thought it might be possible to expand the number of odors by forming an antichamber outside the venturi which is connected to its output by a narrow channel. We hoped the vacuum from the venturi would suck any droplets introduced to the antichamber into the venturi. A little bleed air was introduced to the antichamber to cleanse it. We thought that up to six channels could be fed into each antichamber for a total of 36 odors, but that approach did not work as well as we hoped.

While the shaking loose of droplets is very easy to understand, the fact that the piezo crystals needed room to oscillate and required high voltages to operate added to the complexity of the design, so we experimented with the idea of pumping liquid directly into the outlet of the venturi.

If we could pump liquid directly into the venturi without forming droplets, then we could imagine an array of micropumps or valves that would drive all of the odorant channels. In this case, the odorant channels could be molded or routed out of the same piece of material that the venturi itself is fabricated from. The pump array could then be clamped onto these channels in one operation. In turn, an array of reservoirs could be clamped onto the input to the pump array. We were initially very enthused by a 10 mm x 10 mm x 2 mm self-priming micropump from IMM, a German corporation based in Mainz. However, its output turned out to be too low for our purposes, it was too slow, and its multiple high voltage power supplies presented an additional design challenge.

Instead, we turned to high speed liquid valves from Lee Corporation. We tried the idea of pumping the liquid directly into the outlet of the venturi and found that we were able to meter small amounts of liquid by controlling the time that the valves were open in 1/2 millisecond increments. When the valves are open, odor is released. When the valves are closed, no odorant appears to be drawn into the airflow by suction. (The absence of unwanted odorant release was previously noted with the micropipettes.) By simply controlling the flow of liquid to the venturi, we are no longer forming droplets. Exactly in what form the liquid odorant enters venturi, we cannot know. It may bulge out from the outlet of the channel into the venturi and be torn into droplets by the turbulence or it

may rapidly evaporate in the suction of the venturi.

III.C. Wireless Operation

A twelve odor odor delivery system based on the liquid valves has been developed which can operate at submillisecond rates when tethered. Making it wireless was more of a problem than it had been for the slower demonstration in the previous year.

While the system worked fine on the bench, each step in incorporating wireless control with portable operation ran into difficulties. Enclosing the unit in the carrying case and letting the receiver rotate as the participant walked around made the antenna selection much more critical. In addition, there were many more transmission errors than before.

To combat these problems, a complex error checking and correction scheme was implemented with an onboard microprocessor and the results of each transmission were sent back to the host computer. Unfortunately, this procedure was itself error prone. Experimentation showed that the transmitter and receiver could not be operated simultaneously if they were in close proximity as they are in the portable system. It was therefore necessary to shut off one of these functions when the other was operating. It was further discovered that these devices had to be on for a considerable time before they could transmit or receive reliably. Thus, the wireless function only worked when the data rates were slowed down enough that we were no longer meeting our performance goals.

The solution was to abandon the elaborate error checking, correction, and reporting capability during interactive sessions. Instead, data is simply received by the portable unit and acted upon. If the perceived behavior is not what is expected, the error checking is turned on for health testing and maintenance.

The valves used in this delivery system worked fine during initial testing. However, over time we noticed that some of the valves became clogged. Lee, the manufacturer of the valves, took them apart and found that the coatings had swelled from extended exposure to the odorant liquids. To combat this problem, we chose a more expensive valve with a more inert coating and modified the delivery system so that we could flush the valves with water for an extended period after each use.

Lamentably, the problem has resurfaced. After months of use, even with flushing, the valve coating reacted to the odorant materials. As a consequence, we have ordered the most expensive valves with a Viton™ coating in the hopes that this material will withstand the odorants. Lee is providing us with samples of their coating materials for us to expose to a variety of our odorants. They will then analyze these samples to see how they have reacted to the odorants. It should be pointed out that even the most seemingly benign odorant materials, e.g. vanilla and peppermint, ultimately damaged the valves. If a single coating cannot be used, it would mean that odorants would have to be matched to specific valve coating, making the system much less flexible.

III.D. Microminiature Design Approaches

III.D.1. Ink Jet Print Heads

The current delivery technique releases tiny droplets into an airstream where they are vaporized in a micro-venturi system. If it were possible to vaporize the liquid odorant before it was released into the airstream, the delivery system could consist of just a vapor release system mounted in front of the nose. The air pump, the valves, the micro-venturi apparatus, and the tubing from the back to the nose could all be dispensed with.

Bubble jet printers almost do what is desired in that they heat ink to its boiling point creating a rapidly expanding bubble that forces a tiny droplet of ink out of the nozzle. When the heater is turned off, the bubble collapses and the firing chamber refills with ink. It would seem that this technique could be modified to release the vaporized liquid instead of the droplets. We have seen this possibility since the beginning of the program and have engaged a number of consultants to look at this problem for us. In each case, initial enthusiasm gives way to the frustrations of reverse engineering the printer, because of the lack of documentation about how they operate and the refusal of the manufacturers to provide any technical information.

The investigations of our consultants and discussions with a firm that makes its own printhead gave us enough information to see what the problems would be if we successfully converted an ink jet printer to deliver odorant liquids.

III.D.2. Ink Jet Printers

The simplest ink jet printers channel a single liquid ink to up to 64 nozzles (1000 in one product). Color printers have basically have separate heads for each color as well as black. Each nozzle releases a 25 micron droplet every 25 microseconds. This technology is carefully tuned to the physical properties of the ink and the need to create perfectly formed droplets in the output. We have been looking at how we might repurpose this technology to deliver odors.

Ink jet print heads consist of a sandwich of three layers:

1. the electronics layer which contains the heaters for the bubble jet printers or the actuators for the piezo-electric printers.
2. the polymer via layer containing the channels that distributes the ink to each of the nozzles
3. the nozzle layer from which the ink is actually ejected.

To this end, we attempted reverse engineering ink jet printers to see if we could:

1. get it to deliver odorants instead of ink
2. figure out how to modify the via layer to deliver a different odorant to each nozzle.
3. figure out how to connect the via channels for the individual odorants to separate reservoirs for each odorant.

The appeal of the ink jet print head is that it is the only electromechanical dispenser in mass production. At least one hundred million have been sold. However, the essence of mass production is that enormous engineering and tooling costs have been incurred in making the technology do exactly what it does. The companies involved have no interest in ancillary markets that are anything but huge. For instance, Trident International of Brookfield Connecticut a manufacturer of a custom print head for marking packages has \$200M in sales and plans to reach \$5B in just a few years. They have no interest in a non-printing application. Even the companies that fill or refill cartridges with ink could not be persuaded to provide empty cartridges that we could fill with odorants instead.

Ink jet printer technology appears to point to the possibility of a miniature dispensing devices for liquid odorants, but the fact that existing heads can only print one odorant for each color of ink means that a number of heads would be required to support a meaningful repertoire. In addition, these heads are not so small, are not inexpensive, and require

high voltage power supplies.

There are however many separate nozzles in the print head each of which in principle could be used to deliver a separate odor. This is a problem that none of the printer companies have ever addressed. For them, the trick is to get the via layer in the print head to channel the same color ink to each of the nozzles. They have legions of PhD chemists who control the physical properties of the inks to assure that they will work with the print heads. Feeding a different odorant to each nozzle would not only require a complete re-engineering of the via layer, it would also require a careful study of the physical properties of each odorant. Since none of the manufacturers will provide the components that are assembled into the print heads, either an entire print head would have to be fabricated or an existing device would have to be taken apart and a custom fabricated via layer would have to be inserted.

III.D.3. Micro Fluidics

But what of MEMEs technology? Surely, microfluidic devices are an active area of research in this field. True, but it is seldom noted that the most economically significant MEMEs technology is in the ink jet printer and so the problems described above have significance for MEMEs devices in general.

We talked to a number of the major laboratories including Livermore, Sandia, Oak Ridge, and Sarnoff about their miniaturization technologies. When we approached Sarnoff Labs, we were pleased that they were already working with the ink jet printer manufacturers to see how well the Navier Stokes equations described fluid phenomena in their print heads.

We asked Dr. Anne-Marie Alanzillato whether she could fabricate a microfluidic pump array that we could use for odorant delivery. She was very enthusiastic about the project as was Ken Gabriel who had funded her work when he was at DARPA. However, there were limitations and challenges. Only 9 pumps could put in a single device. This was because of minimum size of the physical connectors that could bring odorant material into the chip. Like the ink jet printer, it could release 25 micron droplets every 25 microseconds. While she felt that the corrosive characteristics of odorants would probably not be a problem, the problem of handling a variety of odorants dissolved in variety of diluents with a wide range of

physical properties has never been addressed let alone solved. Therefore, it was recognized that such a device would have a finite risk of failure.

Though both parties were very interested in pursuing this design, there were some concerns. The 9 odor limit was at the lower limit of what we thought would be sufficient for real applications, so the possibility of two or more chips per systems had to be considered. The replication costs of the chips (\$600) would not be unreasonable to support high end research, but it would not guarantee a market for odors in surgical simulators.

It is important to note that the micropumping element is not by itself a complete odor delivery system. It was to include 1 CC reservoirs for the odorants as well as the drive electronics. The major unknown was how fast the 25 micron droplets would vaporize. If the output of the micropump array was a vapor, it could be mounted on the head and output directly into the wearer's nose. This would eliminate the pumps, valves, micro-venturi systems, much tubing, and reduce the size of the batteries that had to be carried considerably. On the other hand, if the droplets did not vaporize, one would be reluctant to allow them to be directly inhaled, fearing that the liquid odorants that eat valve coatings would also harm nose and lung tissues. In this case, it would still be necessary to keep the batteries, pumps, micro-venturis, and mount the system on the back. While the micropump array would be smaller than one created with individual valves, the total assembly would only be fractionally smaller than the one we have designed.

Even with these concerns, the device would be well worth building because it would have represented an important step forward in approaches to odor delivery. The show stopper was the cost of the effort which was to be \$200K which was the entire budget including our salaries and overhead for the third year of the program in which the final delivery system was to be developed. It would also take a year to get it fabricated and during that time we would have nothing to work with, which meant that we still had to develop an alternative system. Thus, we embarked upon the developing the delivery system described earlier. Ironically some time later, Dr Alanzillato convinced her management to provide half of the support for the effort from internal funds. By then, it was too late for us to take advantage of her offer.

III.D.4. Design Dilemma

One caveat that should be kept in mind when considering a miniature device is provided by careful attention to the sounds that an ink jet printer makes when it is being turned on or when a cartridge has been changed. Even though it has been carefully designed for the exact inks that it is printing (which are chemically benign), every ink jet printer goes through minutes of mechanical warmup procedures that involve spitting ink onto a sponge mounted beyond the end of the print line among many other mysteries. If such precautions against clogging are necessary with the simplest materials, what additional problems will arise with a general purpose device that is expected to handle a wide range of odorants.

The dilemma for the design of the delivery system is that it is circular. Normally, one would start with the requirements and engineer a device that meets the requirements. The requirements would derive from past experience in the design domain. These would include the formulations of the odorant materials, the physical properties of the odorant materials, the sensitivity of the human nose to those materials, the compatibility of the odorant materials with those used in the delivery device, and the safe exposure levels of the odorant materials.

In this case, many of the odorant materials that one would like to use are not yet available. Furthermore, even for the odorant materials that we have been able to acquire, the physical properties, human sensitivity to the materials, and their chemical properties are not available—even from the company that sells them. (Even something as basic as possible solvents was not available.)

The only exception is the toxicity information which provided by the manufacturer for each of the individual chemicals although not for mixtures made from them. This data is very conservative and warns that many of the materials are carcinogenic or otherwise harmful. No dosage level is specified. Getting the toxicity information for diluted odorants required engaging a toxicologist charging hundreds of dollars an hour and she found the task frustrating and raised the cost estimates for future work.

The perceptual information on the human ability to detect each chemical

in specific concentrations is also not available. The only way to acquire it is to build special odor delivery instrumentation which has much more precise control of dosage than is needed for virtual reality simulations. In retrospect, such a device should have been contemplated. Such studies are done in odor research, but both the instrumentation and the methodology seemed crude to the PI. It was aimed at single chemicals, not mixtures. It was very slow and therefore unsuitable for simulations. It was based on passive evaporation rather forced vaporization which was deemed better for complex mixtures.. Thus, the design problem is that it is necessary to have delivery system in order know the requirements of such a system.

IV. Odorant Acquisition

When the project began, we were working with Monell Chemical Senses Center of Philadelphia who assured us that the odors needed for most of our simulations would be easy to obtain. It was their responsibility to identify and obtain the required materials. Unfortunately, it turned out that they had badly miscalculated and few of the materials were available off-the-shelf and many had never been characterized. They had some ability to do perfuming but seemed to be very reluctant to actually do it. After a year and a half, we were only able to get them to produce a very few of the odors we needed; however, since it was not a task they were very interested in and we finally felt forced to seek other sources of support for this part of the project.

IV.A. Fragrance Companies

The first step was to approach and do presentations to a number of the large fragrance companies. These firms found the project fascinating but not commercial from their point of view. The typical question was how many tons of material would we need. Each company provided us four or five odors that they thought might be helpful of which only one would typically be convincing. This experience showed us the paucity of materials intended to imitate the odors in the real world. While floral fragrances and fruity smells are highly elaborated, very few unpleasant odors have been created. These are often developed as models for chemists to work against as they try to mask or neutralize the noxious odor with a deodorant. Thus, some of these companies have developed materials that simulate human sweat, baby vomit, and kitty litter. Unfortunately, these models are highly proprietary and jealously guarded corporate secrets. Several individuals contacted had spent much of their careers developing

just one of these odors.

One reaction that these companies had when presented with the list of odorant materials that we were looking for was that anything that was associated with smoke, vehicle exhaust, and explosives would involve materials that might be considered hazardous and that they did not want to incur any liability for creating such materials. Indeed, almost everyone we encountered was completely spooked by any mention of potentially hazardous materials.

IV.B. Perfumer

The next approach we tried was to enlist the services of a free lance professional perfumer, Geraldine O'Keefe. She was interested in the project and thought that she would be able to contribute. However, the term "free lance" turned out to be misleading. While she does not work for any company, she does use the facilities of large companies to ply her trade. If she has an idea or a commission, she must interest a fragrance house in her project in order to get access to their resources. Usually, they are hoping to produce whatever she develops.

The resources required include a chemistry lab with sophisticated analytical equipment, i.e. a gas chromatograph (GC) and a mass spectrometer (MS) connected in series so the output of the GC flows into the MS. However, traditional lab equipment has several problems. First, the human nose is better than any single laboratory instrument, so substances which smell may elude detection. Second, many of the components of a substance may not contribute to the smell at all. Going to the trouble to simulate these materials would obviously be a waste of time and money.

The perfumer's role in the analysis is to gauge the importance of components that are not picked up by the analysis and to identify the odor properties of those that are. A perfumer working with familiar materials will know which ones are odorous and which ones are not. However, for unknown materials, it is valuable to be able smell the constituents that are separated by the gas chromatograph before they are passed on to the mass spectrometer. While this is usually not possible, a few GC/MS systems are equipped with what is called a "Sniffer Port" which allows the operator to smell the ingredients as they pass from one device to the other. An alternative design would be to have a stand-alone GC that is

identical to the one used in a GC/MS. Then, the operator can smell the output of the GC, characterize the odor, and record the time at which it is emitted. When the same material is put through the GC/MS, it will be possible to correlate the previously recorded smells with the analysis provided by the MS. There are very few instrument systems equipped with sniffer ports which are available to outside users. Even some of the fragrance companies eschew the use of a sniffer port because of concerns about their own safety.

Begin CONFIDENTIAL

IV.C. Odor Mixing Technology

One thing that struck the PI when he visited fragrance companies was that perfumers formulate odorants by mixing liquids. While may seem like an unremarkable observation, the practice does mean that they cannot backup. Once they have added an ingredient, they have no convenient way to remove it. Since the materials are expensive, they must be very conservative as they experiment with new compositions.

It occurred to the PI that the delivery technology being developed under this project offers a radically different approach. Our odor delivery devices are typically used to select one odorant at a time from a small inventory of ten or more options. However, there is no reason that the same devices cannot release more than one odor at a time. By mixing vapors rather than liquids, the operator has almost no investment in the current odor and could in principle change ingredients and proportions through a GUI interface. Indeed, whereas the professional perfumer proceeds tentatively and deliberately, a vapor mixing system could modify the mixture on its own under the direction of a genetic algorithm. As in the graphics work that Karl Sims did when he was at Thinking Machines, the system could provide a set of alternatives, ask the operator which one he preferred, generate four variations on the selection, and repeat the process until he was satisfied or felt that he was in a blind alley. Using Simm's system, it was possible for non-artists to create beautiful images.[3] Our thought is that odors could be mixed the same way.

The limitation of the delivery technology developed so far is that we do not currently have the large inventory (thousands) of odorants that a professional perfumer is typically surrounded by. However for any given project, these individuals create a small working set of from 20-50

bottles and then start mixing. There is no reason that a version of our system that would support such a repertoire could not be developed.

Of greater concern would be the need to provide precise control of the proportions of each of the materials. We currently provide proportional control by pulse width modulation, i.e. we vary the duty cycle, the percentage of the time a valve is open versus the time it is closed for evaporative techniques. With the droplet based systems, we vary the number of droplets per unit time. Since the frequencies that we were using to control droplet generation are quite low (300-400 hertz), we thought we might not have sufficient dynamic range for mixing odorant materials.

Finally, there is the question of correlating the number of droplets vaporized with the liquid proportions that a perfumer would need to create the same odor. Our venturi system assures that all ingredients are vaporized completely and instantaneously. The key physical property associated with perfume ingredients, the vapor pressure or tendency of each component to evaporate is being finessed. In our system, every material evaporates whether it wants to or not. If it was part of a mixture of many ingredients, the most volatile components would evaporate first. Nevertheless, it should be possible to work out the correspondence between vapor proportions and liquid proportions.

For virtual reality applications, the issue does not matter since we display vapors. Therefore, the proposed system could be used for mixing odors for virtual reality simulations. Even for perfume companies, the delivery technology suggests a new way of packaging and presenting fine fragrances. A wearable fragrance appliance could present the out-of-the-bottle experience throughout the day rather one that fades the longer the perfume is worn.

End CONFIDENTIAL

IV.D. Odor Chemical Acquisition

Given the poor substitutes for familiar odors that the fragrance companies had shown us, we despaired of getting truly accurate odors for our simulations. At the same time, there is evidence that people's sense of smell can be fooled. For instance, there was a study in which people tasting an apricot flavored red candy believed that it was cherry because of the color. In some environments where people do not have a very clear

idea what to expect but do know that it should smell somehow, it may be enough to present some reasonable odors rather than the correct ones, e.g. general vegetation odors may be enough to give life and texture to outdoor scenes.

IV.D.1. Direct Purchase

With this thought in mind, we acquired a flavors and fragrances catalog from Aldrich Corporation, but were surprised to discover that they would not sell to us. They explained that their chemicals were only sold in "neat" form, meaning that they are pure rather than diluted. In this form, they are almost all extremely toxic. Since we were not a chemistry lab, they did not want the liability attendant to selling us such materials.

IV.D.2. UCONN Food Sciences

Since we did not want to handle toxic materials or to be responsible for disposing of them, their position seemed reasonable and prudent. So, we approached the Food Sciences Laboratory at the University of Connecticut to see if they would purchase the chemicals, dilute them to safe levels with the proper diluents, and then store them until we needed them. While the initial reaction was very enthusiastic, after several months of indecision the university decided that they also were sufficiently concerned about liability issues that they were be afraid to become involved.

IV.D.3. Environmental Inspectors

Throughout the project we have been talking with a small consulting firm in Bloomfield Connecticut called Odor Science and Engineering, Inc. They primarily work with odors as nuisances or as evidence of pollutants. There are a variety of federal, state, and local regulations that control emissions from sewage treatment facilities, chemical plants, meat rendering plants, hog farms, etc. As a consequence, governmental regulators and the operators of some of these facilities may enlist this firm to determine where the odor that has given rise to a particular complaint is coming from. This focus on environmental odors means that this firm and others like it have expertise about a range of unpleasant odors that fragrance companies have never had any reason to think about, such as those emanating from hog farms.

Of particular interest to us is the fact that they routinely take samples of

noxious air that has given rise to complaints and have it analyzed. Since like perfumers they are as interested in the smell as in the chemistry, they do need a sniffer port to let them know which ingredients of a GC/MS analysis are causing the smell. The closest one that they know of is in California which means that they must fly out to the West Coast each time they want to analyze a sample. By manning the sniffer port themselves, they absolve the testing firm of liability and they assure consistency of their description of odor properties. (One thing that has amazed us is how almost every individual in the industry seems to use entirely different adjectives to describe the odors we have shown them. They all draw on the same set of descriptors, but use them completely differently. This means that they have limited ability to communicate with each other. It would be useful to try to quantify these attributes.)

Getting air samples analyzed requires the cost of the analysis plus the cost of flying the head of Odor Science and Engineering out to California plus compensating him for the service (at \$175 per hour). Since he can only analyze three odors per day, this is obviously an expensive proposition.

There is another difficulty. Air samples must be captured in metallized bags with special valves. There is concern about some of the components of the odors adhering to the insides of the bags. Even more difficult is the fact that the samples must be analyzed within 24 hours after they are collected. Since some of our odors must be collected in different locations under different conditions, this time pressure makes what would seem to be a routine laboratory analysis seem more like a special forces operation.

Given an analysis with a list of chemical components and a subjective judgment of each's contribution to the overall odor experience, there are several additional hurdles:

1. an identified material may be toxic and a similar smelling substitute must be found.
2. an identified material may not be available commercially even though the means of producing it are known
3. an identified substance may not have been studied scientifically in the past in which case a synthetic chemistry lab will need to be enlisted to crystallize it, determine its molecular structure by x-ray crystallography, and synthesize an analog. This process can be very expensive. Monell has had grants of hundreds of thousands of dollars to

analyze a single natural odor.

IV.D.4. Toxicologist

Odor Science and Engineering has been helpful to us in a number of ways having to do with the ingredients of noxious materials. Initially, they were willing to purchase chemicals for us, but upon reflection decided that they were no more equipped than we to do the handle the chemicals. So, they referred us to another firm, TRC Environmental, Inc from which they had once spun off.

TRC is engaged in similar activities to Odor Science and Engineering. In addition, they have a complete chemistry and toxicology lab. Dr Karen Vetrano is a toxicologist and has been enlisted to acquire odorant materials for us. Her tasks are to:

1. determine the toxicology of the substances we are interested in
2. determine the physical properties of each substance such as vapor pressure, surface tension, viscosity, etc to the extent that these are available through the literature.
3. determine what solvents can be used to dissolve the materials
4. determine what concentrations are safe for us to handle and the strongest of these that would be useful for odor display. We will dilute down from these levels ourselves.
5. actually order the materials and prepare dilutions of them for us
6. research the availability of analyses and synthetic formulations for a number of odors that would be used to represent military emergency situations such as gasoline, diesel fuel, exhaust, explosives, burning electrical insulation, etc. While some of these formulations have been identified, none of them are available as mixtures available for purchase. There is also some question as to whether they smell like the real odor they are intended to simulate.

The above process has been pursued for a suite of 30 odors from a list of 180 that we had identified as being of interest to us. (Since the Aldrich catalog only has a few descriptors for each odorant, we can only smell them after we have had them prepared for us.) Only a couple of these odorants will be immediately identifiable. Others have qualities that suggest smoke or vegetation, but are only components from which representational odors would be created. This was an expensive process and one whose cost was revised upwards by TRC for future orders.

IV.D.5. Cornell Food Flavor Laboratory

Another odor search connection has been an effort with the Food Flavor Laboratory at Cornell University operated by Dr. Terry Acree. This laboratory does do analysis and synthesis of organic flavor and odor material for the food industry. They have the analytical instruments to identify the components in an unknown odor. They also have experience of making simulated materials. While their GC/MS machine does not have a sniffer port, they do have a stand-alone GC identical to the one in their GC/MS and they time the output of each odor from the GC before putting the same sample in the GC/MS. They are very concerned about any hint of hazardous materials and are unwilling to ask their students to sniff them. However, for substances which are known to be safe because they are naturally occurring organics such as the smell of blood, this group might be of doing the analysis/synthesis required.

Their funding is almost entirely related to food. In this area, their expertise in fruity tastes and smells. Vegetables have not been investigated very much. Meats and therefore tissues have not been investigated at all. The odors associated with accident and battlefield scenarios will never be addressed. (The continuum from floral essences in the fragrance industry to fruits, vegetables, meats, and combustion odors corresponds to a recognized spectrum of difficulty in odor development. The pleasant odors which are easy to replicate are made up of components with low molecular weight. Therefore, many of the odors needed for medical simulation are inherently more difficult to simulate as well as less lucrative.)

Their lab costs are very high. Having Dick Duffee of Odor Science and Engineering fly out to California to use the equipment there was no more expensive. After many efforts to interest them in what we were doing, we rented their team for a day to brain storm what they could do to simulate a real world situation based on their existing expertise. The result which is included as Appendix B uses individual chemicals to simulate each odor in their scenario. The chemicals identified contained no examples that the PI had not already identified from the Aldrich catalog without being able to smell them.

IV.D.6. Turk Test

After many calls to organizations that would seem to have an interest in

unpleasant odors, e.g. the Environmental Protection Agency, the American Petroleum Institute, and a number of environmental monitoring firms in the private sector, we located the formulation for the Turk Test which was used for testing the effects of diesel exhaust odors on human subjects in the late 1960s.[1] Later, as we were trying to get the chemicals used in the formulation, we found someone who knew how to get in contact with Amos Turk who is now 80 years old.

The PI called him and has had a number of conversations about odor display. He was quick to point out that his simulated diesel odor did not smell like diesel fuel. He explained that what we think of as the smell of diesel exhaust is not exactly a smell at all. It contains droplets of unburned fuel, particulate matter from the combustion process, and fugitive combustion products which are in the process of turning into something else. It also contains benzene which is a known carcinogen. Therefore what he had done was to simulate the qualities of the diesel odor with completely different materials which were known to be safer but which did not necessarily smell similar. These qualities included burnt, oily, pungent, and aldehydic.[2] This information leads to the paradox that the only simulation of a fuel odor does not like it. Since it would cost thousands of dollars to get the Turk Test formulation made up for us, we are reluctant to pursue it if it does not smell like the real thing.

At the same time, the Turk Test points to an alternative approach to odor simulation, the representation of qualities rather than the odors themselves. (Dr. Turk's report on the techniques available for simulating is included as Appendix C.) It also points to the need for broadening the requirements on odor delivery beyond the smells themselves to include droplets and particles. It is possible that water droplets and dust particles of some benign substance could represent those aspects of real odors that are usually caused by more noxious materials. One example of where this would be useful is in urban warfare training simulations where soldiers are trained to clear buildings of enemy personnel by using their weapons to cut doorways through walls. Clearly, this practice would lead to large quantities of dust in the air which would should be represented in the training.

While we will continue to pursue additional sources of odorant materials,

we are confident that our experience so far represents the reality of odor simulation and that we do not have the resources or the willing partners to cause the desired odors to be created. Instead, we will have to work around the odors that we cannot acquire and do the best we can with what we have.

V. Motion Tracking for Odor Delivery During Natural Locomotion

Many of the people working in virtual reality have by now been convinced by the PI's arguments of the past decade claiming that current HMD technology is inadequate for almost any purpose. His repeated question in over one hundred talks and in his book was, "Would you use it, if it was free?" Since even the most committed HMD aficionados had to ruefully admit that they would not and in their own labs did not use HMDs for any length of time.

However, the PI was always quick to point out that the ideal HMD would have some powerful advantages over any other kind of display. Most important of these would be the ability to move around a virtual world by walking naturally rather than by some clumsy control convention such as pointing your finger in the direction you want your eyes to fly. In this project, we have already seen that coupling odor display to natural head movements is very compelling. We have always believed that odors encountered while walking about the virtual world would seem even more so. Natural movement is impossible with the very few systems that permit movement, because the participant's head is connected to the computer by the wires that connect the tracking system to the sensors he is wearing. Therefore, a wireless tracking system is needed for testing odor display in immersive virtual reality.

V.A. Preliminary Tracking System

In the first year of the project, a preliminary wireless tracking system was developed that had performance similar to that of the early magnetic trackers. This system used overhead video cameras looking down at a multi-LED target worn on the top of the participant's head. It analyzed the pattern and determined the location and orientation of the head from that information. Because it was using standard video cameras, it was limited to 30 samples per second. Its spatial accuracy was also limited for the same reason. The tracking worked as did the hand off from one camera to the next down the 40' path. Only the failure of the wireless video

transmission prevented this from being an interesting system. Since then, the video transmission problem has been solved.

V.B. Tracking Design Alternatives

Based on the lessons of that system, a number of much more sophisticated ways of head tracking have been considered. These include:

1. head-worn laser diodes that would project spots on the floor walls and ceiling. The locations of these spots would be analyzed to find the tracking information.

2. laser measurement devices which have been getting very accurate.

3. scanning the environment with a sheet of laser light. The scan angle at the moment the laser was detected by a sensor on the participant's body would determine its location in one dimension. Alternate scanning in X and Y would provide two-dimensional information. A second scanning system would provide the data for stereo three-dimensional calculations.

4. high-speed, high-resolution video cameras to increase the spatial and temporal resolution of the overhead video tracking system.

5. special cameras which can increase their scan rate by aborting a scan when the target is found or can skip over lines in which the target is unlikely to be found.

6. a special camera which had onboard processing that would allow it to in one operation test an entire line to see if it was empty.

7. inertial and ultrasonic techniques which have since been developed as a product by InterSense. (Systron Donner was prepared to make an inertial system for the PI in 1994, but delays in the DARPA funding and the size of the resulting assembly caused that approach to be set aside.) The performance of the InterSense system is good as long as it is tethered. Wireless operation has been reported using an array of ultrasonic transducers.[4]

8. position sensing diodes which are very fast detectors and provide the X-Y centroid of a spot of light that falls upon them. A year ago, the University of North Carolina revealed that they are using these devices. Their system is fast and accurate, but it still tethered and will slow down if wireless transmission is attempted. The PI has been interested in these devices since the early 1970s and always shied away from them because of the analog nature and limited resolution. Consequently, he is very impressed with UNC's achievement.

9. a magnetic system commercialized by Ascension.

Each of the above systems had some disadvantages. The camera-based systems suffered from the low resolution of the video sensors. High temporal resolution is possible but very expensive and is limited to 800x480 pixel spatial resolution. 1Kx1K is possible, but only the expense of speed--no more than 30 samples per second. Higher resolution devices exist, but they are even slower. The other systems that we have considered or that others have developed are inside-out systems as opposed to outside-in systems. This means that the sensors are worn on the participant and the data has to be transmitted back to the computer. While raw sensor signals can be sent over wires or fiber optics at high speed, wireless transmission requires that the data be sent back as a serial bit stream which is much slower.

The PI has designed two outside-in systems in which optical sensors around the environment measure the position of targets worn on the participant. Both of these systems seek to provide very high spatial and temporal accuracy.

V.C. Line Scan Approach

The first approach smashes the resolution constraint suffered by most optical sensors. Whereas existing video sensors max out at about 1Kx1K, this approach uses pairs of line scan sensors to create a virtual 6Kx6K camera which scans at 10Khz. Since multiple LEDs comprise the target and each LED is flashed separately, the actual rate is somewhat slower—about 2.5khz.

When all the target LEDs are illuminated at once, determining which spot seen by the sensor corresponds to which LED from one scan to the next is a complex and error prone calculation. The new technique hinges on the fact that only a single LED is being illuminated at a time, eliminating the correspondence calculation. A traditional video camera cannot take advantage of this simple target, because it must always read out every pixel in the scene to find the one that is illuminated.

V.C.1. Line Scan Concept

By using two line scan sensors mounted orthogonally, we only need to do one-dimensional scanning. Thus, we can scan the 6000 pixels of the line scan sensor much faster than we could scan the 1,000,000 pixels of a high-resolution video camera. By mounting one of these sensor pairs in

each corner of the room, we get complete coverage of the space for stereo measurements of each of the sensors regardless of which way the participant is facing. The very high sampling rate assures that the person will have moved a very small distance since the last sample.

V.C.2. Line Scan Optics

Ordinarily, a line scan camera can only look at a line in the scene at which it is aimed. Special optics have been designed which collapse a two-dimensional camera view of a scene onto a one-dimensional sensor. When the PI first started thinking about using line scan sensors about a decade ago, he was convinced that the optical problem was solvable, but did not have the optical knowledge or resources to pursue it. This time having fully considered many alternatives, he was convinced that the approach was the best option and should be implemented.

Since the optical problem was the unknown, he looked to outside optical designers to look at the problem from the standpoint of feasibility. Bob Perry of Illumination Technologies which does lighting and optical systems for machine vision applications was the first to tackle the problem. He decided that the problem was tractable but beyond his level of expertise. Next, Dr Gary Grimes at the University of Alabama agreed to address it. Just when an approach had been identified and the top student allocated to it, that student received a dream job offer and left school. There was no one else available with the requisite knowledge.

Finally, the problem was discussed with Dr. Jannick Rolland of CREOL (the Center for Research and Education in Optics and Lasers) at the University of Central Florida. She was intrigued by the challenge and spent considerable time analyzing it before coming up with an approach that she was sure could be made to work.[Appendix D]

V.C.3. Anamorphic Optics

At this point, the PI made an insightful but near fatal observation. Since the cameras were viewing the scene from the corner, they needed a 90° field of view in order to provide complete coverage. However, while the 90° of horizontal information was all useful, the 90° in the vertical direction was not. Two thirds of that 90° would be looking at the ceiling or the floor, whereas the participant's head would be in a narrow vertical band no wider than 30°. Therefore, it would be desirable if the optics

could asymmetric, i.e. providing greater magnification in one direction than the other. Such anamorphic optics are much more complex to design and there is almost nothing in the literature about such systems that also have such a wide field of view. At this point, the PI got greedy and opted for the more complex design, even though it would involve more lenses. Neither he nor Dr Rolland realized how much more complex it would turn out to be.

An anamorphic fisheye has been designed in detail. Tolerancing, optical distortion, and color aberration have all been considered. (Color aberration must be considered because the IR LEDs have quite a broad spectrum.) This first stage converts a wide angle rectangle onto a square image. A second stage which is also anamorphic compresses this two-dimensional image onto a line using a series of cylindrical lenses. The design is completely designed and ready to build. A paper has been published on the design.[Appendix E]

As we proceeded to consider fabrication, the size of the lenses required was seen to be a matter of concern. Dr. Rolland has many years of experience with designing and building complex optical systems, but not with such large lenses. The line scan sensor has 6K 10-micron pixels which means that it is 6 cm or 2.4 inches long, implying that the first lens of the fisheye must be 7 inches in diameter with is very large. The cost of grinding a lens goes up with the square of its diameter and the cost of the glass itself goes up with the cube of its diameter. As a consequence, the total cost approached \$40K for each of the eight required assemblies for a total of \$320K for just optical system before adding in the cost of the electronics and computer processing. Such an expense would have distorted the rest of the project and would result in an approach that would be far too expensive for others to emulate.

V.C.4. Line Scan Compromises

As a result, a number of compromises were examined to try to bring down the cost of the design. Several approaches were taken including:

1. beating on the existing design with the existing sensor by using fewer lenses and cheaper glass. This was done and reduced the cost considerably, but still not to the point of practicality.

2. reducing the size of the lenses by finding smaller CCD line scan sensors. This was accomplished by finding a device with 7 micron as opposed to 10 micron pixels, resulting in a 4.2 cm (1.65 inch) sensor.

3. eliminating the second stage by performing its function by some other means.

A number of ways of accomplishing #3 were considered. From the beginning, the PI has chafed at the fact that the second stage, the conversion of a two-dimensional image into a line had to be done using optics at all. Basically, what is desired is to take all of the pixels in a vertical column of the two-dimensional image and to sum them together to produce a single output.

V.C.4.a. Flat Fiber Option

One scheme that has been investigated is to do extend the idea of an optical fiber into two dimensions. An optical fiber is a thin strand of glass which is covered with a cladding material which assures that light that would otherwise leak out along its length is reflected back into it. Devices exist which are basically solid blocks of fiber bundles which are then tapered as a unit to perform magnification functions. Unfortunately, only very small magnifications are possible with this technique with current technology. The PI posed the question of whether very thin flat sheets of glass could be covered with the cladding material and many layers of these sheets formed together. If these sheets formed a very narrow rectangle in cross section at one end and tapered down into a point at the other, internal reflection would take light entering anywhere in the rectangle and reflect it to the point at the other end where it would be fed into a single pixel sensor. While this idea would work in principle, none of the companies approached about it thought that they could fabricate such a device with any process they already had operating.

V.C.4.b. Slit Scan Option

Another variation was to have a single vertical slit that would allow light from a column in the two-dimensional image to go through it. All the light through the slit could be focussed onto a single point detector by a simple parabolic mirror. The slit could then be made to scan across the two-dimensional image at very high speed. Several means of accomplishing this scanning were considered. The most conventional was to use a faceted mirror wheel which would sweep the image of the scene across the slit as the wheel rotated. The problems with this approach were partly the high cost of the motors and mirror wheels which were not in stock, but also the mechanical aberrations that the moving parts would exhibit.

Another issue was the very high speed of the single optical detector and accompanying analog-to-digital converter.

V.C.4.c. Spatial Light Modulator

Another device was a spatial light modulator which is an LCD device that reflects light back from displayed pixels rather than by transmitting it through them as a conventional LCD does. In this case, each column in a two-dimensional array would be a single pixel. When selected, all the light falling on that column would be reflected out where it could be detected by a simple but very fast single-point photodetector. The problem with this approach is about \$250K and one year front end to create the custom chip and \$10K per device after that.

Another approach is to fabricate a special two-dimensional sensor with all of the pixels in each column wired to each other. Using seven micron pixel widths, it would have to be 42 mm wide and 14 mm high. Seven micron pixels are the smallest that are commonly available, but it is not clear whether is a technological constraint or simply that there is a lack of pressure to make smaller devices.

If smaller detectors are developed, the original anamorphic optics design becomes more affordable. With current sensors, it is necessary to either use a symmetrical as opposed to anamorphic fish eye resulting in a 2/3 loss of vertical resolution or to use smaller and therefore lower resolution sensors which has the same effect. Alternatively, the same resolution can be maintained by decreasing the working area from the original 40'X40'.

V.C.4.d. Retroreflective Element

As the approaches that the PI developed were discarded one by one, Dr. Rolland had an idea for an alternative means of collapsing a two-dimensional image onto a single line as required by the second stage of the optical design for the line scan system. Her idea would eliminate five custom lens and replace them with a single off-the-shelf lens and an unconventional optical component. The crucial component is a retroreflective screen manufactured by 3M. A design study was conducted at the University of Central Florida over the summer and a prototype device constructed. Unfortunately, the properties of the retroreflective sheet were far from ideal and the LED illuminated a large area on the line scan sensor not a point.

Subsequent discussions with 3M revealed that the poor performance of the retroreflective sheet was not due to poor manufacturing, but had been deliberately injected into the product in response to customer feedback indicating that users did not want theoretically perfect retroreflection. As a result, 3M has agreed to make experimental sheets with much more controlled retroreflective properties and Dr. Rolland has been ask by 3M to characterize the new sheets. If this approach were to pan out, it would resurrect the moribund line scan approach by greatly reducing the cost of the second stage of the optics. (The cost of the first stage would be reduced by cutting the resolution to 4K by 4K using sensors having 7 micron detectors. The resulting 28 mm symmetrical wide angle lenses could be off-the-shelf and the distortions corrected for in software.)

~~SECRET~~

V.D. Random-Access Camera Option

Another approach that the PI has desired for many years and which only existed in the highest cost systems has recently become available. As mentioned earlier, a video camera looking at a spot of light must read out the entire image to find that spot. Even a line scan sensor must read out the entire line to find the spot. It would seem much simpler and much faster if it were possible to only read out the points near where the spot was last seen to determine where it had moved to since the last sample. CCD cameras cannot do this because the charge received for each pixel must be shifted out pixel by pixel before it can be read.

However, a new CMOS camera can randomly access any pixel at any time. That means that if the last location of the target is known, all that is needed is to search the pixels around that location because the target cannot move very far between samples. The faster this can be done, the fewer pixels need to be checked. As a result, a 10x10 pixel window around a given location can be read out in 40 microseconds or 25,000 times per second which provides a greater temporal resolution than any other method. The spatial resolution is not quite so impressive. 2Kx2K sensors with this kind of operation are now available which would provide sub-millimeter accuracy over a distance of 15'x15'. This working volume is typical of many of the techniques that have been evaluated and the spatial and temporal accuracy is better.

V.D.1. Low-Resolution Random Access

To test this approach, we have acquired a smaller version of this sensor in a 512x512 format which shrinks the working volume much farther. However, the smaller device will allow use to make the whole system wireless over a small area and allow us to test how valuable the higher resolution will be. Since the temporal resolution as well as the spatial resolution is high, it may be that averaging multiple successive very high speed samples will provide stable enough values for our purpose. In an immersive virtual reality system, stability is more important than absolute resolution because the participant does not know where he actually is. Also, the 30 hz video frame rate dictated by the computer graphics coupled to NTSC wireless transmission is really the bottleneck in our virtual reality system. The rest of the system cannot go faster than that.

However, it was hoped that the tracker would also be useful for augmented reality and for fundamental human perception studies like tracking a person's eyes as they move around a real environment and then comparing their eyes movements as they move through a virtual reality simulation of the same space. If the two behaviors are identical, then the VR display has attained a measurable success. If on the other hand, the visual behavior with the VR display contains artifacts that are not present in the natural visual behavior, then it is reasonable to assume that the sense of presence may be affected and that the VR display needs to be improved. In addition, a special low-resolution graphics system could be designed with faster frame rates and controlled by a portable computer carried by the participant. This setup would allow us to investigate the benefits of faster graphics and faster tracking.

At the moment we are building the 512x512 system with the random-access CMOS cameras. A single pair of cameras are tracking the multi-LED target at the speeds needed for tracking head movement. We are currently addressing the registration issues because small errors in the position or orientation of the cameras can lead to apparent erroneous rotations of the head.

V.D.2. Ceiling-Mounted Random Access Cameras

In addition, the random-access cameras are compatible with the original overhead camera tracking technique that implemented early in the program. Remember that the only problem with the performance of that

approach was the slow speed (30 fps) and the fact that multiple samples of the orientation angles had to be averaged to produce completely stable results. Since the random-access camera can locate an LED in a millisecond, the original algorithms will produce stable angles at a speed consistent with the constraint imposed by the graphics speed. In addition, the 512x512 resolution is twice that of the original system which was based a vision architecture developed in the early 1980s for the PIs VIDEOPLACE system. With the four cameras currently in hand, it would be possible to cover a 12' by 12' area. The primary disadvantage of the overhead approach is that a high (16') ceiling is required. Side looking cameras do not increase the performance and in fact add complexity to the system; however, they fit more gracefully into the dimensions of most laboratories.

Finally, the spatial resolution of both the overhead and side-looking-camera approaches can be greatly increased by using the 2Kx2K sensor from the same manufacturer at a small speed penalty. Unfortunately, by the time that we had tested the 512x512 camera sufficiently to be satisfied that it would work for us and tried to purchase the high resolution device, the manufacturer had withdrawn it from the market citing problems with its performance. They promise that they will reintroduce it but do not have a date certain at the moment.

V.D.3. Advantages of Random Access Cameras

There are a number of advantages of the random access camera:

1. it is a home game for the PI in terms of the techniques needed to implement it
2. it is compatible with the original overhead downward-looking camera approach and could be fit into it and the original software employed.
3. its needs for selectable LED targets are common to all approaches now being considered
4. its algorithms for computing location and orientation are also common to all approaches
5. it will give us a short distance wireless tracking capability very quickly.
6. it can use off-the-shelf lenses.

V.E. Smart Targets

In addition, to the design alternatives mentioned above, there are two additional ideas that can be applied to any of those approaches. One is based on the concern that corner-mounted sensors viewing LEDs from the side may suffer from blind spots when the person is in a corner and too close to a sensor for it to see the target. Similarly, we have been concerned that as the person tilted his head too far the sensors' view of the LEDs would not be optimal. (Just as the optics have a limited field of view, so do the LEDs and even though we have the widest field-of-view LEDs procurable, there is less light emitted at oblique angles.) For any configuration of LEDs, there is always a position and head orientation that will make some of the LEDs hard to view from fixed sensors.

One solution to this problem may actually increase the spacial accuracy of the system rather than simply preserving it. The idea is to have redundant targets mounted around the participant's head. At each moment, a virtual target containing enough points to define a plane is created from a subset of these LEDs which are optimally positioned for viewing by the sensors. If selectable target combinations can be made to work, then we can configure the targets to be visible to the nearest sensor pair. If this can be done at operational speeds, it is theoretically possible to increase the resolution by about 50%. (In the original approach, when the person was in one corner of the space, one of the sensors viewing him would be in the opposite corner. By selecting a combination of LEDs that are visible to the two of the other cameras that are closer, the resolution is improved.)

V.F. Steerable Sensors.

Another way of reducing the cost of the optics (or of increasing the resolution) for all approaches is a bit more elaborate. The high cost of the line scan optics was largely due to the desire for a wide field of view (90°) which is necessitated by the need for four detector systems mounted in the corners of a room to provide complete coverage of it. If a narrower field of view could be made to work, the optics would become much more pedestrian and the costs consequently lower.

As noted above, it may often be desirable to select only two or three of the sensors for viewing. At such times, the other sensors could be mechanically steered to aim more directly at the participant. Since the participant does not move very quickly about the physical space, 1/10 or even 2/10 of a second could be available for such aiming. The benefit

would be two fold. First, a cheaper optical assembly with a narrower field of view (say 30°) could be used. Second, the full resolution of the line scan sensor could be applied to that narrower field of view tripling the resolution. The horizontal resolution would be increased because the 6000 pixels of the sensor would be spread over 30° rather than 90° . The vertical resolution would be increased because spreading the 6000 pixels resolution over a 90° vertical field of view—in the symmetric as opposed to abandoned anamorphic design—meant that most of those pixels were looking at points in the environment that were either above or below the elevation of the participant's head. (A 30° vertical field of view was all that was deemed useful with the anamorphic design.) Alternatively, the same resolution could be achieved with smaller sensors which require smaller much cheaper lenses.

This design approach raises several concerns. One is the additional complexity of mechanical scanning. A second is the constraints that may be placed on the speed of the participant's movements. (A participant's movements around the environment would have to be simulated to determine how severe those constraints would have to be.) A third is the need for very accurate measurement of the angle of the steering mirror. While this approach is considered interesting, no action is contemplated on its implementation at the moment.

V.G. Current Tracking Plan

As the random access camera approach is proceeding we will keep beating on the optics for the line scan approach which we have now reduced to \$8K per unit for four first stage optics systems and \$3K each for 8 copies of the second stage optics. This is within our resources; however, we would rather not invest so much money in the optics because these costs do not come down the way electronics costs do.

After the comparative costs are worked out and as we get experience with the short-range random-access camera system, we will decide whether to build the line scan optics or whether to simply move to the high-resolution random access camera system. If the 3M retroreflector does not pan out and the high-resolution CMOS camera is not put back on the market, we will use the four low-resolution cameras mounted overhead to create a 12' square space. In the meantime, the development of the low-resolution random-access camera system proceeds apace.

VI. Odor Studies

Initially, psychophysical studies examining the effect of odors on performance of surgery-related tasks formed a significant part of the project. Two major studies were done in the first year. One tested the effects of odors on spatial reasoning and the other the effects of odors on manual dexterity. Both were definitive studies with 90 subjects apiece. However, while the two issues seemed closely related, the two studies had completely opposite results. Spatial reasoning was found to be positively affected and manual dexterity not affected at all. Thus, the results were equivocal and the very large number of subjects required to swamp out individual differences made them expensive. Since odor acquisition had turned out to be much more difficult than expected, we decided to reallocate more resources in this direction. When the technology issues were all resolved, we would then reconsider how much could be done in the way of studies.

While the odor acquisition continues to be a continuing agony, the tracking and advanced delivery systems are proceeding with some confidence. Therefore, we have been looking at a small series of studies that could be done incrementally.

One area of interest is the use of odors as alarms. There is only one existing example of an odor being used for this purpose and that is the use of mercaptans to signal the presence of natural gas in the home. Even this example is in jeopardy, because elderly people have been found to lose their sensitivity to this odor. However, there are other situations where odors signal emergency conditions. The most obvious of these is the smell of smoke indicating a fire or more specifically the smell of burning insulation to signal a short circuit in an electrical system.

Odors could certainly be used to signal such unique emergency conditions. In addition, they could be used in more subtle ways. For instance, odors could signal the increased likelihood of an event or the presence if not the immediacy of a threat. They could signal the state of a system and activate a set of context-specific expectations. They could display the vital signs of a patient to a surgeon during surgery.

While these applications are probably feasible, there are a number of caveats and subtleties involved:

1. odors are hard to evacuate from a space and so could not be used for commonly occurring events if they are to be displayed to a room full of people. However, if a person is wearing a mask or even a odor presentation device in front of his nose, persistence is not as much of a problem. The very small volumes of odorants used in these cases and the means of evacuation or environmental dilution assure that the odor will be gone from in front of the person's nose.

2. people adapt to odors quickly and then lose their ability to smell them. This feature means that odors can signal transitions but are not as good at displaying a sustained context.

3. people differ wildly in their sensitivity to odors and in their tolerance of them. Indeed, individuals may literally have had a bad experience with a particular odor when they were children and can never forget that association.

Assuming that odors can be used as alarms and as cues in practical applications including surgery, what kinds of research questions need to be asked? The following candidates have been identified so far:

1. what kinds of odors should be used? For instance, pleasant versus unpleasant, stimulating versus soothing, trigeminal versus pure smell.

2. can odors break the concentration of a person who is involved in a highly involving task?

3. how many odors can be identified with different conditions?

4. how long do people remember the significance of odor associations that they have learned?

We spent time developing a small set of studies with the Dr. Joel Warm and Dr. William Dember at the University of Cincinnati. These studies will be implemented only if the financial needs of the tracking and delivery systems permit.

VII. Next Years Effort

The final year of the project will see the completion of the individual technologies and their integration into a single virtual reality system. These efforts will include:

1. completion of a preliminary wireless tracking system based on the random-access cameras.

2. completion of the final wireless tracking system using either the line scan sensors if the 3M's new retroreflectors are successful or the high-resolution random-access cameras if the latter become available.

3. integration of the tracking and odor delivery into a wireless virtual reality system which permits natural ambulation. This will involve the upgrading of the current HMD which is the most inexpensive available.

4. integration of the wireless advanced delivery system and possible reduction of its weight.

5. continuing acquisition of odorant materials needed for various scenarios.

6. development of the following virtual environment scenarios for displaying odors:

A. an easy odor environment such as an outdoor market or a suburban home

B. a surgical simulation

C. a battlefield mass casualty scenario set in the countryside

7. the final documentation of the project

References

1. Turk, A. Sensory Evaluation of Diesel Exhaust Odors, U.S. Department of Health, Education, and Welfare, Environmental Health Service, National Air Pollution Control Administration Publication No. AP-60, 1967.

2. Ibid, p. 19.

3. Sims, K. Artificial Evolution for Computer Graphics, SIGGRAPH91, p. 319.

4. Foxlin, E. Harrington, M. Pfeifer, G. "Constellation™: a Wide-Range Wireless Motion Tracking System for Augmented Reality," SIGGRAPH98, pp. 371-8.

Vibration-Induced Atomization of a Droplet

summary report by

Cornell University
Sibley School of Mechanical and Aerospace Engineering
Ithaca, New York 14853-7501

Task Leader: Professor C. Thomas Avedisian
607-255-5105
cta2@cornell.edu
Student: Mr. Rajeev Shah

to

Artificial Reality Corporation
P.O. Box 786
Vernon, Ct.

July 17, 1996

Appendix A -- 47

1. Introduction

The technology for odor generation begins with a bulk liquid followed by its evaporation to produce molecules which are subsequently inhaled in the respiratory tract. An intermediate step to evaporation often involves atomization of the bulk liquid to produce droplets, followed by droplet evaporation. Reaction of the molecules with the tissues involved creates the sense of smell. A common example is the perfume industry and the squeeze atomizers used to vaporize the liquid and produce a fragrance. The application of interest here is the incorporation of odors into the artificial reality (AR) experience. The goal is to introduce odors which match the sense of sight and sound experienced in the AR environment. For that purpose, several technologies are under consideration, including flow of the liquid through a porous medium within which the liquid evaporates, and atomization of the liquid.

In this brief report, we describe a method for atomization of liquids that is both simple and cheap to use. We first give a brief review of the current technology for atomization, then discuss the new approach. Advantages and problems are pointed out. Preliminary results are presented to demonstrate the concept.

2. Liquid Atomization Technologies

A device which disintegrates a bulk liquid into droplets is termed an 'atomizer'. Atomizer types can be classified according to the type of energy used for atomization. These include energy from the liquid itself which is to be atomized; gas energy; mechanical energy; electrical energy; or vibrational energy. Bayvel and Orzechowski (1993) and Lefebvre (1989) provide extensive discussions of the various technologies for atomization of liquid.

3. Vibration-induced Atomization

A little used technology for atomization is based on passing the liquid over a transducer which vibrates at frequencies to produce short wavelengths that result in break-up of the liquid into droplets. This approach appears to be suitable for applications that require low spray velocities.

The precise mechanism for atomization by this vibratory process is a matter of debate. It is generally thought (Lefebvre 1989) to include result in the unstable growth of capillary waves on the surface of the liquid into macroscopic ripples that eject liquid and thereby form droplets. Though the concept of atomization by this approach has been known for over 30 years, it has not been extensively studied. Only recently has atomization that involves some form of vibration excitation of the liquid been incorporated into a commercially available atomizer design.

Analysis of free-surface waves generated by vibration excitation was developed by Peskin and Raco (1963) in terms of a Taylor instability mechanism. The analytical results show that the mean droplet size, D , is related to the surface tension, σ , liquid density, ρ_l , and frequency, f , as

$$D \approx (4\pi\sigma/(\rho_l f^2))^{1/3}$$

Thus, high frequency vibrations produce small droplet diameters. Mochida (1978) studied ultrasonic atomization of distilled water flowing in a ultrasonically excited tube at 26Hz. A correlation for the 'sauter mean diameter' was developed as

$$D_{SMD} \approx 0.158 (\sigma/\rho_l)^{0.354} \mu_l^{0.303} f Q_L^{0.139}$$

where Q_L is the flow rate and μ_l the liquid viscosity. Note that frequency does not appear in this correlation because it was fixed at one value in the experiments. The results of Land and Mochida are similar in that $D_{Land} (1963) \propto (\sigma/\rho_l)^{.33}$ while $D_{Mochida} (1978) \propto (\sigma/\rho_l)^{.354}$.

Vibration atomization has recently been proposed for drop formation in a thermal control device for microgravity cooling applications (Smith and Glezer (1996)). In this approach, a single 'large' droplet is placed onto the surface of a piezoelectric crystal that is vibrated at a frequency at which surface wave disturbances break up the droplet into smaller droplets. The present study further examines this concept experimentally. In the next sections, we describe the experimental design and procedures and discuss preliminary results.

4. Description of Experiment

Figure 1 is a schematic of the apparatus of the experimental design. It consists of a single 'large' droplet placed onto the surface of a piezoelectric crystal, the drive electronics to vibrate the crystal and cameras for recording the results. The components are the following: a HP 214B pulse generator; an HP 54600A oscilloscope; the piezoelectric crystal attached to an aluminum support; a halogen light source; and a 35 mm motor driven camera to record the atomization process. In the experiments reported here, water droplets were first deposited onto the crystal by hand using a glass pipette, then the crystal excited. The droplets flattened into a 'lens' shape or 'sessile' drop shape depending on the volume of water. For the results reported here, the wetted diameter before excitation was from 4mm to 6mm. Some limited results were attempted with an organic liquid, heptane, but were unsuccessful because heptane rapidly spread into a thin film over the surface of the crystal due to the comparatively low surface tension of heptane relative to water: about 30 dyne/cm to over 70 dyne/cm).

Figure 2 shows a top view of the aluminum housing used to secure the piezoelectric crystal. The crystal is attached to the plate with 10-24 threaded bolts, and flat washers at four corners. This arrangement secures the edges and allows the active area to oscillate freely. The crystal has one lead soldered to the back and another wire is attached to one of the fastening screws to complete the circuit. Excitation of the crystal was via a pulse generator (HP 214B). Input signals were observed on a digital recording oscilloscope (HP 54600A). In all cases, a square wave input was used. The frequency, voltage, and pulse width were varied. The limits on these parameters was controlled by the pulse generator until a 'overload' condition was observed.

Figure 3 is a detailed schematic of the piezoelectric crystal. Dimensions are indicated in the figure. The back side of the crystal is brass. It was not polished for the experiments reported here. The crystal was oriented horizontally with the back side facing upward, and test droplets were gently placed on it.

The photographic arrangement used to capture the sequence of events consists of a 55 mm/2.8 Nikkor lens connected to a PB-6 bellows, Nikon F-3 body, and a MD-4 motor driver. The droplet is illuminated by direct back lighting using a halogen bulb. This set-up

created a direct line of sight from to the camera through the droplet. Film used in these preliminary experiments was Kodak color print film.

5. Experimental Procedure

The experimental procedure involved first depositing the test (water) droplet onto crystal and then gradually increasing the system variables until an explosive atomization process occurred. The piezoelectric crystal produces a ringing noise which corresponds to the rapid oscillations of the active area, growing louder with increasing voltage and higher in pitch with increasing frequency; this gave us a basis to determine our starting ranges. The lowest voltage amplitude examined was about 20 millivolts and the maximum was 33.44 volts at which the pulse generator indicated an 'overload' condition.

To identify the combination of variables in which droplet atomization occurred, we systematically varied the variables as follows. First, the voltage and pulse width was fixed and then the frequency was varied until either the droplet exploded or an 'overload' condition occurred. Then, the voltage was increased to a new value while holding the pulse width constant and the frequency again increased until atomization or 'overload'. After that limit was explored, the pulse width was changed and the process repeated.

The frequency range was limited by the pulse generator characteristics; the upper limit was found to be about 3300Hz. The optimal range was 1500 - 2000 Hz. The pulse width ranged from 0.1 milli-seconds to 0.25 milli-seconds.

To capture the time sequence of the droplet atomization we kept the voltage and pulse width constant, and increased frequency starting at 1000 Hz until atomization occurred. The motor driver on the camera was set at 5 frames per second.

6. Results

A sequence of photographs is shown in figures 4 to 6. A color print film was used which is the reason for the pink 'tint' to the images which are largely devoid of any color (future studies would use black and white film). The magnification of the images are evident for the lens arrangement used. An approximate scale is shown on the figures. The same nominal conditions were used for the three sequences shown.

Figs. 4a to 6a show an undisturbed droplet. Figures 4b to 6b show surface ripples prior to the shattering of the droplet. Figs. 4c to 6c show the dynamics of the droplet disintegration process. The speed of ejection is suggested by the blurring of some of the microdroplets produced. Furthermore, some of the atomized droplets are in focus and appear to be more than one order of magnitude smaller than the wetted diameter of the original lenticular droplet (figs. 4a to 6a).

Figures 7 to 9 show the frequency/voltage/pulse width conditions at which atomization occurred. Generally, for frequencies below 1400 Hz, no atomization was observed. Similarly, above 1700 Hz, an 'overload' condition tended to be reached. It should be emphasized that these combinations of variables are likely to be strongly dependent on the physical dimensions of the crystal used. Thinner crystals can, for example, produce atomization at lower frequencies. Furthermore, while an intense 'ringing' was observed during excitation of the crystal, this problem could be avoided by using ultrasonic frequencies. The voltage and pulse widths needed to atomize the droplet using ultrasonic frequencies will be different than reported here.

7. Future Work

- Future experiments should explore a higher frequency domain to avoid the audible sound that can make this technology prohibitive for incorporation in the AR environment.

- Different crystal designs should be examined.

- The photographic process should explore different lighting schemes and use black and white film

- Finally, a system to deliver liquid to the crystal needs to be automated.

8. References

Bayvel, L. and Orzechowski, Z. 1993 *Liquid Atomization*, Taylor and Francis, New York.

Lang, R.J.S. 1962 *J. Acoust. Soc. Am.* **34**, 6.

Lefebvre, A.H. 1989 *Atomization and Sprays*, Hemisphere, New York.

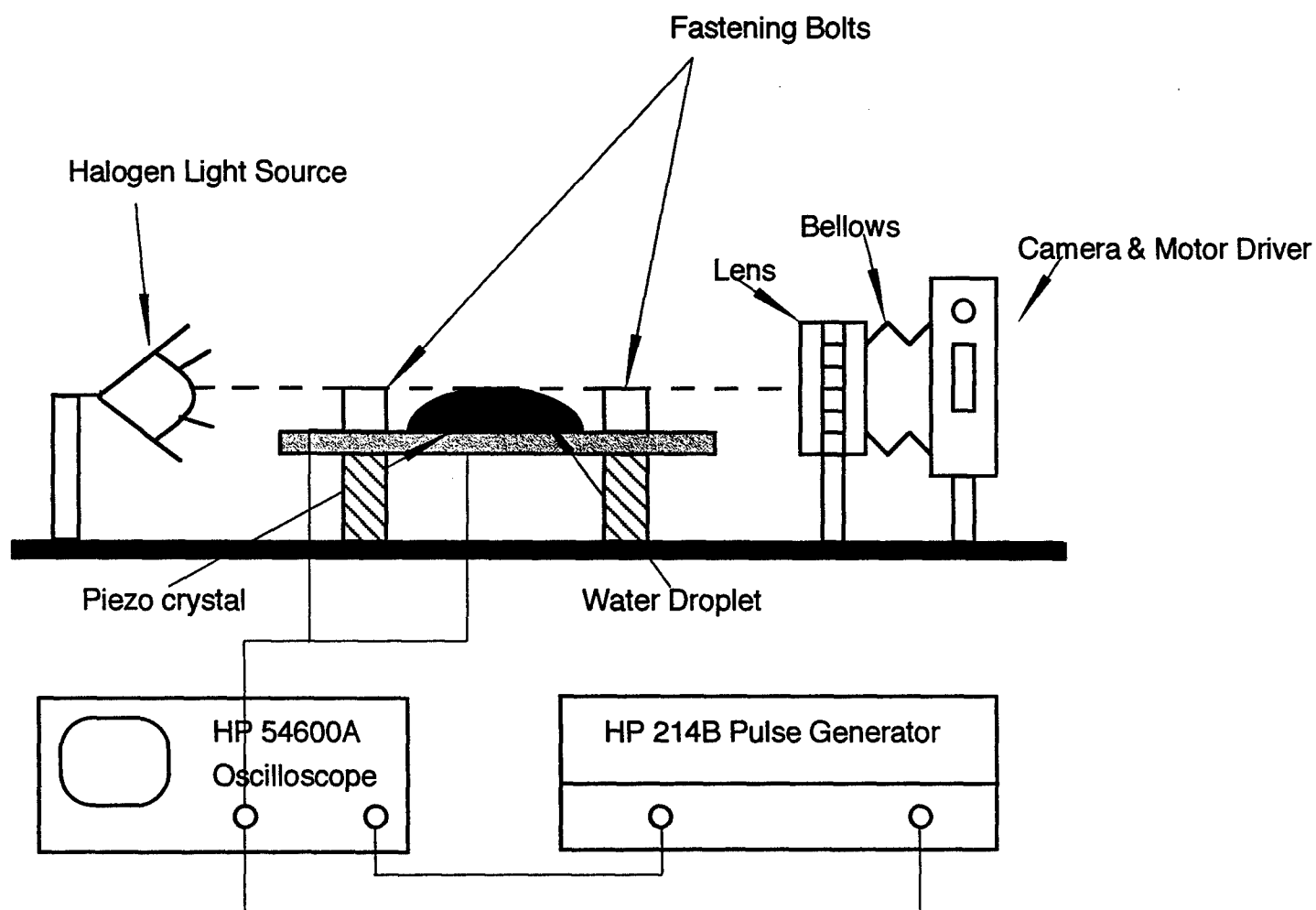
Mochida, T. *Proc.* 1978 *ICLASS* pp. 193-200.

Peskin, R.L. and Raco, R.J. 1963 *J. Acoust. Soc. Am* **35**, 1378.

Smith, M.K. and Glezer, A. 1996 *3rd Microgravity Fluid Physics Conf.* NASA CP-3338.

Aparatus to Produce Droplet Atomization

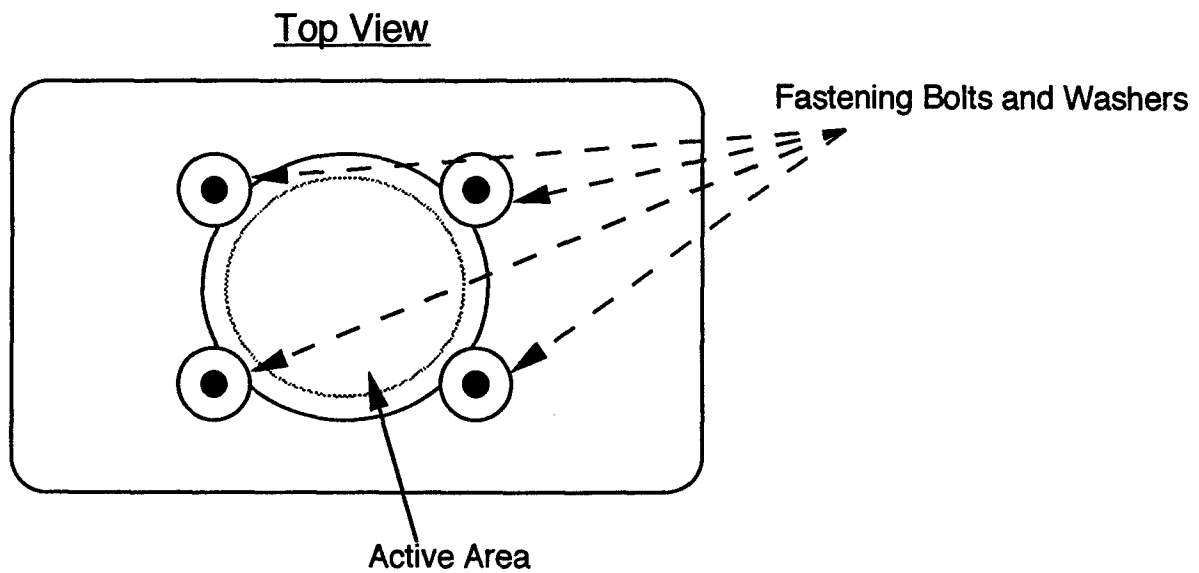
Figure 1



* Not to scale

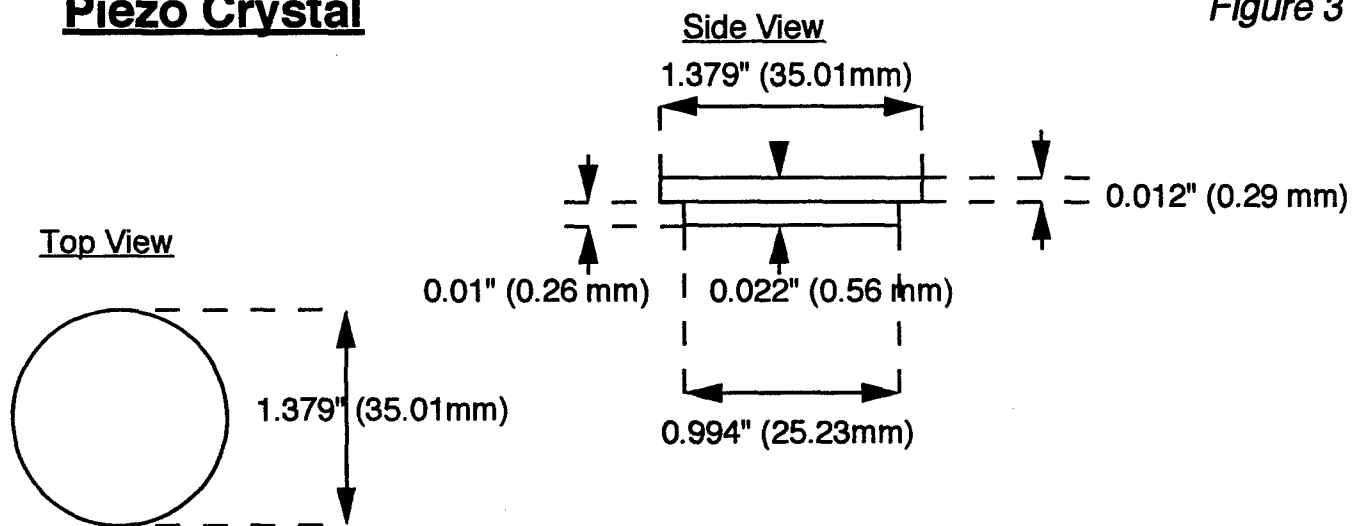
Aluminum Housing

Figure 2



Piezo Crystal

Figure 3



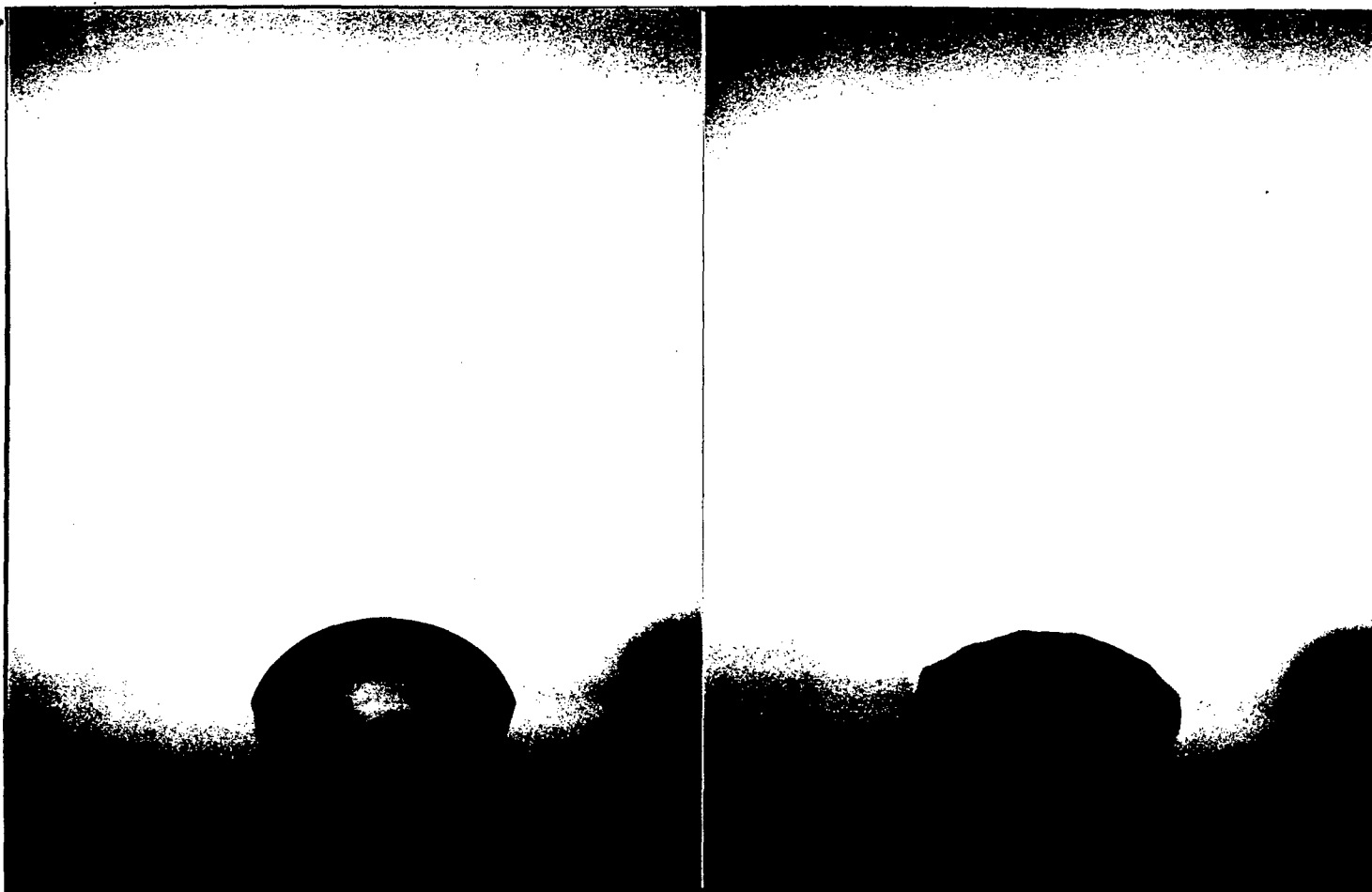
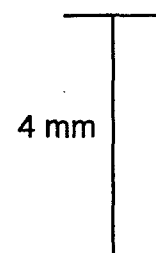


Figure 4

Approximate scale



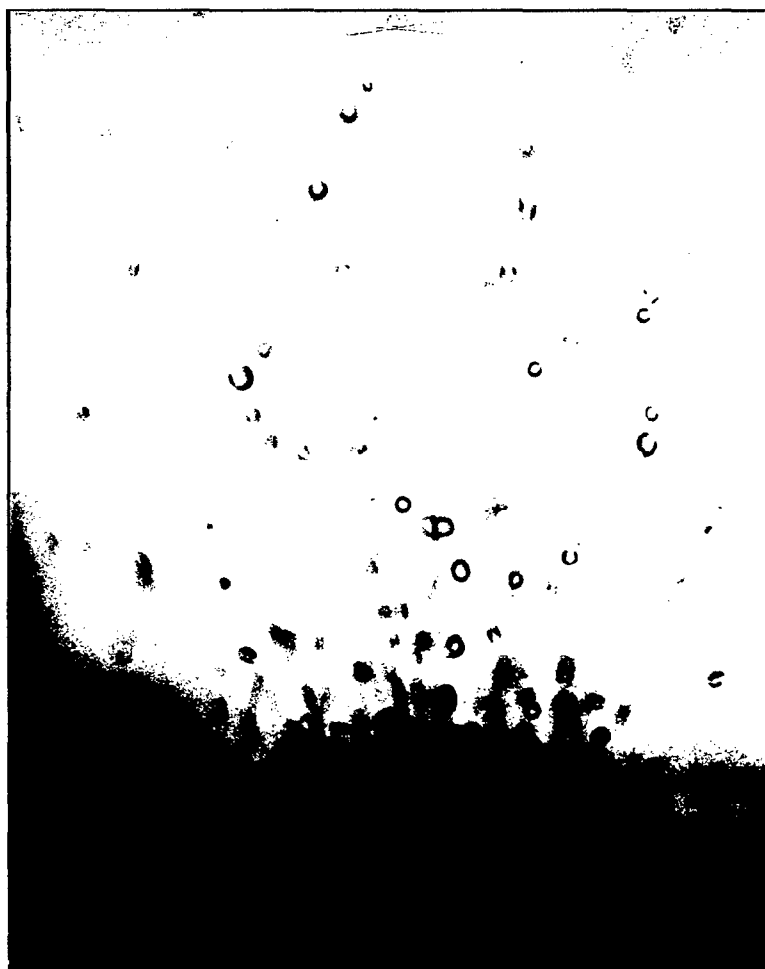
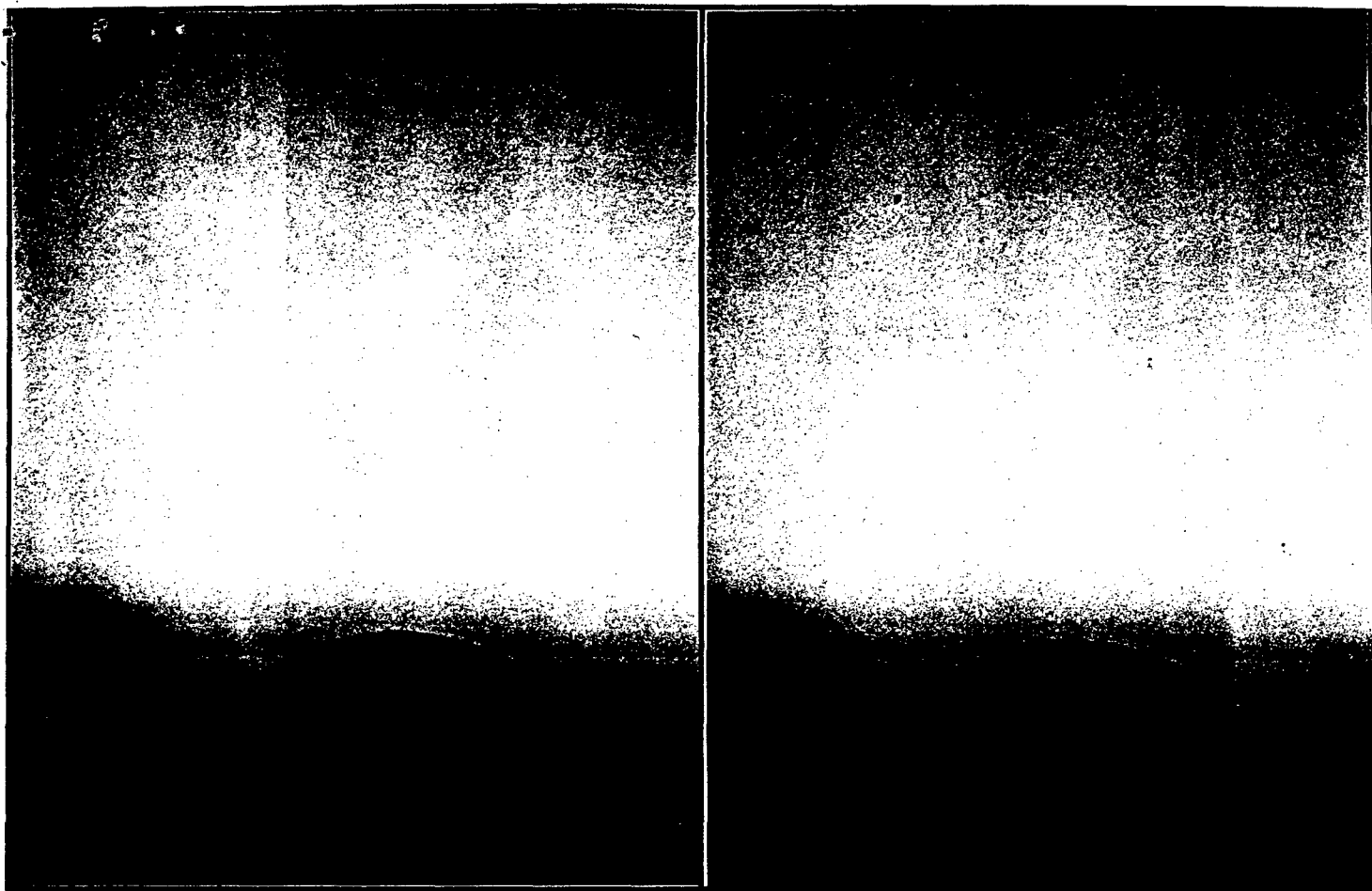
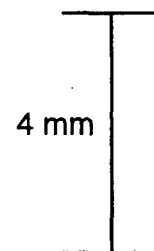


Figure 5

Approximate scale



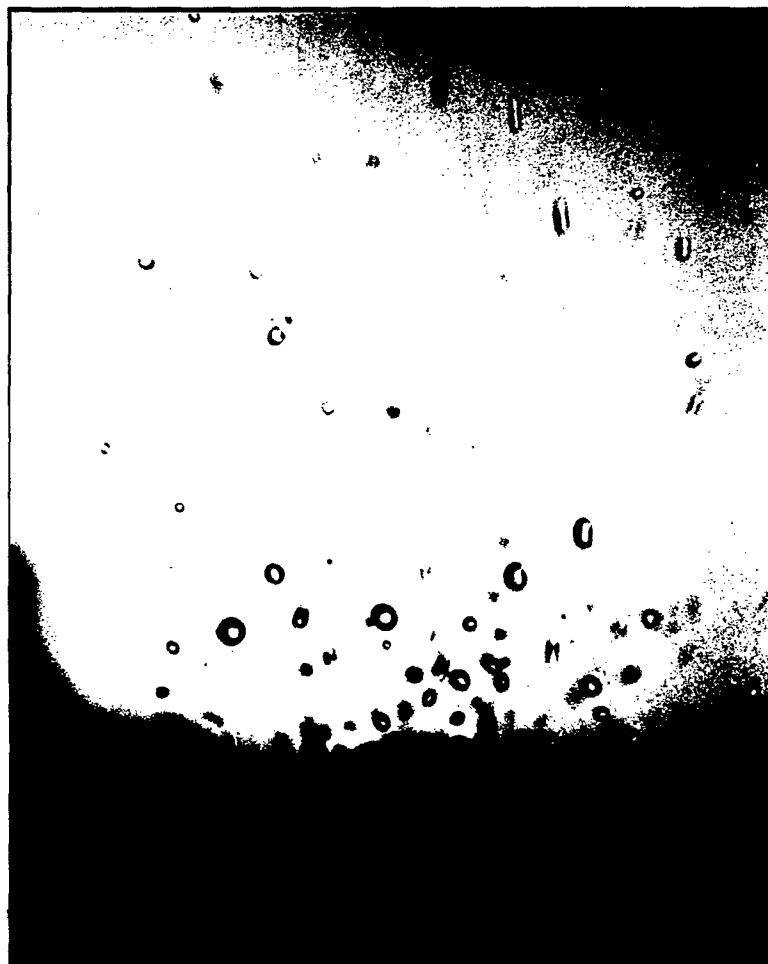


Figure 6

Approximate scale

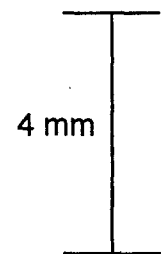


Figure 7

Atomization Response to variable voltages and frequencies at 0.1 milli second pulse width

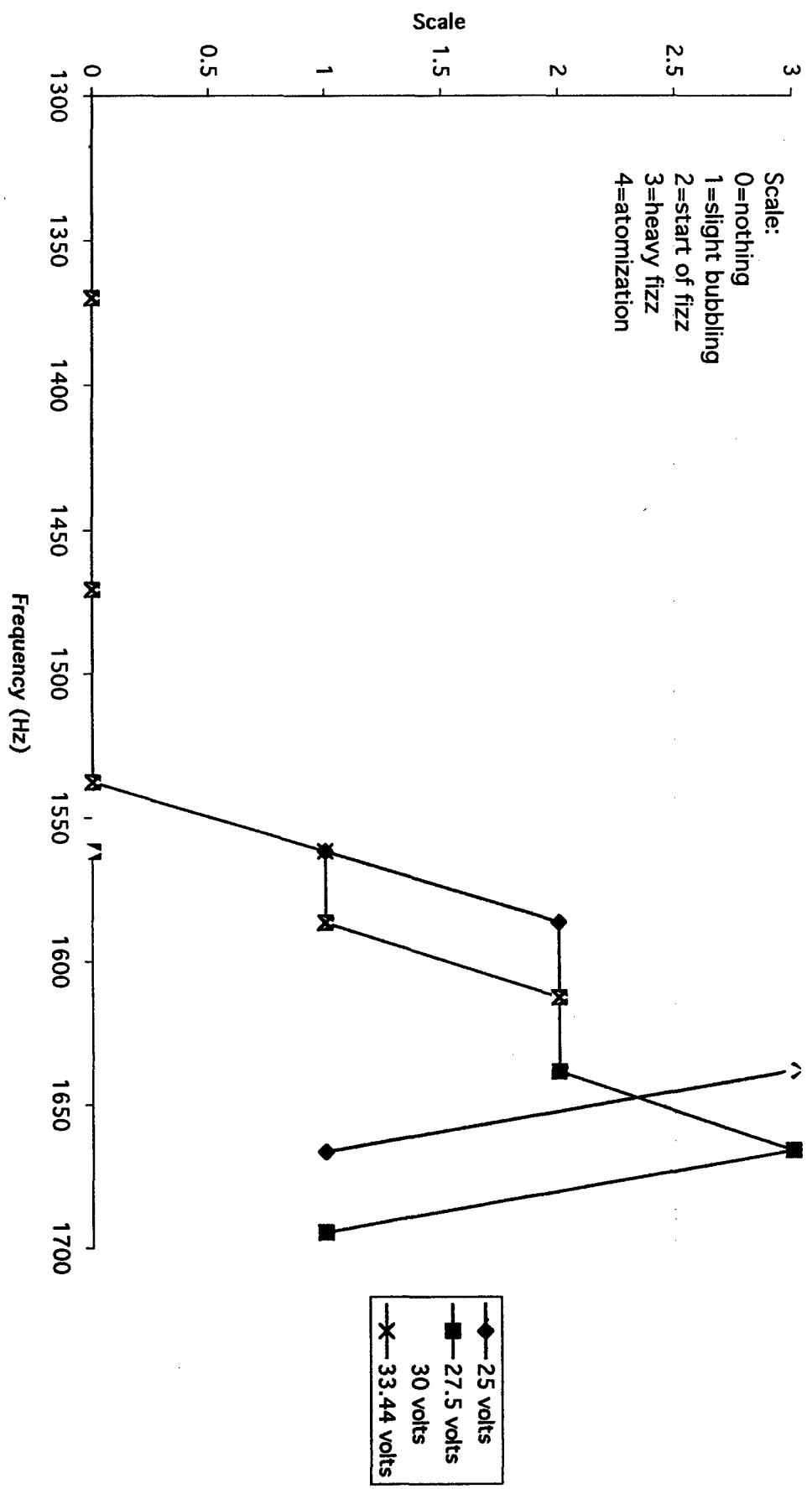


Figure 7

Figure 8

Atomization Response to variable voltages and frequencies at 0.17 milli second pulse width

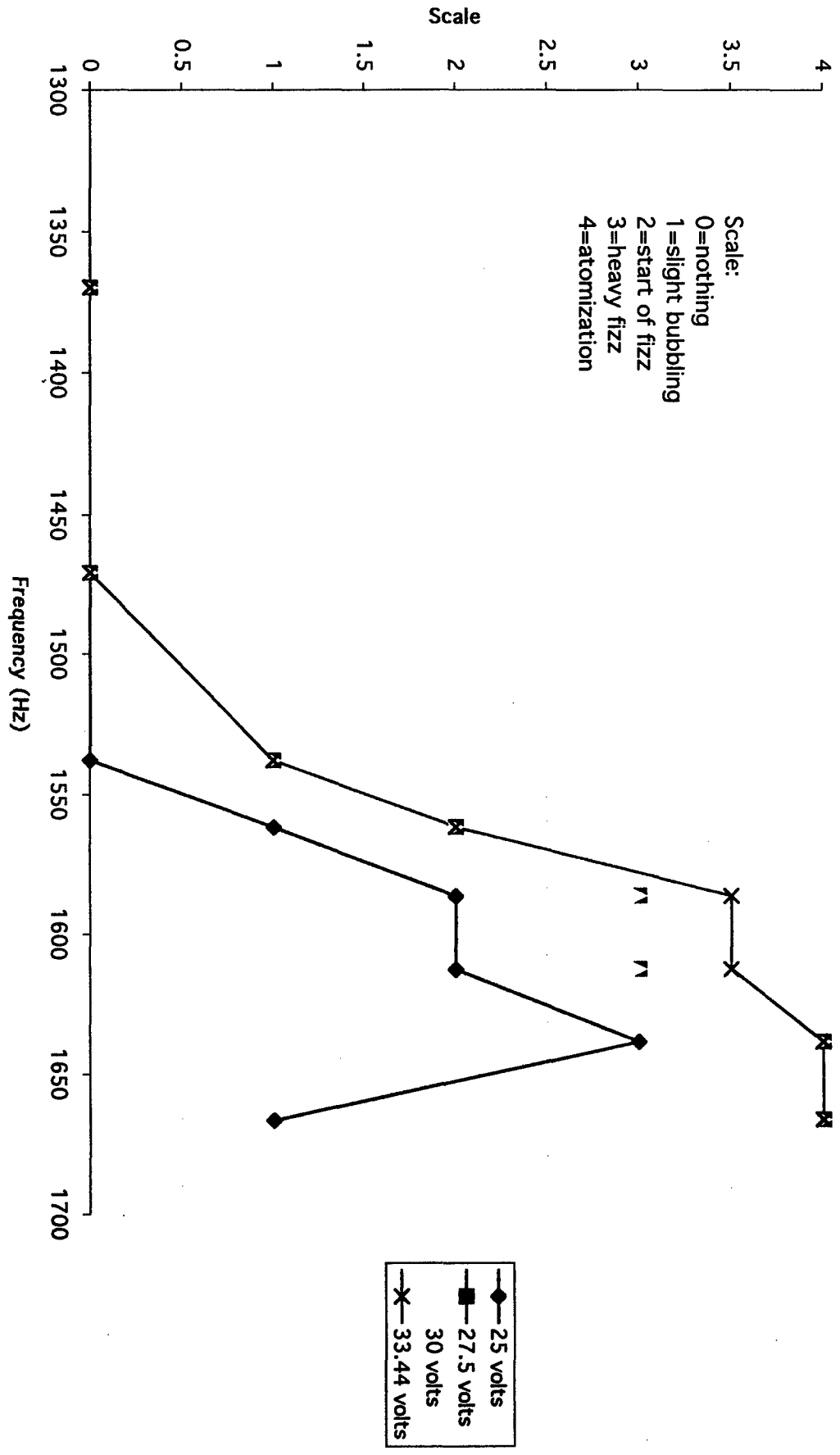


Figure 9

Atomization Response to variable voltages and frequencies at 0.25 milli second pulse width

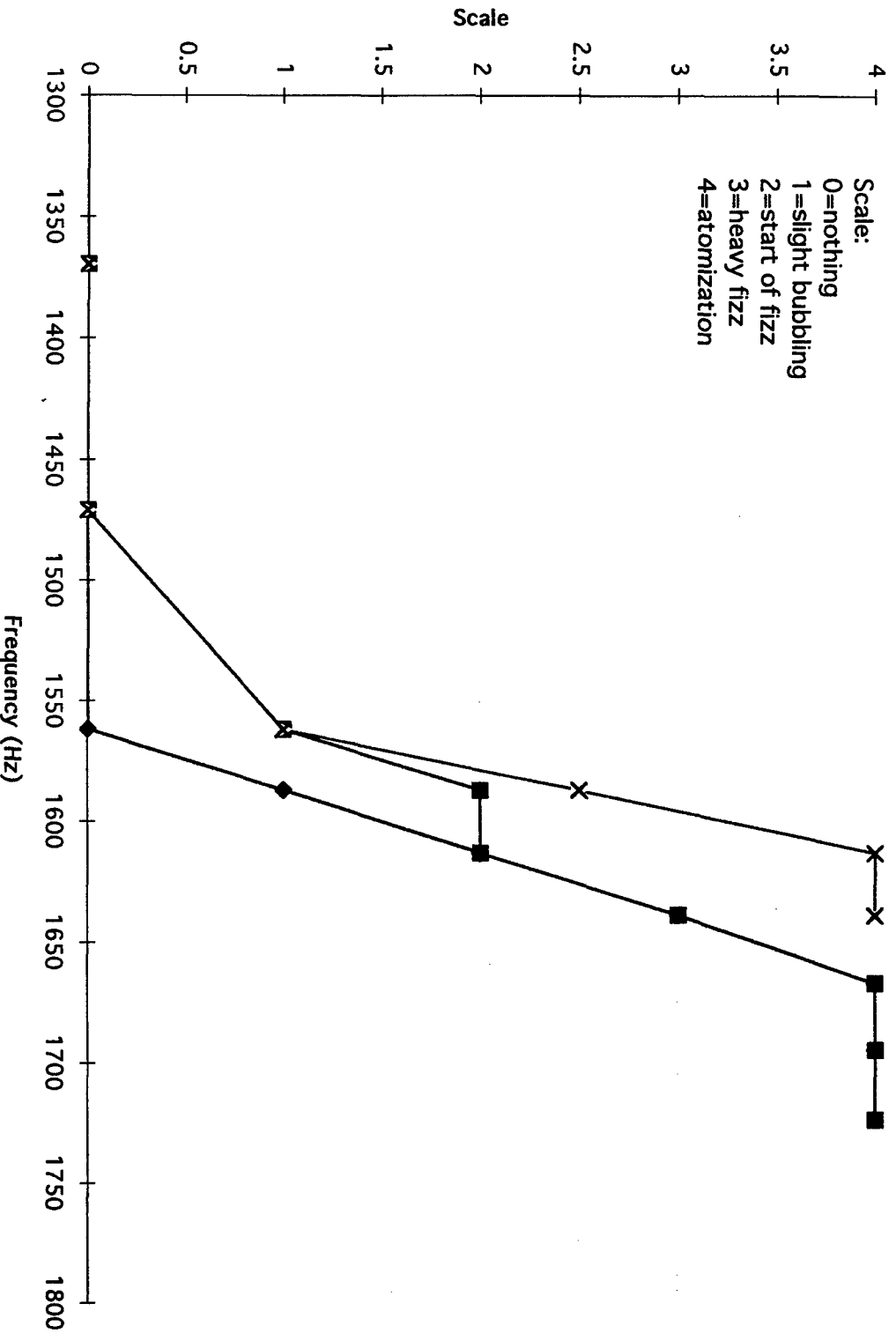
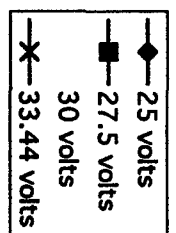


Figure 9



Possibilities to Consider in Promoting the Concept of Aroma Enhanced Virtual Reality

(The following report is based on the ideas discussed during roundtable meetings on the subject of aroma enhanced virtual reality held in late Jan. 1998. Leader of the discussions was Dr. Terry Acree, Professor of Biochemistry at Cornell University and head of the Flavor Labs at the New York State Agricultural Experiment Station in Geneva, New York. Contributing to the discussions were five graduate students from the Cornell flavor labs: Jane Friedrich, Peter Ong, Grace Feng, Olivier Perrin, and Kathryn Deibler. Also present was flavor labs research support specialist Ed Lavin who compiled this report)

There was a consensus from the group that the concept of adding the dimension of odor to a virtual reality system is both a worthwhile and exciting one. To better consider the concept, the group decided to focus its ideas into two categories: promotion and execution. This report will deal each of these individually.

I. Promoting the Idea

If the overall goal of your group is to research and then demonstrate the impact that aroma could have when integrated into a virtual reality system, perhaps the most effective way to achieve this would be to produce a small scale aroma-enhanced "virtual reality" video using odor delivery systems that are already in use in industry. Our group feels that an aroma enhanced video could be made employing scenarios that would include a number of common everyday life situations. Inherent to these situations would be moments where a specific aroma would be delivered to the viewer that would clearly enhance the one-dimensional nature of the scene on the screen. Such a video could demonstrate the positive impact that adding the extra dimension of aroma would have on a total virtual reality package.

We are not familiar with the current state of the art in aroma delivery for these purposes. Basic to the premise of course is that a method would have to be devised to deliver and vacate the aromas used and to synchronize them with the on-screen activity. It is probable that current options consist of the old scratch and sniff method in which the viewer responds to an on-screen cue by scratching and sniffing a card containing the various odors. Another

and more attractive method would be a system which delivers airborne puffs of odor chemicals directly to the viewer from a remote location.

Aroma delivery systems aside, our expertise is in the realm of food science. The vast majority of known aroma producing compounds are associated with foods, therefore our suggestion is to make a video which displays the enhancement aroma lends to food. To give you an idea of what we mean we have scripted a video sequence which will demonstrate the concept of aroma enhanced virtual reality. The compound name and the approximate amount that would be needed to produce the desired effect is noted. This script is a rough sketch which can be used to demonstrate aroma enhanced virtual reality.

Our script begins with a medical professional on his day off doing an everyday task and ends with his re-entering the professional realm of medicine. It was thought this might be an effective way to bring in the medical angle which is ultimately the driving force behind this research.

Scene 1 (S1)-- Doctor in home, says good-bye to wife "going down to the market" , exits front door. Says good- bye to son who is mowing grass. > Aroma 1 (A1) *hexanal (smell of fresh mown grass-- 25ppm)*

S2-- Physician goes to car and gets in > (A2) *vinylchloride (new car smell)*

S3 -- Pulls out of driveway, then pops a piece of gum in his mouth > (A3) *carvone (peppermint odor -- 50ppm)*

S4 -- Arrives at open-air market in a park like setting.

S5-- Sees popcorn stand near market and stops to buy popcorn > (A4) *2-acety-1-pyrroline (popcorn aroma-- 50ppb)*

S6 -- Stops at cheese stand > (A5) *butyric acid (cheesy-- 5ppm)*

S7 -- Walks by cotton candy vendor > (A6) *furaneol (burnt-sugar smell of cotton candy -- 25ppm)*

S8 -- Walks by peanut vendor > (A7) *2-acety pyrazine (roasted peanut--1ppm)*

S9 -- Stops at fruit vendor, buys apple, takes a bite > (A8) *ethyl butyrate & E-2-hexenal (apple and apple peel-- 10ppm)*

S10 -- Checks out orange stand, buys a dozen oranges > (A9) *orange oil (1% by vol.)*

S11 -- Stops by bell pepper stand > (A10) *3-methoxy-2-isobutylpyrazine (green bell pepper aroma -- 10ppb)*

S12 -- Stops by fish vendor--sniffs fish to test for freshness. > (A11) *trimethyl amine (unfresh fish aroma -- 10ppb)*

S13 -- Stops at vendor and buys a cup of concord grape juice > (A12) *methyl anthranilate & furaneol mixture (concord grape 50ppm)*

S14 -- Tries a sample slice of cucumber > (A13)- *E-2-nonenal (green cucumber like -- 1ppm)*

S15 --Approaches mushroom vendor > (A14) *1-octen-3-one (fresh mushroom like -- 1ppm)*

S16-- Stops and eats a banana > (A15) *isoamyl acetate (banana aroma--10ppm)*

S17 --Buys chocolates for his kids > (A16) *vanillin (100ppm)*

S18- Buys roses from vendor for wife > (A17) *2-phenylethyl alcohol (rose-like aroma -- 50ppm)*

S19 -- There is a sudden commotion. Sirens are heard and an ambulance pulls up in a park adjoining the market. Doctor moves to help and comes upon a scene with a man down, apparently unconscious surrounded by onlookers and EMT's. Doctor identifies himself and begins to work on the man.

S20 -- Doctor begins to check for vital signs. He rips open the patient's shirt and puts his face close to body of patient to check for breathing and pulse. > (A18) *hexanoic acid (body odor aroma-- 500ppm)*

S21 -- Doctor loosens victim's belt to assist breathing. Further examination shows patient has urinated > (A19) *phenylacetic acid*(urine smell -- 100ppm)

S22 -- Patient remains unconscious and appears to be going into cardiac arrest. Doctor decides to begin CPR, as is often the case the patient aspirates during the procedure > (A20) *butyric acid* (vomit aroma-- 500ppm)

S23 -- Patient is loaded onto a gurney and doors of the ambulance open and patient loaded on with doctor climbing on board > (A21) *heliotropin* (odor of cleaning solutions associated with sterile environments like hospitals etc.)

S24 -- Doors close on the ambulance. Text on screen: To be Continued.

End of Video

Discussion

If the video and aroma concepts are produced correctly, the video will demonstrate the positive effect of aroma when coupled with video. But to drive home the point that not much is known about the olfaction of medical/surgical environs, the video ends with the words "To Be Continued" rather than "The End". We feel this will drive home the point that the idea of aroma-sustained virtual reality is a good and exciting concept but one that needs a lot of development to make a reality. Our group feels that this type of ending could be an effective lead-in to discussions including prospective project supporters, developers, and of course, funders.

II. Executing the Concept: Is it Feasible?

It is important to note that the aromas that would be delivered in the aforementioned video were the result of many years of research by food scientists throughout the world. Their efforts to isolate the

trace active aroma constituents in the complex matrices of natural foods took generous amounts of time, effort and of course, money. In addition, the chemicals listed were only the major character compound for each of these foods. There are many lesser compounds that add the complexity and a three dimensional nature to real food aromas. Considering that, the challenge of capturing, isolating, and identifying the multitude of smells associated with surgical/medical procedures is better understood. There are many questions to consider. For example:

How do we isolate, capture , concentrate, and identify the important components in an odor event of interest?

Odor compounds are usually present in quite minuscule amounts (ppb to low ppm levels) when compared to other naturally (or unnaturally) occurring compounds in any given environment. Samples may contain many scores of compounds of which only a handful have any odor at the levels they are present. Allowing that we are able to gather enough sample from the airspace to do this analysis (of course there are also issues of accessibility to surgical settings, bureaucratic and ethical red tape, insurance issues etc.), it will be necessary to do extensive bioassay work to determine the most important characterizing candidate compounds. Capturing enough of these airborne volatiles to do an effective analysis will be a challenge although recent introduction of Solid Phase Micro Extraction (SPME) technology which provides a portable and cost effective method of sampling for airborne volatiles. Once samples are collected, bioassay work will be necessary to begin the process of identifying the major character impact compound(s) in a given sample. This bioassay will likely entail use of Gas Chromatography/Olfactometry (GCO), a system that employs feedback from human "sniffers" and sorts through a mixture of odor compounds in a sample and rates their odor potencies. Identification of unknowns and verification of known odor compounds will depend on good GC/MS (Mass Spectrometry) and high quality mass spectral libraries for data interpretation. In addition, it may be necessary to employ Nuclear Magnetic Resonance (NMR) to verify identifications done via GC/MS .

Another possible source of information will come from literature searches carried out using the multiplicity of medical research sources available. It may be possible to gather some useful

information on research already done on certain organs which may act as guides as we try to identify odor active agents.

Once identified, how do we find a source of the compound or how to synthesize it?

It is likely that compounds we will identify are not commercially available for purchase. Those compounds not available will need to be synthesized. This can be a tricky and/or expensive proposition. One resource is to look for a commercially available analogue or closely related species of chemical and determine its acceptability as a substitute. If there is not an acceptable alternative, it will be necessary to contact a commercial synthetic laboratory and investigate the feasibility of synthesizing the target compound(s).

How do we set the intensity levels of odors to match those found in a real situation?

One of the real challenges in re-creating an aroma profile in a virtual reality type setting would be the fact that there is huge variation in the abilities of average people to smell. The actual variation can be measured in orders of several magnitudes where one person will have one hundred times more sensitivity to a compound than another person. The challenge will be to deliver doses of odor that are detectable to a wide range of subjects but don't lose their authentic character due to over-dose saturation.

What type of delivery system would be appropriate?

We are not aware of any specific delivery systems in use at this time. One of our staff has seen a system used by Toyota which delivers a stream of air through a manifold system and delivers it to an outlet on the headrest of the chair to the front of the subject. This was found to be an effective method of delivery in a room with multiple stations. The issues here are precise delivery and a system that moves the odor through without leaving trailing "ghosts" of odor behind to contaminate the next odorant. Special care must be taken to ensure the use of non-odorabsorptive materials in the hardware of the system.

Will it be possible to produce aroma that demonstrates a gradient or very subtle change in odor from one part of a surgery to another?

Such a subtle action will be very difficult, although not impossible to achieve. The best way to achieve this would be by changing delivery levels of an aroma. Effectively delivering odors showing minor differences will prove challenging due to differing acuity levels and saturation and acclimatization factors.

Summary of Technical Issues

To summarize, we see the challenges to be faced in producing aroma enhanced virtual reality in a surgical/medical setting to be the following:

Challenge #1

Devising a system to capture the odor events as they happen in the surgical environment.

This could mean using SPME devices in and around surgeries of various types and performing bioassays to identify the odor-active components. The challenge will be to get the right sample from the right place at the right time and to get enough of the volatile compounds in the short time available to collect the sample to do an effective bioassay. Currently, the SPME system is effective for gathering a fairly wide range of compounds from an airspace. However, it has not to our knowledge been adapted for the dilution analysis techniques of bioassays like CharmAnalysis. Since the SPME system is an equilibrium-based collection method, it is not especially well suited for a dilution-based bioassay. It appears that a method employing the split injection mode of the gas chromatograph injector would have to be developed to make this technology compatible with a dilution-based bioassay such as CharmAnalysis.

Challenge #2

Identifying trace level odorants determined by CharmAnalysis or some similar bioassay using GC/MS, NMR, or some combination of similar analytical tools.

Most odorants are present at trace levels therefore identifying them for use in an aroma delivery system will be labor intensive. For many compounds the human nose is more sensitive than the instruments we have to measure them. The Charm bioassay may be able to tell us where to look for answers on a GC/MS chromatogram but it does not provide structural information. Often in areas where odor is detected by charm, the GC/MS will detect nothing thus making compound identification difficult or impossible. The challenge thus will be to collect enough of the trace level odor-active compounds to be identifiable using standard analytical tools available. The SPME technology is unproven but promising in this regard.

Challenge #3

Identifying and reproducing subtle odor changes as they occur.

If the task in virtual reality is to reproduce odors of very different types and intensities, the goal is more achievable. If the goal is for doing this with very subtle changes that are occurring, the task is much more formidable. Subtle changes in odor character can be very difficult to detect instrumentally and thus may be difficult to reproduce.

Challenge #4

Delivery of odor compounds to the subject.

The goal here will be to construct a system that will deliver packets of aroma at the correct intensities in an appropriately humidified airstream with no carryover from previously delivered odors. The system will require some type of manifold delivery design with digital feedback etc. to accomodate the interactive elements of virtual reality where the subject is allowed to make free choices in his movements and activities.

III. Conclusions

Based on our discussions, challenges 1-3 (above) are formidable but for the most part should be achievable with the right amount of research support. Challenge #4 should not prove to be an obstacle since elements of this type of odor delivery system are already in use at exhibits around the world. One of those systems could be adapted for your purposes.

Overall, the largest stumbling block for the surgical/medical application of aroma enhanced virtual reality will probably be the quality of the delivered smells. The necessary level of authenticity of the delivered odors will determine how much effort needs to be expended to achieve the goal of an aroma enhanced virtual surgical/medical reality system. It may well be that the odors which you will be dealing with are intense and will be more easily identifiable than we currently imagine. It really becomes more of a matter of scope. If the goal is to provide odors associated with antiseptics and gross bodily functions such as body odor, bowel, urine etc. then the current knowledge exists to achieve this relatively easily and inexpensively. However if the aim is to reproduce other more subtle and obscure odors associated with surgery, the playing field changes shape a bit. As food scientists we do not have the requisite experience with surgical/medical odors to make a definitive statement as to the true feasibility or cost of effort that will be necessary to produce authentic surgical aromas. However, based on our experience with identifying food flavors and aromas the challenge of identifying odors produced by human organs during surgery may be the biggest challenge confronting developers of an aroma enhanced virtual surgery/medical reality system.

Amos Turk, Ph. D.

CONSULTING CHEMIST

7 TARRYWILE LAKE ROAD / DANBURY, CONNECTICUT 06810

(203) 748-6067

June 15, 1998

To: Virtual Reality Corp.
Box 786
Vernon, CT 06066

Simulated Odors: Methods and Possibilities

Introduction

Conceptually, it is attractive to think of the simulation task as comprising analysis, reconstitution, and delivery at an appropriate concentration.

An alternative, perhaps easier, approach would be the selection of a reference odorant to "stand for" the real odorant and be accepted as such. I will discuss the pros and cons, as well as the history, of both approaches.

This report will also deal with the task of removal of odorants by ventilation or other methods.

I will also discuss some of the odorants of specific interest to you.

Analysis and reconstitution: single-component* odorants

The task would seem to be easiest for odorants such as ammonia, hydrogen sulfide, vanillin, isovaleric acid (for body odor), and the like. There are two caveats here: Is your "single-component" substance compromised by impurities, and does it smell like the "real" odor you are simulating?

*I prefer the terms "single-component" and "multi-component" to "simple" and "complex," which have different chemical meanings.

Impurity is a problem when the contaminants have different and stronger odors than the major component. So if you wanted the odorant to be pure n-octane, and it were actually contaminated with the other 17 octanes (I've smelled them all), it would make little difference, because they all have mild, paraffinic odors. If the substance of interest has a very strong odor, and the impurity does not, there may be no problem, as would be the case, for example, with a sulfide contaminated with a paraffin. But my experience with n-octyl benzene, which I selected as a reference odorant for the "oily" note of diesel fuel, (as I discussed with you by phone) included a batch that had another strong non-oily odor. I traced this to a different synthesis batch, but the nature of the difference was never disclosed. Another, chemically more interesting, example was on the occasion of a NATO-sponsored Summer School on research methods in odor perception, which involved working with mixtures of acetophenone and eugenol. A study of the presumably pure acetophenone (Turk and Turk, 1975) showed that it was contaminated, and that the impurity seriously changed the odor quality.

What should be done to avoid such difficulties? It is easy to demand "pure" materials, but that is not always reliable, and extensive analysis and purification (as by zone-refining) is not generally feasible. My suggestion is first, of course, to obtain the most reliable "pure" sample available, then to sequester an ample supply of it as a reference against which to

match later batches. Ideally, the base supply should be stored under refrigeration, preferably in separate sealed ampoules, but do the best you can.

Next question is, "Does your pure odorant smell like the real odor you are simulating?" Sometimes it does. For example, isovaleric acid is said to smell like human body odor, and especially foot odor. In a recent legal dispute regarding commercial foot deodorizing products, both sides agreed that control of isovaleric acid odor was a fair basis for comparison. And some years ago, when my wife and I were hiking alone in Glacier National Park, we smelled body odor. We traced it to some withered valerian flowers along the trail. (Many common chemical names are of botanical origin.)

Sometimes it's close enough. For example, dimethyl sulfide would be a good standard to represent the odor from a pulp mill, even though it is only one of 23 identified from such a source (Himberg et al., 1987), because it is a major component and would not be overwhelmed by other more highly odorous or very different odor notes.

Analysis and reconstitution: multiple-component odorants

A frequent recommendation is to use GC-MS analysis to identify the components, then to reconstitute the mixture from a supply of pure odorants. Obviously, only the odor-relevant components would be needed, so these would have to be identified -- possibly by sniffing the exit stream from the chromatograph. Is such an approach ever successful? From my knowledge--

rarely, and only with considerable effort. One successful effort was by Roy Teranishi, a chemist with the U.S. Dep't of Agriculture, who was able, after much effort, to reconstitute the flavor of green apple essence with three odor-relevant components. (I do not have the reference, but it could be searched. He told me that his boss asked him why he had to analyze for all those other non-odorous components.) But when a substance undergoes partial decomposition or other conversion, as by cooking, scorching, smoldering, burning, exploding, putrefaction, or fermentation, the product practically always is much more odorous and has more components, often a great many more. These are the mixtures that have more interesting odors and are much more difficult, often hopelessly so, to reconstitute. I know of no instance where such a reconstituted odor is indistinguishable from the original. The task is further complicated by the circumstances under which the real odorant is sensed: (1) The substance may be in more than one state, such as vapor, liquid droplet, solid particle, dissolved in the liquid, or adsorbed on the particle. (2) The substance may be unstable or otherwise reactive, so that the reconstituted mixture, even if representative, may be difficult to preserve.

Reference odorants

It would be convenient if you could represent a real odor by a known substance, either a pure material or a mixture of a few components, that was stable and reproducible. But what if it didn't smell right? The history of the so-called "Turk diesel

odor kit" is worth summarizing in this regard.

The increasing awareness in the 1960s of odors as an air pollution problem led the petroleum and diesel engine industries to focus their attention on diesel exhaust odors. It was recognized that a method of measuring these odors had to be devised before control techniques could be evaluated. Early attempts to use category scales of perceived intensity (weak, moderate, strong, etc) were unsatisfactory: they did not yield reproducible results and did not address the different "qualities" of the exhaust odors. I suggested that an overall reference standard be developed that would serve to anchor different intensities of diesel exhaust odor, and that the various "qualities" of the odor be referenced by individual standards (Turk, 1970). The number of such quality standards was limited by the sensory capacity of judges to distinguish among them. Perfumers, despite their reputations, cannot factor out hundreds of odor notes in a mixture -- they usually work with multiple paired comparisons. I concluded, after tests and interviews, that a workable number of different sensory odor qualities was four. The next task was to define and make up the separate quality standards and the overall "diesel odor" standard. We smelled diesel exhaust under different conditions of engine operation (idling, cruising, acceleration, and deceleration) and prepared concentrates of them. We also identified the most commonly described qualities of diesel odor as burnt/smoky, oily, pungent/acid, and aldehydic/aromatic. The

only single-component quality selected was n-octyl benzene for the oily standard. The overall diesel odor standard consisted of a mixture of three of the quality standards. Each of the quality reference standards was compounded in four different dilutions, and the overall diesel standard in 12 dilutions, making a "kit" of 16 + 12, or 28 standards in the kit.

How well did the kits serve? They were used in extensive studies by Southwest Research Institute and by various manufacturers of diesel engines and fuels. No one thought the diesel standard smelled just like diesel exhaust, but none of the test groups had any difficulty in relating the standard to the real thing. The quality standards were also very useful in distinguishing between odors from different fuels and different modes of operation. Shortly after this work, I was asked by the City of New York to evaluate the effect on the odor from its diesel buses of using a catalytic converter offered by a supplier. Our results, obtained with the aid^{of} my odor panel and the diesel kit, showed clearly that the converter would reduce the overall diesel odor intensity and the burnt quality of its odor, but would increase the perceived pungency. I recommended it not be used, and the City rejected it.

What do these findings imply for your "virtual reality" objectives? In my opinion, subjects can comfortably associate an artificially simulated standard with a real odor if the simulation is not too far-fetched and is not otherwise strongly reminiscent of a different familiar odor. The latter point is

important. For the "oily" quality of diesel exhaust I could have selected linseed oil, or olive oil, for example. But these are too familiar, and it would be difficult to reassociate them with another odor. N-octyl benzene is not familiar, so no transfer had to be made, and there was no problem with the new association. Similarly, I would not use burnt meat for the burnt diesel odor quality, etc.

The ease of sensory association of different odor qualities for the purpose of testing was taken a step further with the development of the butanol odor standard (Moskowitz et al., 1974). This standard is now the basis for an A.S.T.M. method and is widely used. Judges have no difficulty in rating the perceived intensity of an odor with the intensity of a butanol-air mixture. Dravnieks' (1985) compendium of odor quality profiles offers a tempting approach to selecting "virtual" odor standards. I think you should have a copy, and it may be a moderately helpful guide, but its value is limited and much of the data will be confusing.

My recommendation on odor simulation

It would be very helpful if reference odors that do not duplicate the real ones would work for you. They do work for odor measurement, and for gas odorization (Cain and Turk, 1985), but no one has tested them for your application. You should do such testing. If they are accepted, you will be blessed. You would then be able to make and store a supply from which aliquots could be selected as needed.

Dissemination and removal

The dissemination options include scratch-and-sniff, permeation tubes (for a steady dose), and diffusion through a capillary. I am not familiar with the mechanics of your systems, but these or other methods could be tested.

Removal may be by ventilation or activated carbon adsorption. The latter method is very rapid, once the vapors reach the carbon, but the changes of vapor concentration with time in a space are subject to the constraints of chamber volume, mixing efficiency, and air flow rate (Turk, 1963 -- the photo was old even then -- and 1968).

Your statement of work

Diesel and gasoline

Diesel fuel can be readily simulated as per the reprint enclosed, with the caveats regarding reproducibility as discussed above. Toxicity is very low for intermittent and occasional exposure. Gasoline, now often referred to as BTEX (for benzene, toluene, ethylbenzene, and xylene) contains these components as well as the mostly C₇ and C₈ paraffins, olefins, and alicyclics, and MTBE (methyl-t-butylether). Most people don't have much occasion to smell gasoline now, with the new recycling hoses at filling stations, so a reasonable hydrocarbon simulation at low toxicity should not be difficult to do. It should be easy to make 100 mL or more of each. Particulate matter is irrelevant here, because odor exposure is only to vapors.

Lubricating oil

Not difficult to simulate, but the odor is mild unless the oil is hot. Simulating hot oil at ambient temperature could be tricky, but I believe it could be done.

Explosives

Mild odor from TNT mostly from undernitrated toluene and some oxidation by the nitric acid, which does more than nitrate the toluene. The "red water" effluent from TNT manufacture contains some of these by-products. Also some sulfur notes from the reduced H_2SO_4 in the mixed acid. RDX and HMX are white crystals, practically odorless. Nitroglycerin and particularly EGDN (ethylene glycol dinitrate), both in dynamite, can be smelled by dogs, but not much by people. Ammonium nitrate is a crystalline salt -- no odor.

It's different when they explode, of course. The resulting aerosols include particles from the blasted surroundings, as well as from the explosives themselves. Depending on their experiences, people associate these odors with battle, accidents, demolition, or fireworks. They could be simulated to some degree, but not from the real thing. I think it could be done.

Other forms of combustion

Combustion of substances containing carbon and hydrogen always presents a toxicity problem because the oxygen reacts preferentially with the hydrogen, increasing the C-to-H ratio, which leads to the formation of benzenoid and ultimately the carcinogenic polycyclic aromatic hydrocarbons. But one doesn't

have to go that far to get a burnt odor. I did use oil of cade (Juniper tar) for the diesel burnt note, but that may have been pushing it a bit too far toward toxicity. Caramelized odors are on the early chemical pathway to tarry and then burnt odors, and they may be reasonable substances to use. There are also synthetic hickory-type odorants for barbecue applications, and it would be good to check these out.

For burning plastic and insulation, it is essential to avoid any source that contains chlorine in any form, because combustion of such materials always leads to at least some dioxins and furan derivatives, which are toxic. Polyvinyl chloride depolymerizes to vinyl chloride, a known carcinogen. The acridity of these odors can be simulated by other reference compounds.

I don't have experience with odors associated with surgical processes, but I would want to check first to establish how much of the sensory impact in such environments comes from the anesthetics, and how much from the sterilizing and cleaning compounds. Cauterization gives a burning flesh odor. Have these effects in hospital environments been established?

Conclusion

I think the chances are fairly good, but by no means certain, that your objectives can be accomplished at reasonable cost. It would be prudent to carry out some of the preliminary tests I have suggested before large investments of money and effort are committed.


Amos Turk

Non-odor aspects

The generation of aerosols such as those that accompany diesel exhaust would add, in my opinion, an unnecessary complication, especially at the outset, when there will otherwise be complications enough. Remember, diesel engines are not necessarily smoky, and should not be when they are well tuned. Explosions and uncontrolled fires from organic matter are always smoky, and range from white to black, depending on moisture and carbon contents. If smoke is to be simulated, white is preferable to black, which generally includes toxins. Hold it for later.

The role of moisture is interesting and not generally understood. Tests conducted years ago at the then Cleveland labs of ASHVE (predecessor of ASHRAE) showed that, other things being equal, atmospheric humidity tends to decrease odor intensity, but that things are rarely equal. Much more common is the effect that moisture has on displacing adsorbed odors from furnishings, coatings, and other materials, so that intensity actually rises when humidity does.

References

Cain and Turk (1985), "Smell of Danger: An Analysis of LP-Gas Odorization," Am. Ind. Hyg. Ass. J. (46) -- copy included.

Dravnieks (1985), "Atlas of Odor Quality Profiles," A.S.T.M. Data Series DS 61 -- sample pp included.

Himberg et al., (1987) Atm. Environ. 7, 1671.

Moskowitz, Dravnieks, Cain, and Turk, (1974), "Standardized Procedure for Measuring Odor Intensity" Chem. Senses & Flavor 1, 235.

Turk (1963), "Measurements of Odorous Vapors in Test Chambers: Theoretical," ASHRAE J. -- copy included.

Turk (1968), "Concentration of Odorous Vapors in Test Chambers," in ASTM STP 433 -- copy included.

Turk et al., (1970) "Sensory Evaluation of Diesel Exhaust Odors," National Air Pollution Control Admin. Publ. # AP-60 -- copy included.

Design of an Optical Orientation Sensor

1. System Specifications

(Discussed with Myron Krueger ; Formalized by Jannick Rolland)

Given a 40 feet square room with Light Emitting Diodes (LEDs) at various locations (e.g. on the head of a person), design an optical system that can measure the orientation in azimuth and elevation of an LED in the field of view (FOV) of the optical system. Moreover, as a special requirement the system must be designed to use a linear detector array (1D) instead of a two dimensional (2D) array. Cost, speed, and resolution are issues in favor of a 1D array. Finally, the optical system will preferably be able to image a 90 degree FOV horizontally and a 20 degree FOV vertically while the same optical system should be used if possible whether the 1D array is positioned horizontally or vertically. The final FOV and ratio of the x-component to the y-component should be specified taking into account a required resolution for the overall system.

- The 1D detector array will be a 6K DALSA sensor with 10 μm pixels (see attached documentation)
- The source will be a high-power GaAlAs illuminator (model OD-100) with a peak emission of 880 nm; the spectral characteristic at 20% spectral output is about 150 nm (810nm-960nm) (see attached documentation). The physical size of the LED source is 1 mm x 1mm. The radiant intensity of the source depends on its mode of operation, continuous or pulsed. The lower bound will be used in the calculation of the SNR in the last section of this report. LED model OD-666 was originally chosen and this study influenced the decision to work with the OD-100 model which has a smaller source area.

2. Overall Design Approach

Such specifications can be achieved using a double stage anamorphic optical system.¹ The first stage will consist of an anamorphic *fish-eye lens* which will allow imaging of a 90 degree x 20 degree FOV onto a square virtual detector array also known as an intermediary image plane. No real detector is needed here since the image will be used by the second stage and only a final detector is required. The second stage will be an anamorphical imaging system that will map the square intermediary image onto a 1D linear CCD array.

Two questions arose:

- Can a fish-eye lens be designed to be anamorphic ? (a novel approach is presented)
- Will such a mapping allow enough light collection from one LED on the 1D CCD array?
(Radiometry calculations indicate that the S/N ratio is >1 in all cases considered)

This report discusses the optical system design approach to the overall system (section 3 and 4), the resolution and field of view tradeoff (section 5), the impact of the size of the image of the

¹ Anamorphic here means that the optical system yields different magnifications in the two orthogonal x and y directions. An anamorphic system usually requires cylindrical optics of one sort or another.

LED on detection (section 6), and presents the light collection calculations for feasibility of the system (section 7). This report does not include the final lens design; It includes, however, some preliminary optimization of the anamorphic fisheye lens.

The study reported here focuses on demonstration of feasibility. We show a case study assuming a 80 degree FOV in x and a 20 degree FOV in y. There is no fundamental limit to go from 80 to 90 degree FOV, only more complex optics is usually required as the FOV increases for a given image quality. The 80 degree was chosen for this feasibility study because the fisheye lens chosen as a starting point and shown in section 3 was optimized up to ± 43.5 degrees. Increasing the FOV by only a couple of degrees at such wide angles is significant and not necessary in completing this first phase of the study. To insure that all rays were imaged with high quality as a starting point, we decided to select an 80 degree FOV (± 40.0 degrees) in x. Because only 4 cameras covering 90 degree each and placed at the corners of a room would be ideal for the application at hand, the FOV in the final system will be increased from 80 to 90 degree in one dimension. In the other dimension, while 20 degree would yield higher precision of tracking, a larger FOV may be beneficial to cover a larger tracking volume (e.g. including height of children's head instead of essentially adults). Some considerations of the trade-off between the application requirement and the engineering requirements still need to be made. The engineering requirements are given here.

3. Design of an Anamorphic Fisheye Lens

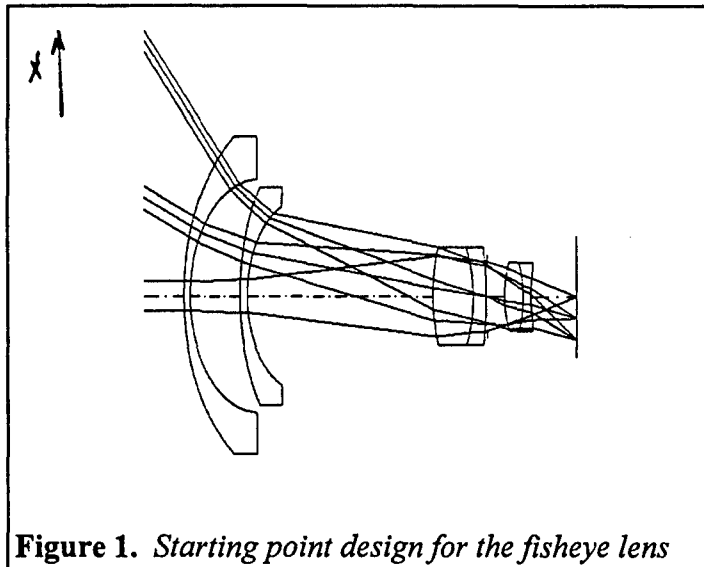


Figure 1. Starting point design for the fisheye lens

The starting point for the design was chosen to be that of a fisheye lens that we carried out a few years ago for the design of miniature video cameras for a video see-through head-mounted display (Edwards, Rolland, and Keller, 1995). This lens consisted of two single front meniscus lenses and two doublet lenses close to the aperture stop of the system as shown in Figure 1. This lens will need to be scaled to the proper focal length for the design of the proposed system.

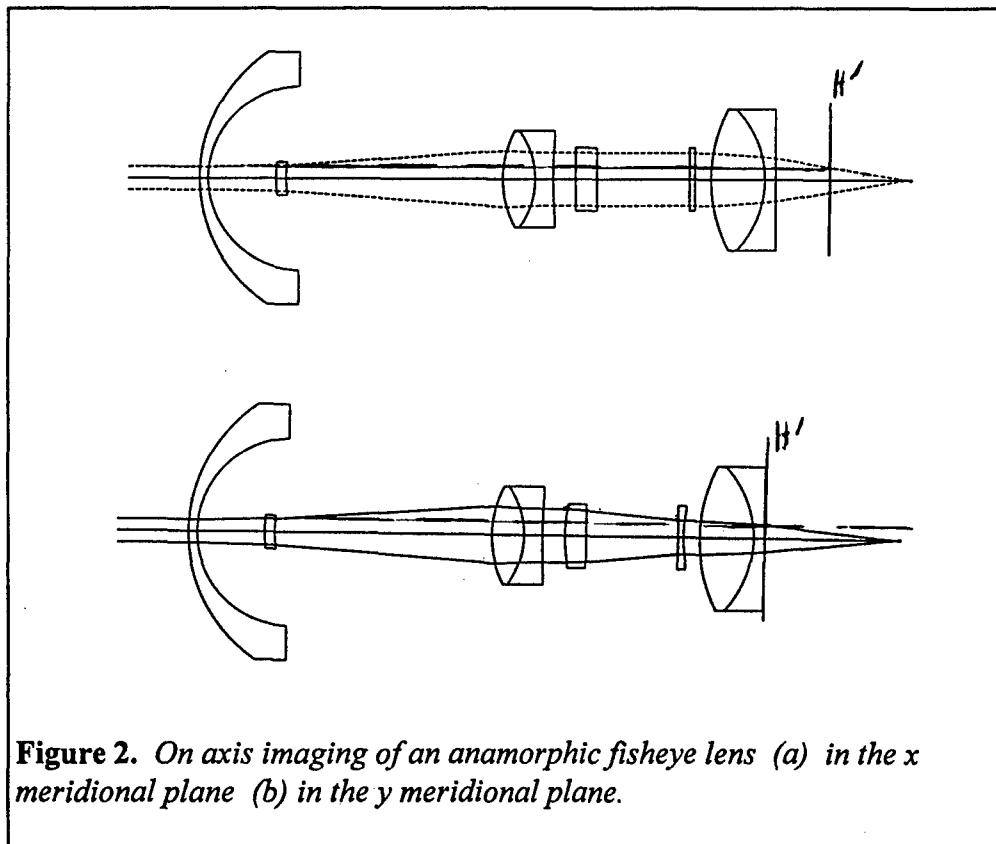


Figure 2. On axis imaging of an anamorphic fisheye lens (a) in the x meridional plane (b) in the y meridional plane.

We demonstrate here that a fisheye lens can be made anamorphic by insertion of an *anamorphic focal attachment* located appropriately within the system. The attachment, in this case, is positioned between the two doublets as shown in Figures 2a and 2b which show the imaging of a point on axis through the *anamorphic fisheye* lens for an x and y meridional plan, respectively.

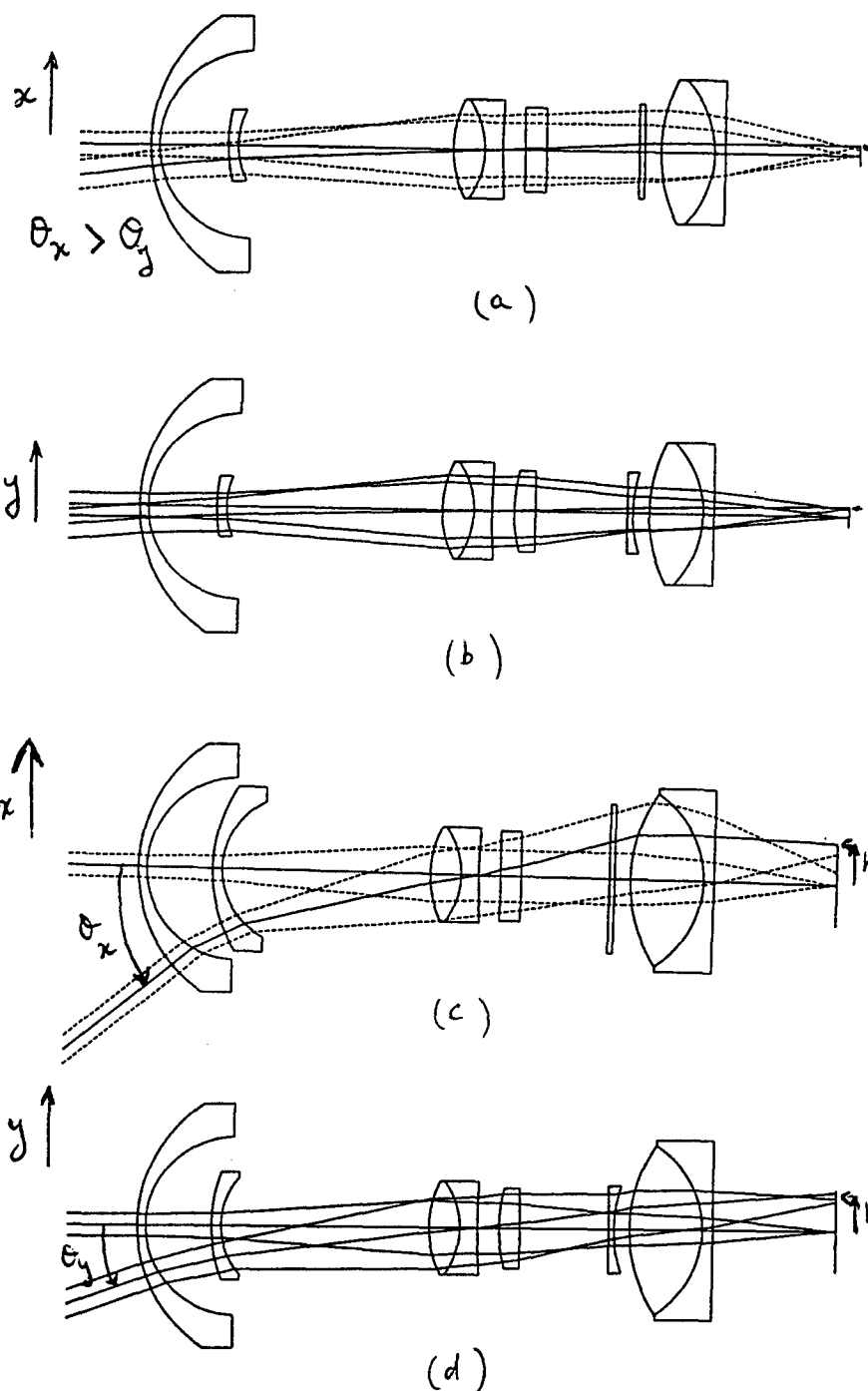


Figure 3. Off-axis imaging of the anamorphic fisheye lens. (a) and (b) correspond to a small field of view, while (b) and (c) correspond to a large FOV before optimization ; (a) $FOV(x) = 15.7$ degree ; (b) $FOV(y) = 10.0$ degree ; (c) $FOV(x) \cong 87$ degree ; (d) $FOV(y) \cong 55$ degree.

Figure 3 show the imaging of the anamorphic fisheye lens for a point off-axis but close to the axis (small field of view) (a) and (b) and a point further off-axis (c) and (d). No attempt to optimize the lens was conducted at this point in time. These figures are only meant to illustrate feasibility of a fisheye lens with anamorphic properties.

While the field of view is larger in x than in y, the image of the field of view by the fisheye is square. This image will be fed to the next stage of the optical system.

At this stage of feasibility, no attempt was made to match the ratio of the x and y field of views to required values. Proper scaling will be done at a later stage of the design when all optical quantities have been determined. We now have

demonstrated that we can transform a fisheye lens into an anamorphic fisheye lens where two

different field of views in x and y will be mapped on a square intermediary image. Latter in this report we shall calculate the specification parameters of the overall system. These parameter will be used to scale the fisheye lens appropriately. The anamorphic lens will be designed to be part of the scaled fisheye lens and the anamorphic fisheye lens will then be optimized for satisfactory performance which will be discussed in section 5.

The next stage of the design is to take the square intermediary image and image it on a linear array. Another anamorphic imaging system is needed.

4. Anamorphic Lens From The Output Of The Fisheye Lens To The CCD Array.

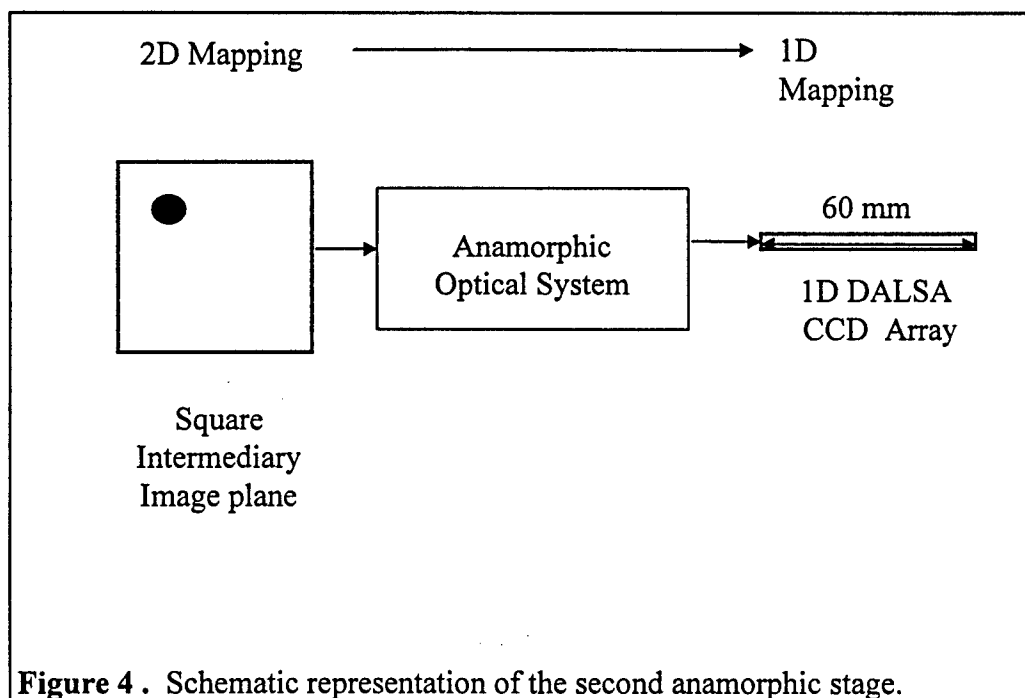


Figure 4 . Schematic representation of the second anamorphic stage.

Such a mapping as illustrated above is quite unusual in optical systems. The rationale for such a mapping is to be able to use a 1D linear array sensor. A first order layout of a system which would allow such a mapping is given in Figures 5a and 5b. The idea is to create an astigmatic image (property that one usually strives to eliminate). This can be accomplished using cylindrical optic in a specific assembly. In a first order calculation one requires only two positive cylindrical lenses satisfying EFL_2 or F_2 equal $2 EFL_3$ or $2 F_3$ where EFL of F denotes the focal length and 2 and 3 refer to Lens 2 and Lens 3 shown as L2 and L3 in Figure 5.

The image plane of the fisheye lens (also referred to as the intermediary image plane) is located at the anti-nodal points (i.e. twice the focal length) of Lens 3². At the anti-nodal point image of Lens 3 is an image of the x-dimension of the intermediary image plane. The magnification is -1

² Antinodal points in optical systems are defined as the optical conjugates of angular magnification -1, which also correspond to a linear magnification of -1. They often present interesting properties of symmetry for imaging.

so the size of the detector sets the overall dimension of the system. The detector has 6000 pixels of 10 μm x 10 μm , thus it is 60 mm long (see Figure 5a). The image plane of the fisheye lens is also located at the focal point of Lens 2 and is therefore imaged to infinity after Lens 2 in Figure 5b. Lens 3 in Figure 5b, is equivalent to a plane parallel plate. In the focal plane image of Lens 2 is an image of the exit pupil from the fisheye lens. The height h of the exit pupil is given by

$$h = \frac{\text{EFL}_2}{\text{EFL}_1} \rho_i,$$

where EFL1 and EFL2 are the focal lengths of Lens 1 and Lens 2, respectively; ρ_i is the height of the exit pupil of the fisheye lens. Knowing the height h of the "exit pupil" at the final image plane (i.e. the detector plane) will be useful in the calculation of energy reaching each pixel at the detector plane. We will also have to consider the width of the line due to the finite size of the LED.

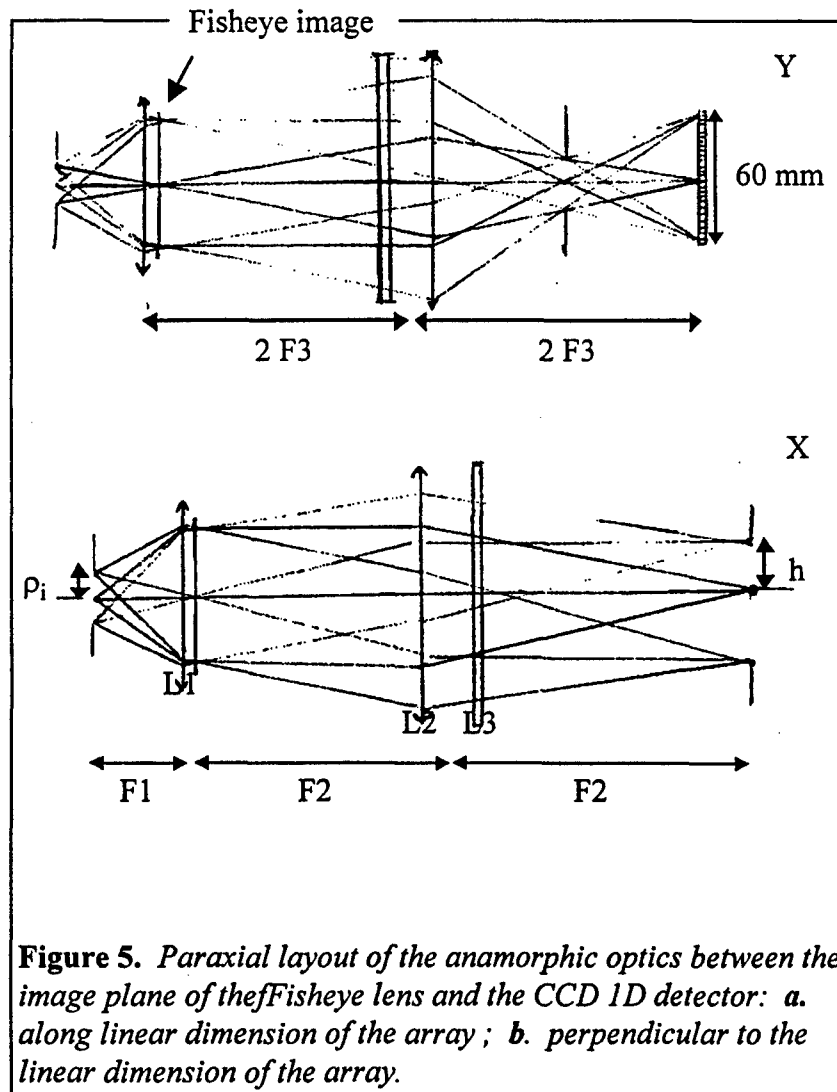


Figure 5. Paraxial layout of the anamorphic optics between the image plane of the fisheye lens and the CCD 1D detector: a. along linear dimension of the array; b. perpendicular to the linear dimension of the array.

Given the size of the detector we know that the image size of the intermediary image plane is 60 x 60 mm. This allows specification of the focal length of the fisheye lens given the FOVs to be imaged.

For $\text{FOV}_x = \pm 40$ degrees and $\text{FOV}_y = \pm 10$ degrees we can calculate the focal lengths EFL_x and EFL_y of the fisheye lens ($y_i = 30$ mm).

$$\text{EFL}_x = \frac{y}{\theta_x} = 42.97 \text{ mm}$$

$$\text{EFL}_y = \frac{y}{\theta_y} = 171.89 \text{ mm}$$

(Fisheye lens specification)

Note: want a linear mapping so use θ in rad.

Given a FOV_x equal to four times FOV_y, the magnifying power MP of the afocal, anamorphic attachment is 4 and the ratio of the aperture stop of the fisheye lens to that of its image through the afocal attachment is 4 as well. A paraxial raytrace gives the values of 34.75 mm and 8.70 mm for the height of the marginal ray at surface 8 (the aperture stop) and surface 12 (the back side of the afocal attachment, respectively).

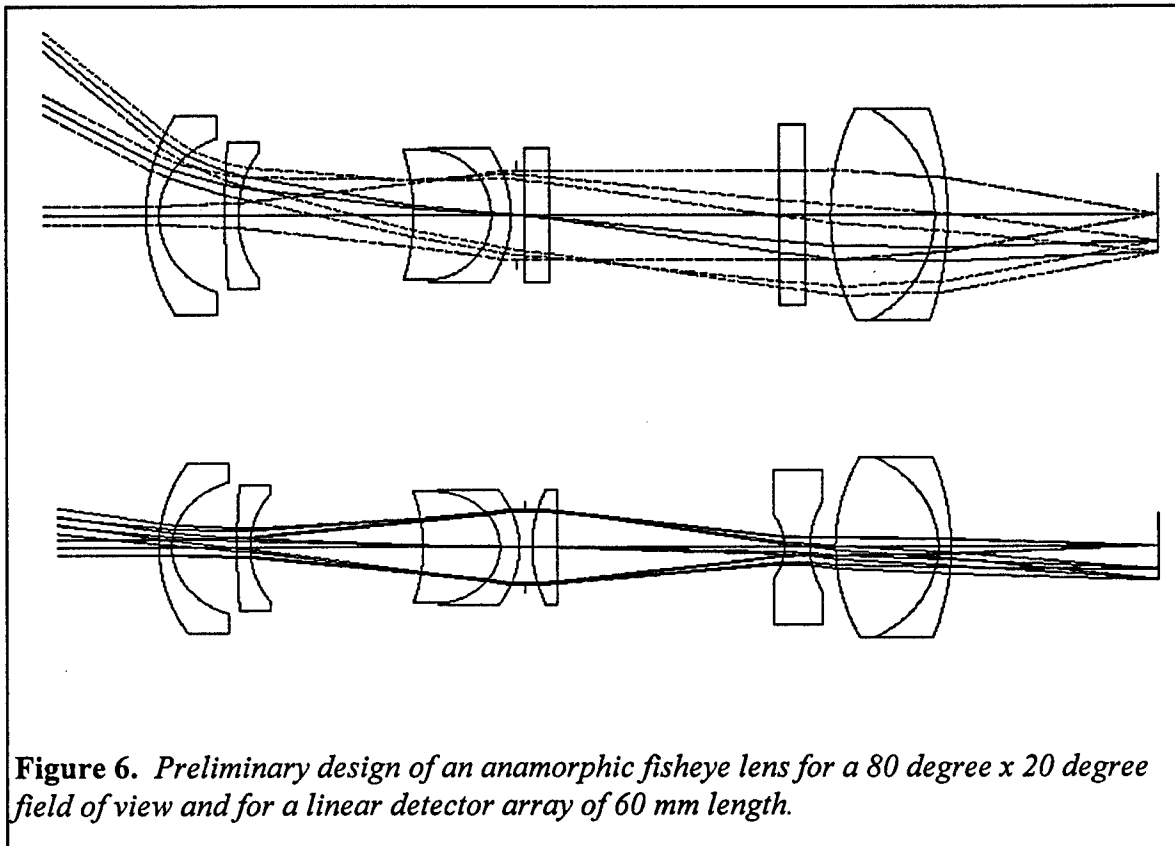


Figure 6. Preliminary design of an anamorphic fisheye lens for a 80 degree x 20 degree field of view and for a linear detector array of 60 mm length.

The lens shown in Figure 6 has been optimized to satisfy paraxial properties, such as FOV_x equals four times FOV_y. EFL_x = 42.972 mm and EFL_y = 171.887 mm (EFL stands for effective focal length). The RMS spot size at various points in the FOV are currently without full optimization : on axis: 0.22 mm ; FOV_x = 28 degree, RMS spot size = 0.35 mm ; FOV_x = 40 degree, RMS spot size = 0.61 mm ; FOV_y = 7 degree, RMS spot size = 0.45 mm ; FOV_y = 10 degree, RMS spot size = 0.80 mm. For such a system with a CCD detector where the centroid of energy needs to be extracted as accurately as possible, two important criteria are a symmetrical spot image and a uniform illumination over the image of the LED. To yield a symmetrical image, one image quality requirement will be to have no coma³. Currently, image quality is

³ Coma is one of the third-order optical aberrations in optical systems. Unlike various other aberrations, the image spot size of a system limited by coma is non symmetrical around the centroid of energy. In systems relying on the centroid of energy to locate a point in the FOV, coma should be eliminated. Other types of aberrations (e.g. spherical aberration, defocus, field curvature, astigmatism) which do not shift the centroid of energy are not as

degraded by coma and further optimization of the lens will allow to satisfy all requirements, paraxial and symmetry of the spot size. As part of the optimization, we will also aim at decreasing the RMS spot size. A 3 pixel image spot size is desirable to get good centroid estimation as also indicated in the literature on stellar tracking systems and subpixel resolution.

Given the intermediary image formed by the anamorphic fisheye lens, the next stage will image the square intermediary image onto a 1D linear CCD array. The magnification of the second stage will be one. We need to calculate the length of the astigmatic line formed on the 1D CCD array. The principle of imaging was given in Figure 5, assuming that the exit pupil is the same in x and y location for the fisheye lens. From the preliminary design of the first stage, however, we also note that the exit pupil of the anamorphic fisheye lens is located in different planes for the x and y imaging directions. This is somewhat of a complication. The solution seems to lie in observing that the location of the exit pupil for the x imaging which is currently +800 mm, can be made to be infinity (which we will do in the next stage of optimization) and that of the pupil in the y dimension is at -385 mm. So by using a cylindrical lens for Lens 1, we can put the exit pupil at infinity in both directions. Then imaging after Lens 1 resumes as illustrated in Figure 5.

Currently, in the y dimension, the diameter of the exit pupil of the fisheye is equal to 34 mm, and its distance from the intermediary image is 385 mm to the left. For the design of the second stage we shall start with a cylindrical Lens 1 of $EFL_1 = 385$ mm placed close to the intermediary image as shown Figure 5. The pupil will then be at infinity after the intermediary image for both the x and y dimension (assuming the fisheye lens images the pupil at infinity in the x dimension). Then depending whether we want to image the x or y dimension on the linear array we flip the module L2-L3 and the detector 90 degree. There is no need to have two different optical systems for the two scenario x or y imaging. If we want to image simultaneously the x and y directions, however, we may consider placing a half-silvered mirror after the intermediary image following the fisheye imaging and have in each path the same module flipped 90 degree. One linear area in each path would also be used.

Calculation of EFL of Lens 2 and 3 can be conducted based on their required diameter and assuming that lenses are open at F/2 or less for fabrication feasibility. In the thin lens approximation, the half-height H of the astigmatic line is given by

$h = \theta \cdot f_2$, where θ is given by the angle subtended by the exit pupil of the anamorphic fisheye lens (see Figure 5b). Indeed, $h_{ex} = \theta \cdot f_1$ with $f_1 = 385$ mm, and $h_{ex} = 17$ mm, then $\theta = 2.5$ degree.

Now we have $f_2 = 2 f_3$; and from the design of the first stage the angle of the marginal ray θ_m at the last surface is less or equal to 0.04 rad for the case where the pupil is far away (approx ∞). Given that the exit pupil of the fisheye is almost at infinity in that case, we can estimate the diameter of Lens 2 and Lens 3 with

critical. Spherical aberration which is constant over the FOV may be desirable to enlarge the point spread function to a 3 pixel spot size in the detector plane.

$$\phi = \text{size of the intermediary image} + 2 f_2 \cdot \theta_m = 60 + 2 \cdot f_2 \cdot 0.04 \cong 60 \text{ mm}$$

let's assume f_2 is open at $F/2$, then ϕ also equal $f_2/2$. Therefore $f_2 \cong 2\phi = 120 \text{ mm}$;
 Consequently $f_3 = f_2/2 = 60 \text{ mm}$. This yields a Lens 3 open at $F/1$, which is the maximum one would want to work with. In the design stage, depending on the required image quality, we may have to assume Lens 2 open at $F/3$ or $F/4$, which will increase the length of the optical system.

Estimated minimum lens of the optical system for a 60 mm linear detector array is

$$\text{Total Minimum Length} = \text{Fisheye lens Length} + 2 f_2 = (776+240) \text{ mm} = 1016 \text{ mm} \cong 1 \text{ m}$$

Options for decreasing the overall length are either choosing a smaller detector or decreasing the ratio of FOVx to FOVy.

The length of the line in the plane of the detector array in a direction perpendicular to the array is given by $h = (34/2) \cdot (120/385) = 5.3 \text{ mm}$ if the large field of view FOVx is imaged on the linear array. In that case, the pupil in the perpendicular dimension (along the y dimension) is what matters in terms of the length of the line perpendicularly to the array. This is relatively small. For the length of the line if the lens is used in the other direction where the small field of view (FOVy) is imaged on the linear detector array, what matters is the angle subtended by the pupil in the x direction from L2. Half the length of the line is then given by the product of the angle subtended by the pupil from L2 (estimated to be 0.17 rad) times the focal length of L2 (120 mm); the length of the line is then estimated to be 42 mm. Given these estimated values of the lines perpendicular to the array in the two configuration of imaging, a calculation of energy transfer through the system allows to estimate whether enough light will be sensed by the detector array. This is expanded in the next section.

5. Discussion of field of view and resolution trade-off

Let's assume a linear mapping of the field of view on the linear array detector. In other words, y equal $(f \cdot \theta_y)$ if the linear array is along the y dimension (respectively $x = (f \cdot \theta_x)$ if the linear array is along the x dimension). We are close to this mapping right now and will optimize the system to satisfy this mapping exactly during full system optimization.

Given a FOVx equal to 90 degree (± 45 degree), and a detector size of 60 mm (± 30 mm), this set an overall EFLx of $(30 / 0.7854)$ equal 38.22 mm. Similarly EFLy equal $(30 / 0.1745)$ 171.89 mm.

Assuming that we can resolve the centroid of energy of the detected LED within the 10 μm resolution of the detector array (subpixel resolution can in fact be achieved), the variation in angle $\Delta\theta$ corresponding to a Δy (let's say) of 10 μm is given by $\Delta\theta = \Delta y / f$, which yields $\Delta\theta_y = 0.01 / 171.89 = 0.2 \text{ arc minute}$. In the x-direction we have, $\Delta\theta_x = 0.01 / 38.22 = 0.9 \text{ arc minute}$. This simple calculation indicates that even in the worse case scenario of pixel resolution (instead of subpixel resolution), precision of tracking is fairly high (less than 1 arc minute). We

remmend that a complete analysis be carried out to determine what angular resolution is required ofr the y dimension. Overspecifying the system will increase the full design cost and perhaps the cost of the prototype as well.

6. Considerations of imaging of an "extended" light source

The imaging range for the light sources spans 1.5 m to 15 m from the optical system. At near range, the source will subtend the largest visual angle. We estimate here the size of the image of the LED at the extreme of the range. The calculation is based on a light source of physical dimension 1 mm x 1 mm (we have decided upon the OD-100 ; this calculation influenced a change from the OD-66 to that of OD-100). Given the largest dimension of 1.4 mm (the pixel diagonal), the size of the image of the LED through the optical system is summarized in the table below:

size of the image of the LED (using the 1.4 mm)	x = 1.5 m	x = 15 m
imaging of 90 degree on a 60 mm detector (f' =38.22 mm)	0.04 mm or 3.7pixel (x'=39.2 mm)	0.004 mm or 0.37 pixel (x'=38.3 mm)
imaging of 20 degree on a 60 mm detector (f' = 171.89 mm)	0.18 mm or 18 pixels (x'=194.14 mm)	0.05 mm or 1.8 pixels (x'=173.88 mm)

In the table the image size is given by $y = \theta x'$, where x' is given from first order optics principles by

$$x' = \frac{x f'}{x + f'}$$

and θ is given by the ratio of the source size 1.4 mm divided by the distance x . x is the distance of the LED to the object principal plane of the optical system and f' is the focal length in the corresponding dimension x or y . In the above formula x is negative and f' is positive.

Thus, within the working volume, the image of the LED on the detector varies from 0.37 pixel to 18 pixels. Increasing the FOV in y will help decreasing the size of the LED on the detector plane. The challenge with having a large image of the LED is to insure uniformity over the overall size for precise detection of the centroid. Also, some edge effects will have to be taken into account. If 18 pixels is too large to conserve uniformity, a larger FOV_y may be considered.

In the cases where the image is less than 3 pixels, the point spread function will be adjusted to cover at least a 3 pixel area. This will be achieved by allowing some remaining spherical aberration, aberration that yields symmetrical spot size and invariance over the FOV. Coma will be eliminated and field curvature will be minimized.

7. Flux Detection Calculations

7.1 Some fundamentals of detector devices

A detector is characterized by its responsivity $R(\lambda, f)$ where λ is the wavelength of the light and f is the electrical frequency of the modulated signal or chopping frequency. Usually manufacturers report values of R when measured with standard test sources (500K for deep infrared, 2856K for visible and near infrared are typical sources).

An important quantity is the *Noise Equivalent Power* (NEP, measured in Watts) defined as the required source power to yield a S/N ratio of 1. NEP (λ, f) as well. $NEP = \phi_e / (S/N)$; Given ϕ_e , a good detector has a high S/N ratio, therefore a low NEP. Given a detector NEP or an equivalent, and given ϕ_e , we will use this formula to derive the expression for the S/N ratio. In some case, the Noise equivalent exposure is given instead of the NEP. More on this and the relationship of NEE to NEP is given thereafter.

Also, an overriding principle is that given the integration time t_d of a pixel element (which is equal to the readout time in our case), the noise equivalent bandwidth is given by $1/2t_d$. Also the NEE scales as the square root of the noise equivalent bandwidth.

7.2 Application to the orientation sensor

This calculation first assumes that the width of the image of the LED is one pixel wide and off axis at some angle of view θ_l . The led off axis is also seen from the pupil under an apparent area. The actual width will be accounted for in the final figure of merit for the SNR. The final result will be divided by the actual spread of the source in number of pixels that is a maximum of 18 according to the calculation in Section 6.

$$\phi_{\text{pixel}} = R_v \cdot L_{\text{source}} \cdot A_{\text{source}} \cdot \Omega_{\text{lens}}$$

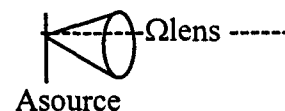
$$\Phi_{\text{pixel}} = L_s (A_s \cos \theta_s) \Omega_l = (L_s (A_s \cos \theta_s) A_l \cos \theta_l) / (x / \cos \theta_l)^2 = (L_s A_s A_l \cos^2 \theta_s) / x^2$$

where we set $\theta_s = \theta_l$ by geometry; Let's formulate the expression for the pixel-SNR based on voltage outputs:

$$V_{\text{signal}} = T \cdot \frac{1}{N} R_v \cdot \phi_{\text{pixel}} \quad (\text{from basic radiometry theory})$$

where:

- R_v is the responsivity (v refers to a voltage output)
- L_{source} is the luminance of the source in $\text{W/m}^2 \cdot \text{sr}$
- A_{source} is the area of the source (m^2) (we are assuming here the more general case of an extended source)
- Ω_{lens} (sr) is the solid angle subtended by the lens at the source
 $= A_{\text{lens}} / x^2$ on axis where x is the distance source to lens.



- N is the number of equivalent pixel elements in the astigmatic line formed in the image plane, given that the system performs point to line imaging. This factor allows taking into account the fact that energy in the line outside of the pixel detector element is lost. Still, here the width of the line is assumed to be one pixel wide.

$$\text{Thus, } V_{\text{signal}} = T \cdot R_v \cdot L_{\text{source}} \cdot A_{\text{source}} \cdot A_{\text{lens}} \cos^4 \theta_s / (Nx^2) ,$$

where $R_v \cdot L_{\text{source}} = \int_{\lambda_1}^{\lambda_2} R_v(\lambda) L(\lambda) d\lambda$ where $[\lambda_1, \lambda_2]$ represents the intersection of the source spectral range with that of the detector.

Therefore the SNR is given by

$$\text{SNR} = \frac{V_{\text{signal}}}{V_{\text{noise}}} = \frac{T \cdot R_v \cos^4 \theta L_{\text{source}} A_{\text{source}} A_{\text{lens}}}{V_{\text{noise}} Nx^2}$$

where V_{noise} is the rms noise for one pixel. Also, by definition, for one pixel $\text{NEP} = V_{\text{noise}} / R_v$

Instead of providing the NEP (W), the manufacturer specifies a quantity called NEE to denote the noise equivalent exposure in pJ/cm^2 . The NEE is related to the NEP as

$$\text{NEE} (\text{pJ}/\text{cm}^2) = \text{NEP}_a (\text{pW}/\text{cm}^2) \cdot t_d (\text{sec})$$

(NEP_a is used here for conversion units purpose)

$$\text{and NEP (pW)} = \text{NEP}_a (\text{pW}/\text{cm}^2) \cdot A_{\text{pixel}} (\text{cm}^2)$$

where A_{pixel} is the area of a pixel and t_d is the pixel integration time, in our case $3000\text{pixels}/20\text{Mhz} = 150\text{ us}$ (note: this is based on a readout time of 20Mhz and the fact that 2 pixels are read simultaneously during each readout). An important point is that the NEE is often given for a certain bandwidth, and a correction factor will need to be computed to account for the working bandwidth.

$$\text{SNR} = \frac{T \cdot t_d \cos^4 \theta L_{\text{source}} A_{\text{source}} A_{\text{lens}}}{\text{NEE} A_{\text{pixel}} Nx^2}$$

Note: the NEE is likely given for peak wavelength. We must theoretically Multiply by the ratio of the responsivity at the wavelength; the SNR decreases in proportion.

Numerical Application:

The minimum value of integration time τ_d was estimated to be 150 us. The calculation is based on a 20MHz readout time knowing that a pair of pixels is read simultaneously. Therefore, the integration time is given by $3000/20\text{MHz}$ or 150us.

NEE = 25 pJ/cm^2 according to spec sheet ; this is however for a 7.5Mhz instead of our actual 20Mhz bandwidth. 20 MHz corresponds to an integration time of 150us which yields a noise equivalent bandwidth of 3.3Khz. 7.5Mhz corresponds to an integration time of 400us which yields a noise equivalent bandwidth of 1.25KHz. So the effective NEE should be $25 \times 1.6 = 40 \text{ pJ/cm}^2$ where 1.6 is the ratio of square root of 3.3KHz to the square root of 1.25KHz.

$$A_{\text{pixel}} = 10 \text{ um} \times 10 \text{ um} = 0.001 \text{ cm} \times 0.001 \text{ cm} = 10^{-6} \text{ cm}^2$$

Radiant intensity of the source $I_e \text{ (mW/sr)} = L_{\text{source}} \text{ (mW/sr. cm}^2) \cdot A_{\text{source}} \text{ (cm}^2)$ - From the specification for the OD-100, the minimum power is 100mW. What we may be able to drive out of the LED may be higher by a factor of 2 to 5 but we will use the most pessimistic power value in the estimation of the SNR.

$$A_{\text{lens}} = \pi d^2/4 \text{ with } d=1.5 \text{ cm in our case (d is the entrance pupil size of the fisheye lens).}$$

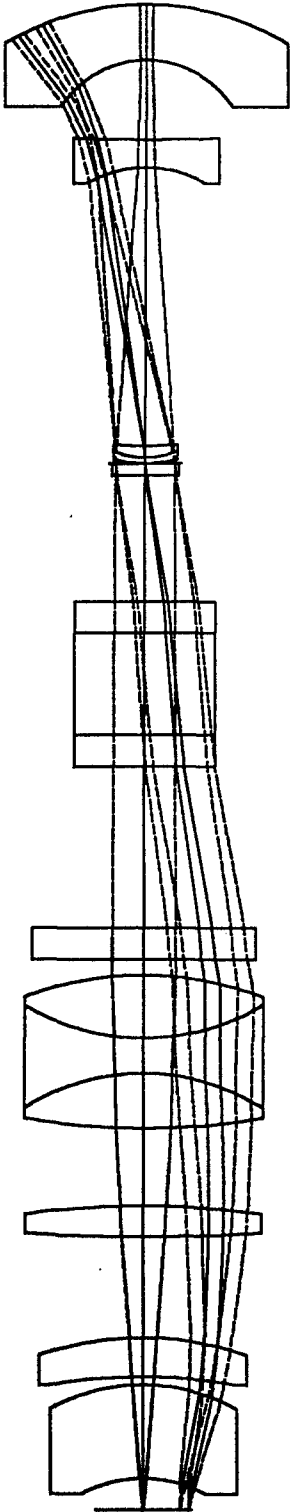
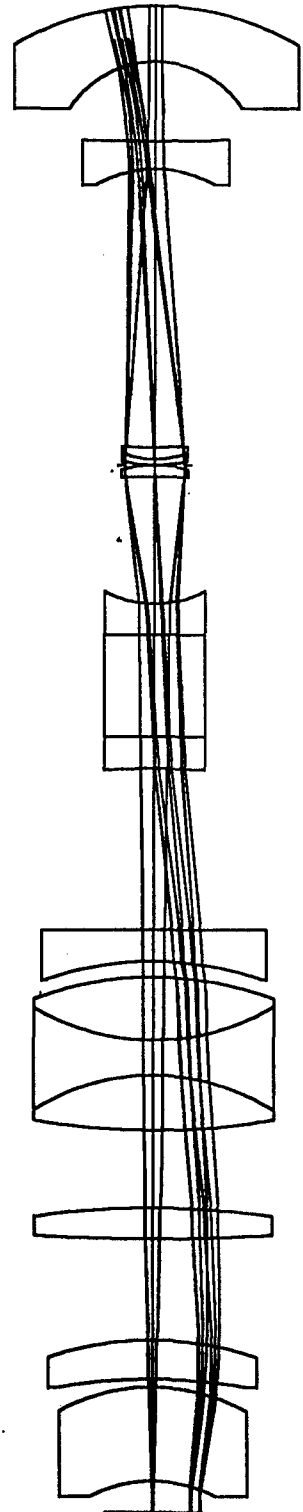
N for the x and y directions are given by (line length (um) / pixel size (um)) equal $(5300 \text{ um} / 10 \text{ um} = 530)$ and $(42\,000 \text{ um} / 10 \text{ um} = 4200)$, respectively.

In the worse case, $x = 15 \text{ m} = 1500 \text{ cm}$. For $T=1$; angle θ is zero (led on axis)

$$\text{SNR} = \frac{1}{N} 18 \cdot 10^4$$

Thus in the worse scenario where N equals 4200 equivalent pixels, the pixel-SNR is estimated to be equal to $43 \gg 1$. This assumes a pulsed source of 60mW/sr and a 150us integration time. The pulsed source may indeed be of higher intensity since we used the most pessimistic case of the power from a continuous source. In the case where the light source spread over 18 pixels, the $\text{SNR} = 43/18 = 2.4 > 1$. In a more typical case where the light source will be spread at least over 3pixels, the SNR is estimated to be around 14. In all cases considered, the $\text{SNR} > 1$.

Note: we computed SNR for various sensor DALSA IL-C8 (6000pix 10um), DALSA IL-C7 (4096 pix 7um at either 20 or 30 Mhz); EG&G (4096pix 7um 20 or 30MHz or 8192pix 7um 20Mhz); did not have the responsivity for the Sony Ilx503A 2048 pix or Kodak KLI-5001 5000pix. The SNR was found > 1 for all cases.

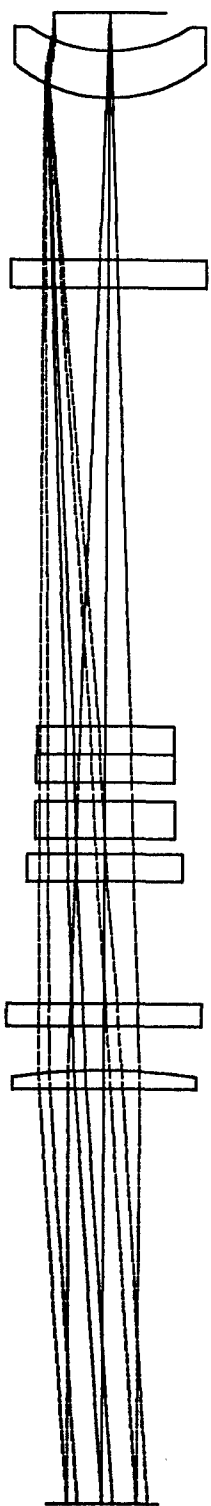
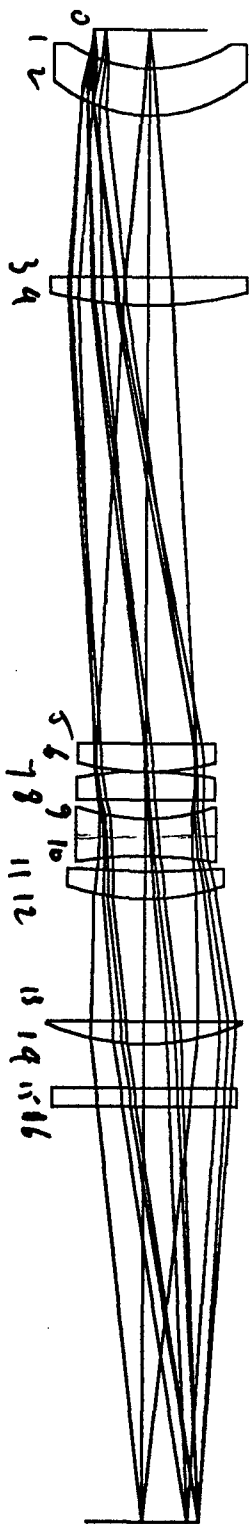


Anamorphic Fish-eye Lens System

Position: 1
Scale: 0.22

113.64 MM

XZ



96.15 MM

X2

RELAY LENS

Scale: 0.26

13-Jan-98

Technical Report of A 1:1 Anamorphic Relay Lens System

1. Overview.

1.1. Presentation of the system.

Given a room with Light Emitting Diodes (LED's) at various location on an object (e.g. on the head of a person), an optical tracking system must be able to measure the position and the orientation in azimuth and elevation of the object in the field of view (FOV) of the optical system. Two perhaps unique features of the system are the use of a linear detector array (1D) instead of a two dimensional (2D) array, and an anamorphic field of view (FOV) in the ratio of 3. Cost, speed, and resolution are issues in favor of a 1D array.

1.1.1. System Specifications.

Source	OD-100 from Optodiode TM) with a peak emission at 880 nm; the spectral width at 20% of the maximum output is about 150nm (810nm-960nm)
Field of view (FOV)	90 degrees horizontally and 30 degrees vertically
Numerical Aperture	To be assigned for sufficient signal/noise at the output
Bulk	As compact as possible
Detector	1D CCD sensor array with 10µm pixels
Cost	Less than \$10,000

1.1.2. Overall Design Approach.

The system was originally conceived using a double stage anamorphic optical system (anamorphic here means that the optical system yields different magnifications in the two orthogonal x and y directions. An anamorphic system typically requires cylindrical optics of one sort or another). The first stage consists in an anamorphic fisheye lens which allows imaging of a 90 degree x 30 degree FOV onto a squared array intermediary image plane. The intermediary image is then imaged by the second anamorphic relay lens onto the linear detector array. The main drawback of the system as conceived is its cost. The idea of a new design for the second stage emerged in order to make the system more cost

effective. The layout of this second stage as well as its testing on an optical bench is now presented.

1.2. A new design for the second stage.

If we look at a schematic representation of the functioning of the second anamorphic stage, it seems simple: a square is transformed in a line (Fig. 1). The LEDs are sequentially fired so that the position of one LED at a time is computed.

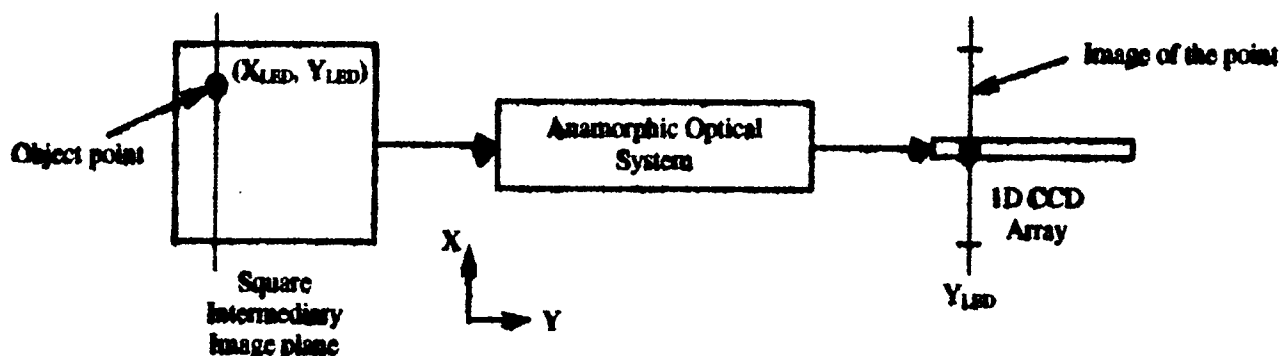


Figure 1. Schematic representation of the second anamorphic stage

In the former relay lens the one-to-one imaging was achieved successfully to specification by using a set of refractive lenses whereas conceptually a simple mirror should be able to perform this mapping. Actually, if we use only a mirror, the image which corresponds to this one-to-one mapping is virtual and symmetrical with respect to the mirror (Fig.2a). So came up the idea of using a retroreflective surface in combination with a semitransparent plate to make rays converge toward the virtual image given by a mirror and to make the image real (Fig. 2b). At the output of the first stage the system was telecentric setting the chief rays parallel to the optical axis.

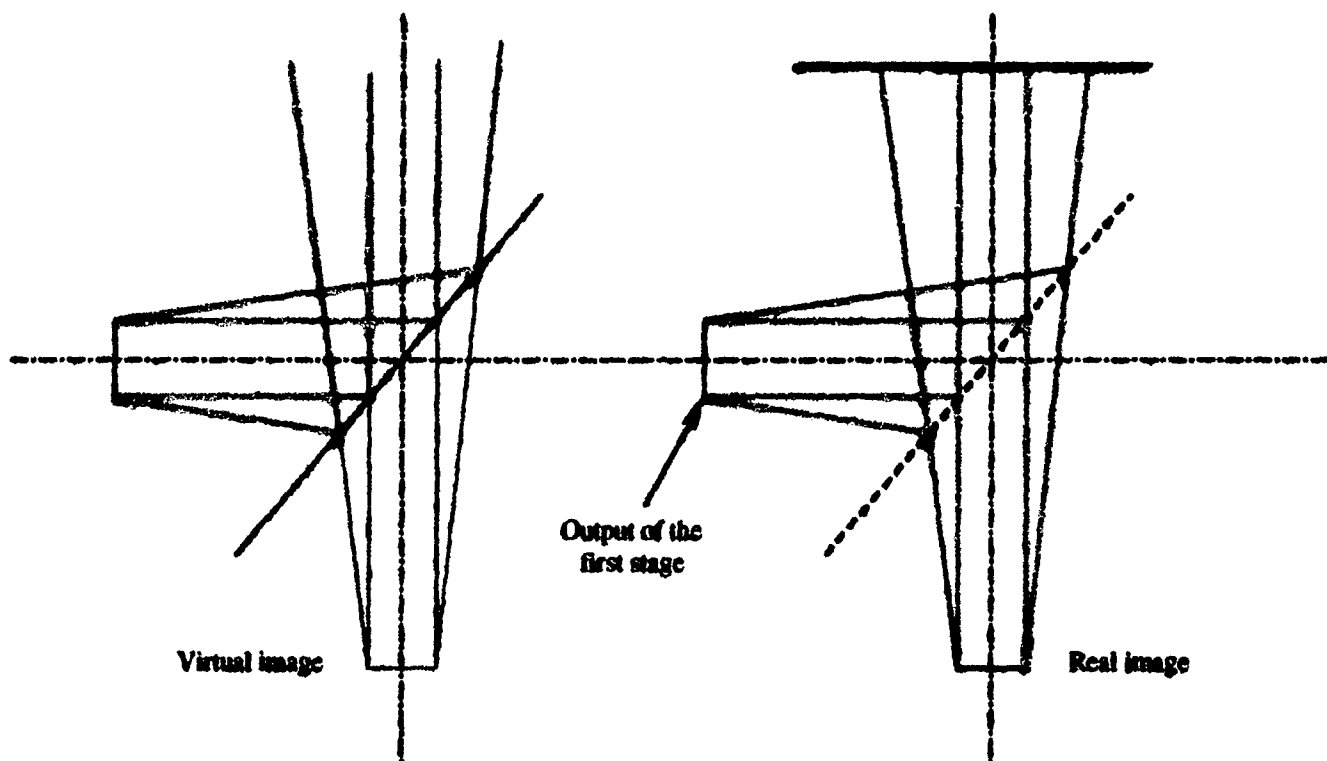


Figure 2a. Virtual one-to-one mapping with only a mirror

Figure 2b. One-to-one mapping thanks to a retroreflective surface and a beamsplitter

Therefore, we are able to do a one-to-one mapping by simply using a retroreflective surface. In the other dimension, we must add cylindrical optics following the beamsplitter in order to create a line in the image plane. The image plane becomes then conjugate to the exit pupil of the first optical stage in one dimension, that of the line. The system could then be presented according to Fig. 3 in which the two dimensions are represented: in one dimension we have a one-to-one mapping and in the other we have a line image.

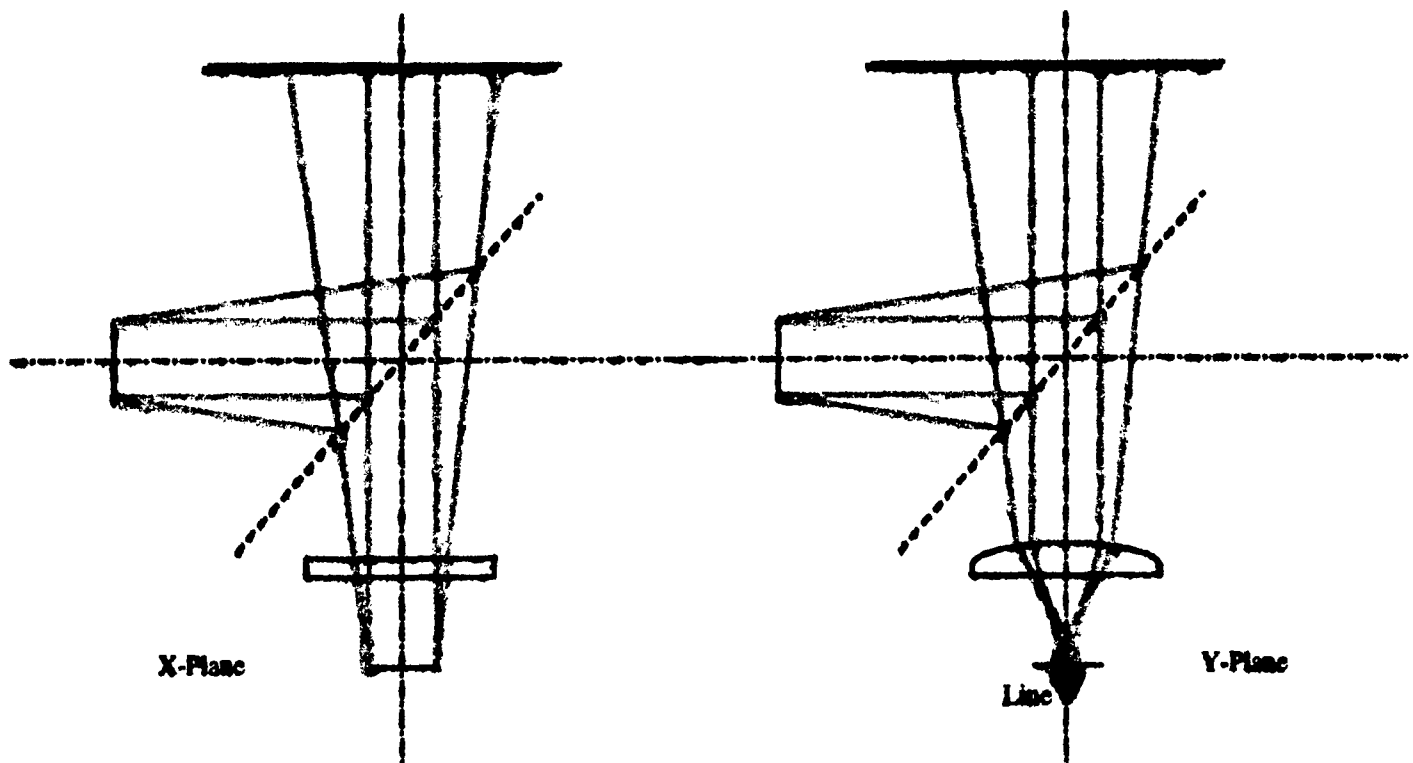


Figure 3. Concept of the new second stage.

Such a system is quite simple compared to the former system using refractive optics and the critical component to its working is the quality of the retroreflective sheet. The next step is to design this system so that it will be as compact as possible and to test its image quality on the bench. We shall proceed first with a first order optical layout and then optimize the optics using a lens design software; CODE V was used in our case.

2. First Order Layout.

The first order calculations will allow us to foresee the space between the system's elements to make it as compact as possible. It will also allow provide a starting point design for CODE V.

First of all let us have a larger diagram to introduce the notations we are going to use (Fig. 4).

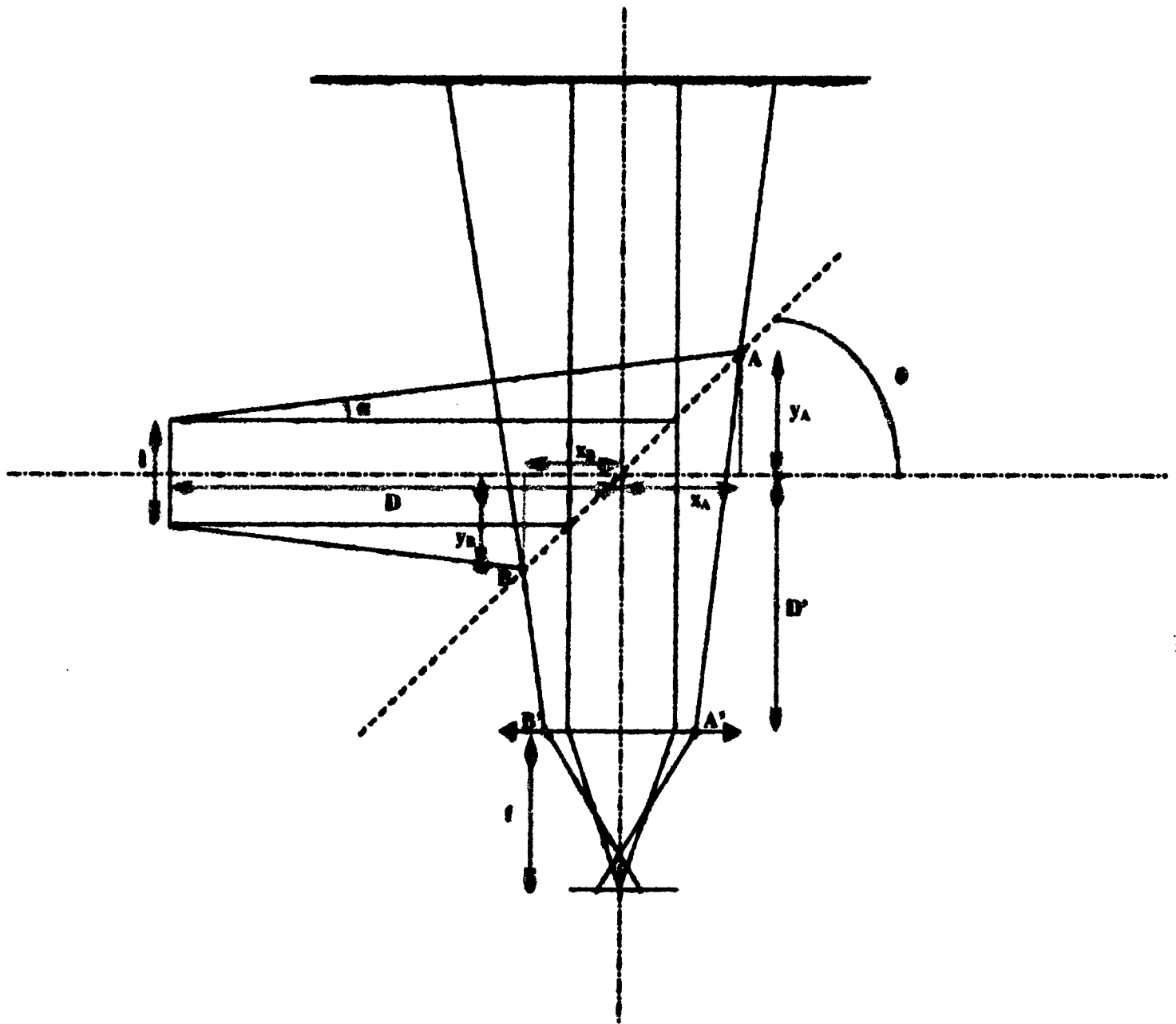


Figure 4. Notations for the first order layout.

The knowledge of the position of A' and B' allows us to constraint the diameter of the cylindrical lens. The focal length f of this lens must respect the relationship $f = D-D'$. The system is then solved for $x_{A'}$, $x_{B'}$, $y_{A'}$, $y_{B'}$; The intermediary results x_A , x_B , y_A , y_B are also computed to constraint the beamsplitter diameter.

2.1. Search for a solution using a single lens.

The object and the image are symmetrical with respect to the beamsplitter. In our application, the object will be a 14-millimeter square. We can choose D and compute the other parameters in order to see if the system yields a valid solution.

We keep in mind that the system must be as compact as possible using off-the-shelf components. With a single lens, the system has a lot of constraints:

- We cannot have a small focal length (to limit the bulk) and a large diameter because the f -number ($=f/\text{diameter}$) of the lens must be greater than 1.
- D and D' must satisfy $f = D \cdot D'$
- D' and the diameter of the lens must be so that the lens doesn't collide the beamsplitter.
- The dimensions of the lens must be sufficient to collect all the light beam.

If we look again in the catalogs, we notice that the larger dimension for a cylindrical lens is 60*50mm and the minimal focal length for such a lens is 100mm. We could put the lens far away from the beamsplitter, but then we have no chance to have a compact system. As a 50mm wide lens is enough to receive the image spot just after the beamsplitter, we can think about using this kind of lens. The problem is that a 100mm focal length imposes putting the object at least at 150mm from the beamsplitter; moreover these calculations are very approximate as we are not taking into account the thickness of the elements, so that real dimensions can be far bigger. That's why we must keep a small focal length.

We have highlighted rapidly that with the lenses available in the catalogs, the system was overconstrained and no solution appeared. Then we must reconsider the structure of our system.

2.2. Search for a solution using two lenses.

For thin lenses the power C resulting from putting two lenses (power C_1 and C_2) together is $C=C_1+C_2$. If we consider the focal lengths this relationship becomes:

$$\frac{1}{f} = \frac{1}{f_1} + \frac{1}{f_2}$$

The main point is that we can make a 50mm-focal-length lens with two 100mm-focal-length lenses. An other advantage for using two lenses is that geometrical aberrations decrease when the number of lenses increases.

3. Optical Design under CODE V.

We use the first order layout as a starting point to the optimization under CODE V.

3.1. First drawing.

To model the system in CODE V, we decide to unfold the system and to consider it only after the reflection on the retroreflective sheet because there is no preprogrammed surface in CODE V that could model such a sheet. We then analyze the part of the system composed of the beamsplitter and the two lenses. We define the object as a virtual object at which the rays will aim. So instead of defining a real object with the entire system we define a virtual object with the unfolded system. As a matter of fact this virtual object takes the place of the virtual image given by a single mirror. A simplified diagram for this unfolded part is shown in Fig. 6.

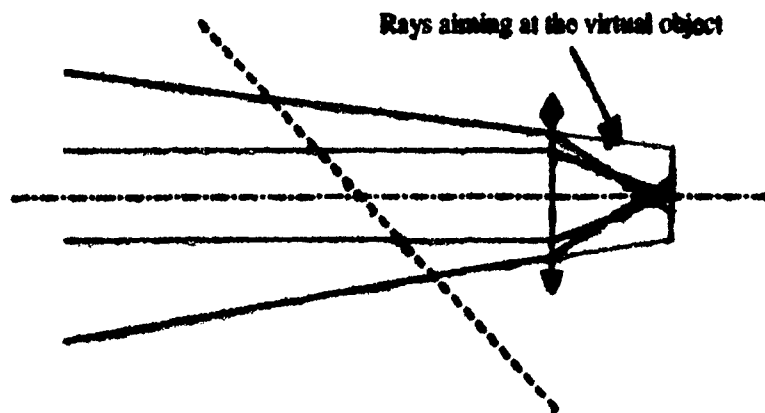


Figure 6. Unfolded system

In this simplified drawing, the image and the object are superimposed, but it certainly will not be the case in the real modeling because of the optical elements' thickness which are going to introduce a shift. Moreover for the moment we don't tilt the beamsplitter because we only want to know if our configuration is valid or not. After entering data in CODE V, the system in the two dimensions is shown in Fig. 7. On this drawing we can see the shift between the object and the image and we can notice that the concept of our system is "raytraceable": There is a one-to-one imaging in the Y-dimension and a line is formed in the X-dimension. If we zoom in, we can notice that the image is out of focus and it leads us naturally to the optimization phase.

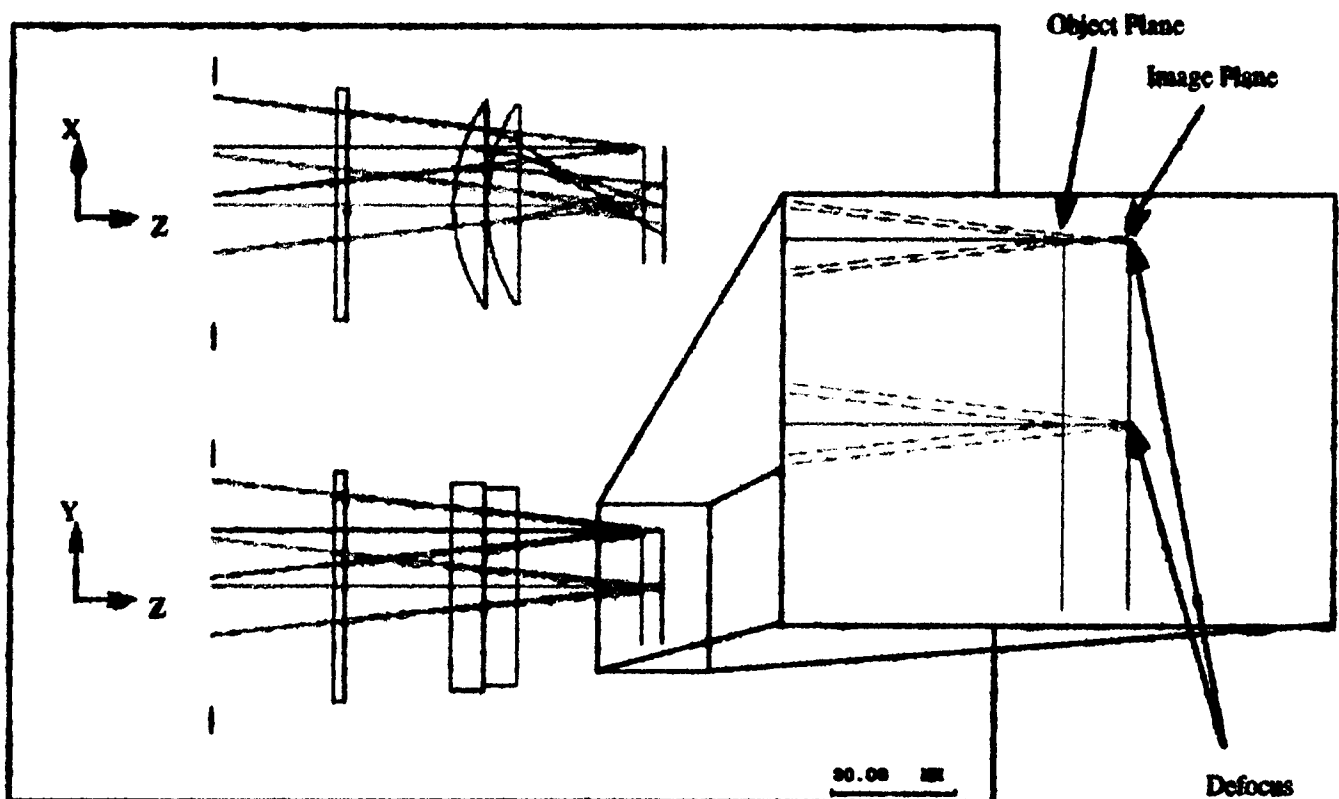


Figure 7. Drawing of the first attempt & zoom to highlight the defocus.

3.2. Optimization of the system.

3.2.1. First AUTO macro.

We now optimize the system. The result of this first optimization appears on Figure 9.

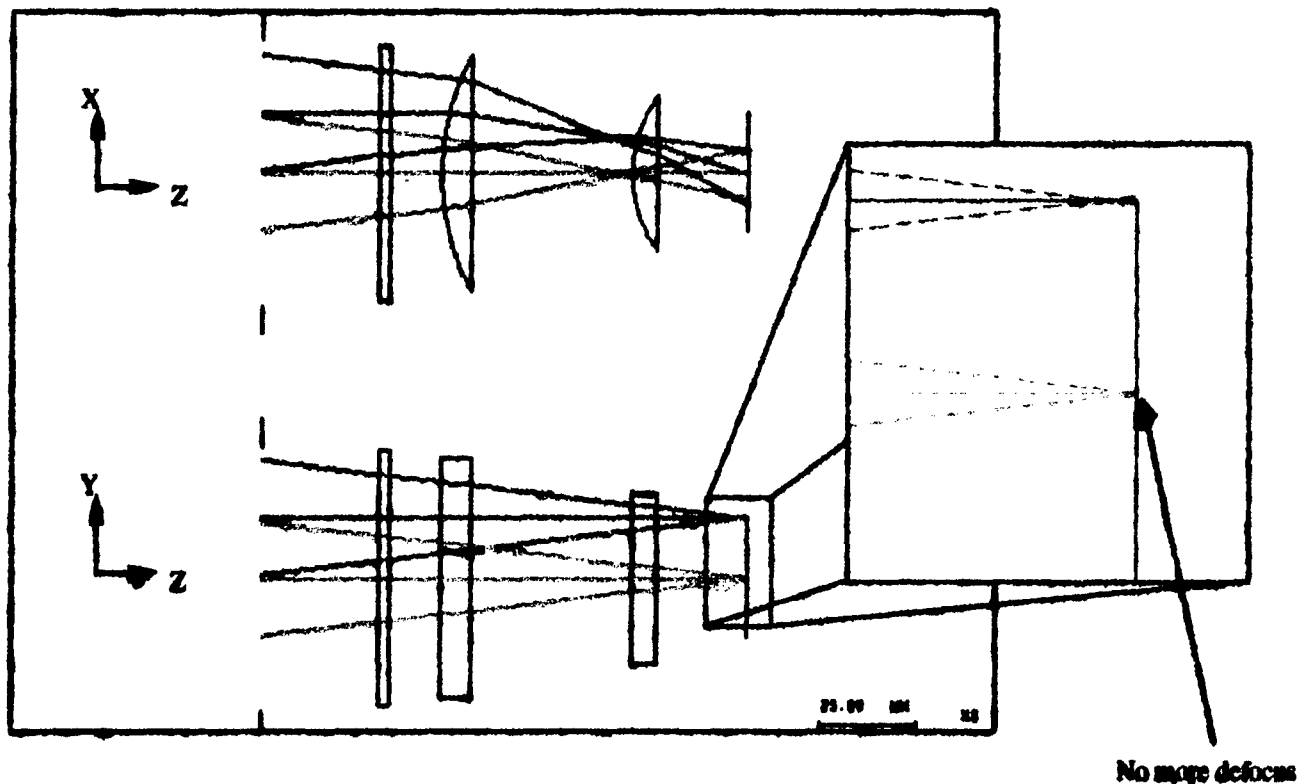


Figure 9. Drawing of the first optimization & Zoom to highlight the correction for the defocus of the center field of view. (the object is not represented)

But now we must think about tilting the plate because it has an important part to play for the positioning of the lenses. Actually we can notice that in our first optimization CODE V placed the first lens in a position that won't exist anymore when the beamsplitter is tilted.

3.2.2. Final optimization and analysis of the final system.

The final result of the optimization is shown in Fig.10&11.

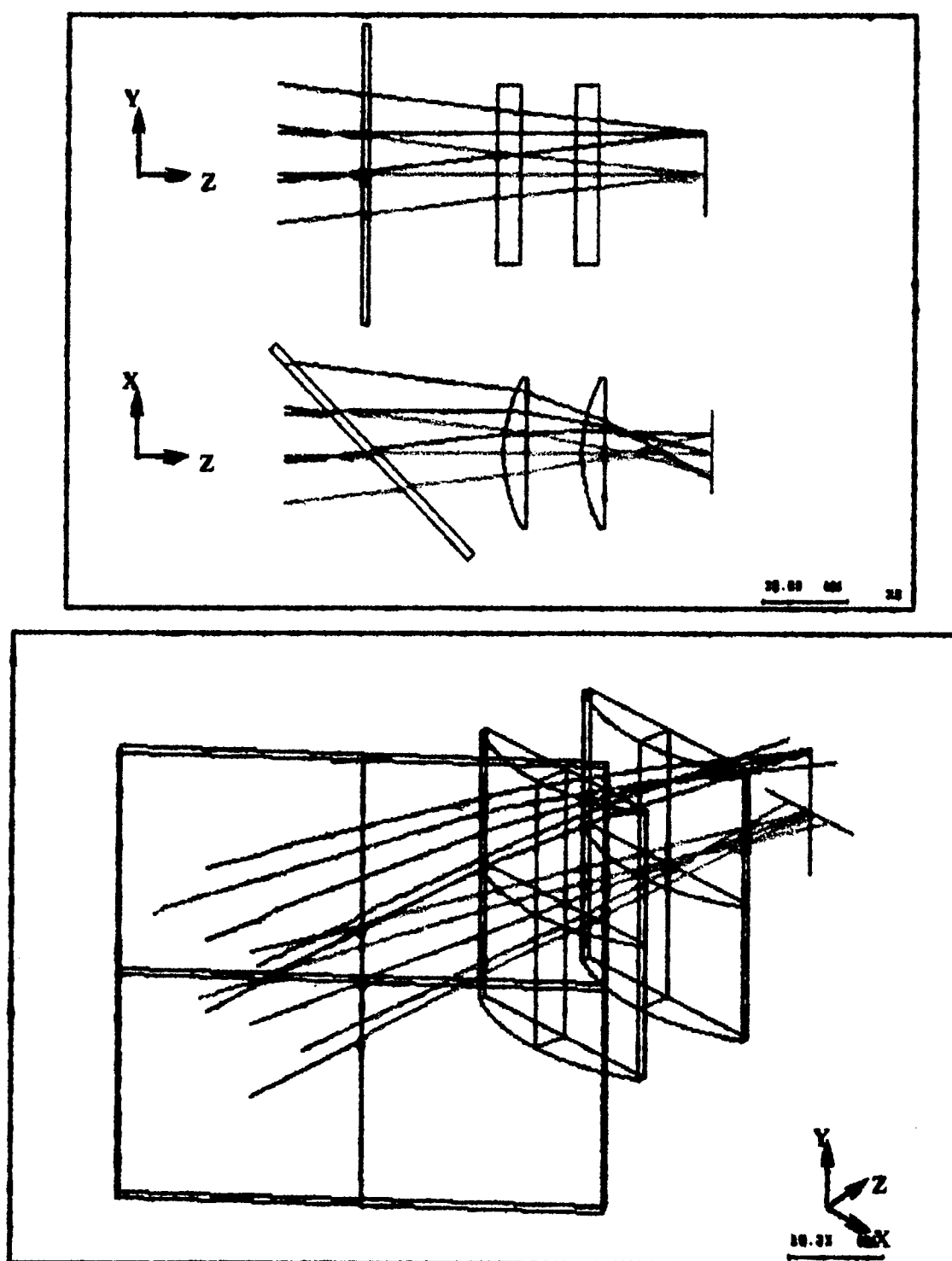


Figure 10&11. Drawings of the final system.

The optical elements that I used are the following:

- Cylinder lenses: MELLES GRIOT⁽¹¹⁾ Model 01 LCP 011
- Beamsplitter: EDMUND SCIENTIFIC⁽¹²⁾ Model D61260

1	INFINITY	-146.93314146			
2	INFINITY	-0.1e7			33.2398
3	INFINITY	0.1e7			
4	INFINITY	30.00000000			33.2398
5	INFINITY	3.00000000	BK7 SCHOTT	REFR	Special
6	INFINITY	46.93879358			Special
7	51.479009	0.00000000	BK7 SCHOTT	REFR	Special

Figure 12. Data sheet of the final system

3.2.3. Spot Diagram.

The spot diagrams are obtained by tracing a grid of equally spaced rays on the entrance pupil from each point in the object. The distribution on the image surface is then reproduced at a correct scale. The interest of these diagrams is that they show the geometrical structure of the image; moreover when they are drawn in color they allow to see the chromatic aberration insofar as each color corresponds to one wavelength. Fig. 13 shows the spot diagrams for five fields: (0,0), (9.8,0), (14,0), (0,14), (14,14) which correspond to the normalized fields (0,0), (0.7,0), (1,0), (0,1), (1,1).

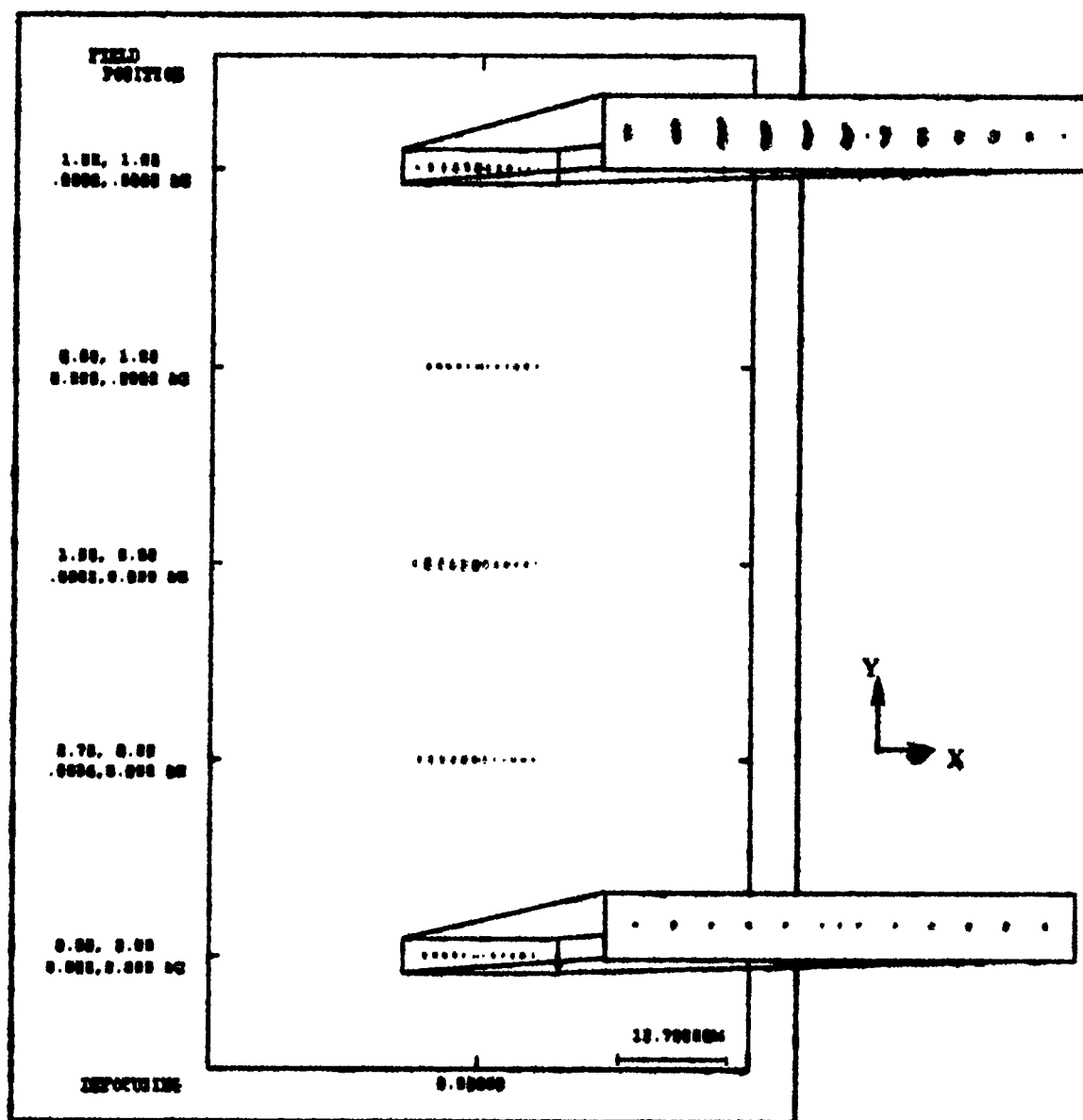


Figure 13. Spot Diagrams for the final system

We can notice that the chromatic aberration is not a problem for our application because it causes no spread in the Y-direction. As it was previewed the quality of the line is far much better for a field point that belongs to the YZ-plane, where as for those which move along the X-axis we see some defocus; and the greater the field, the greater the defocus. But the quality of the image along the X-axis is not important. Actually what we are glad to observe is that there is no important spread along the Y-direction in the center of the line. But we must admit that the scale of these spot diagrams is not appropriate. Because

the line of the sensor along the Y-direction has a 10um width, we conducted further analysis. That is the purpose of the Detector Energy.

3.2.4 - Detector Energy (GDE).

GDE measures the relative proportion of passable rays at each field. The convolution in the nominal image surface with a detector is included. We specify a detector that is 1mm long in the X-direction and 10um long in the Y-direction. Then GDE adds a 21*21 display of points in the image showing the energy on the detector when it is centered at each of those points. We specify an increment for this 21*21 grid which is 40um.

The results are shown in Figures 14a/b&15a/b. They are the results for the center field and the corner field. We can see that for the center field the line is perfect; but for the corner field the line is spread along the Y-direction. Fortunately, we can notice that the distribution along the Y-direction is symmetrical with respect to the center line. So we can go around this blur problem and we can capture the point we are interested in thanks to that symmetry. However we must be careful because for an extreme corner point the image points that are above the center line will be out of the sensor line. That's why we lose a little part of the object. In Figure 15b, we can see that the spread is 320um (the increment we have chosen the grid is 40um) so that we are able to capture 13.680mm instead of 14mm we judged acceptable.

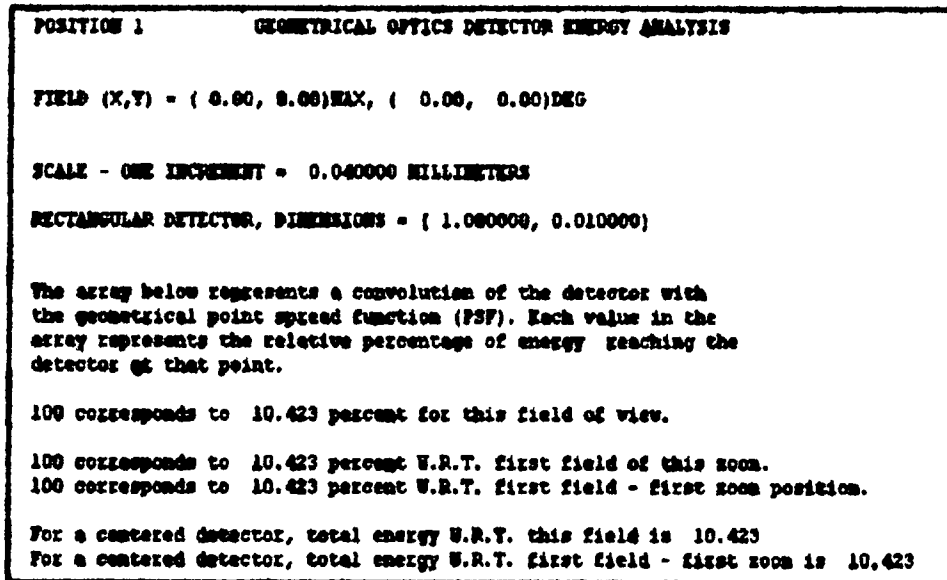


Figure 14a

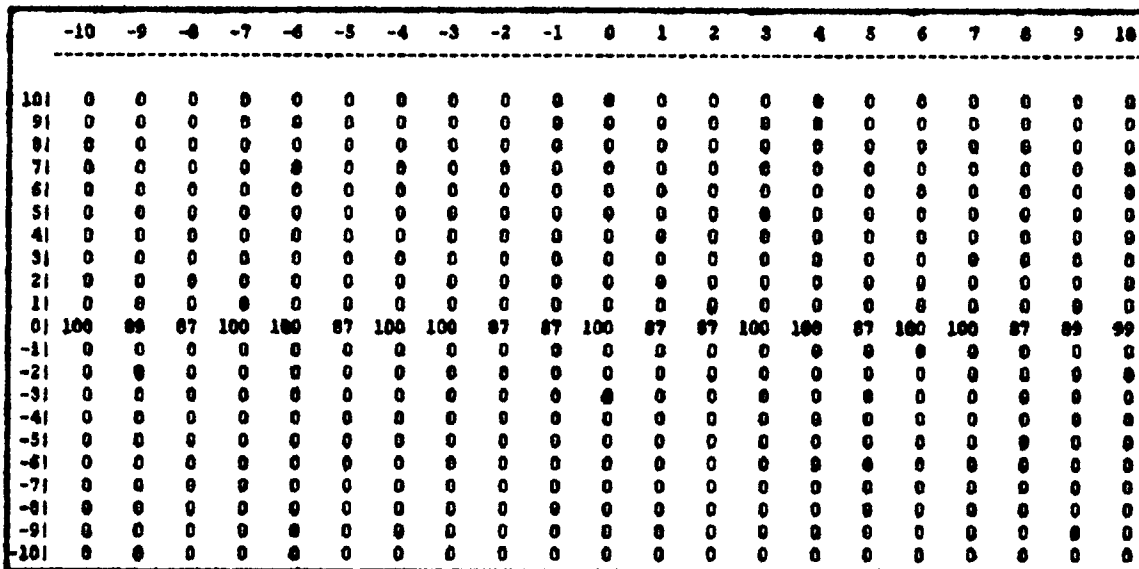


Figure 14b

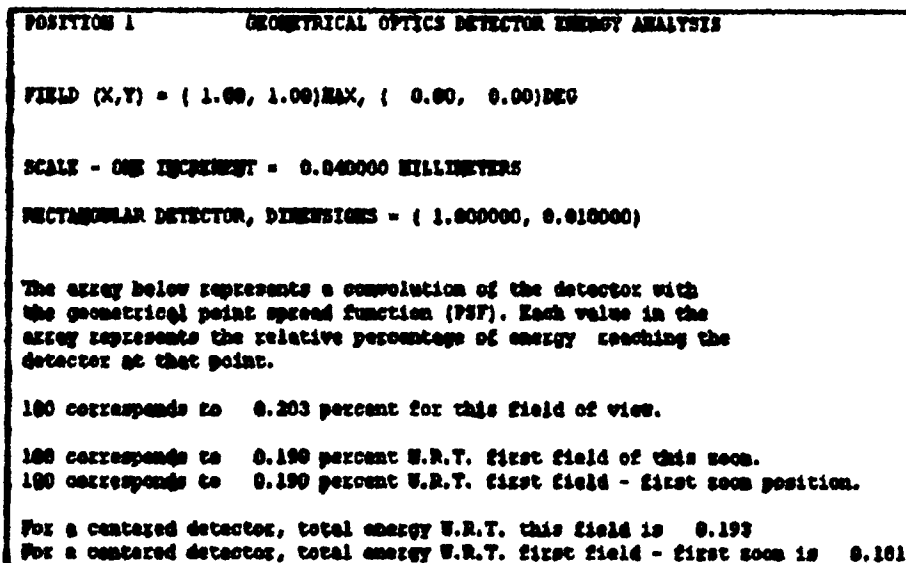


Figure 15a

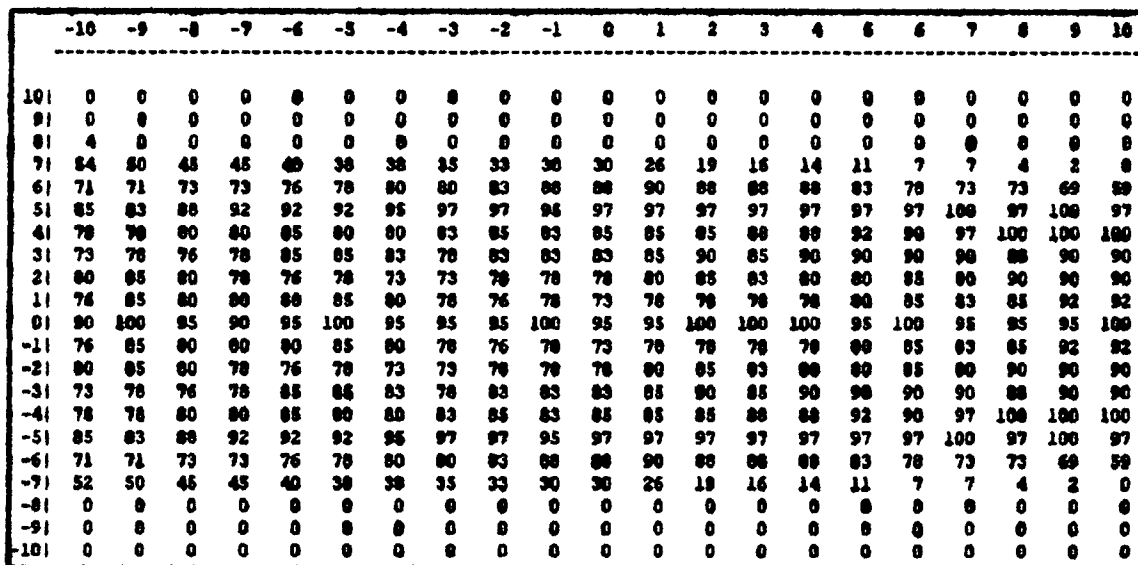


Figure 16b

3.2.5. Tolerances Analysis.

Tolerances of the finished design are also needed in order to have the units built at a reasonable cost. In our case we have focused our optimization effort on having off-shelves elements, so this analysis is going to ensure us that tolerances given by the manufacturers are sufficient. We measure the performance change by RMS (Root Mean Squared) wavefront error or MTF (Modulation Transfer Function). No sensitive tolerances were observed.

3.2.6. Increasing of the object's dimensions.

We now increase the dimensions of the object from 28*28mm to 42*42mm to investigate other field of view requirements. Of course such a modification can have important consequences on the system we have designed. So we took the latest configuration and increased the object's dimensions in order to fit those new needs. The results are shown on Fig.16.

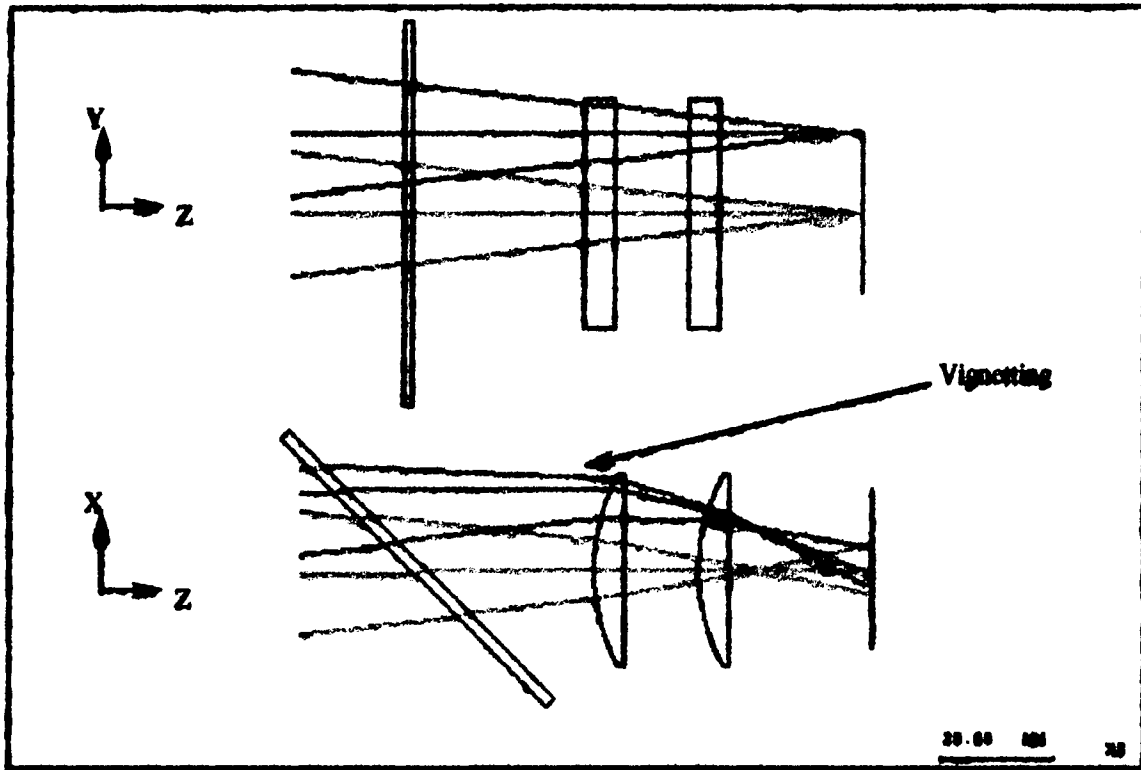


Figure 16. The increasing of object's dimension makes vignetting occurred

Fortunately, we can notice that vignetting occurs only in the X-dimension, i.e. the dimension in which is formed the line. As a matter of fact if we lose a part of the light in this dimension, it is not really important because we are focused on the center of the image (the 1D CCD array will be perpendicular to the image line); so losing a small part of the line's edges is not critical. On the contrary we are satisfied to see that we collect all the light in the other dimension. Then our system is still valid for a 42*42mm object.

3.3. Modeling of the retroreflective surface.

The next challenge is to model the retroreflective surface because CODE V does not include a type of surface that has the optical property to send a ray back on itself. We have to "build" this surface manually. Moreover, we also have to specify to CODE V that the plate we had in the unfolded part is in fact a beamsplitter.

3.3.1. A first solution using Non-Sequential Surfaces.

The idea of this first solution is based on the fact that CODE V traces default rays for each field of view and there are the rays in the X-Z plane and the rays in the Y-Z plane. For these rays, we have to identify their position on the surface representing the retroreflective sheet and we then have to send them back on themselves. An idea is to divide a surface in small square patches (2mm squared for example) and when a ray hits one of these surfaces, we identify which one it is and we orient it so that the ray concerned is sent back on itself. In such a configuration, Non-Sequential (NS) ranges are perfectly appropriate not only for modeling the beamsplitter but also for entering all the small patches which compose the retroreflective surface. The results we get are pretty nice and we can see the whole system on a CODE V's drawing (Fig. 17a).

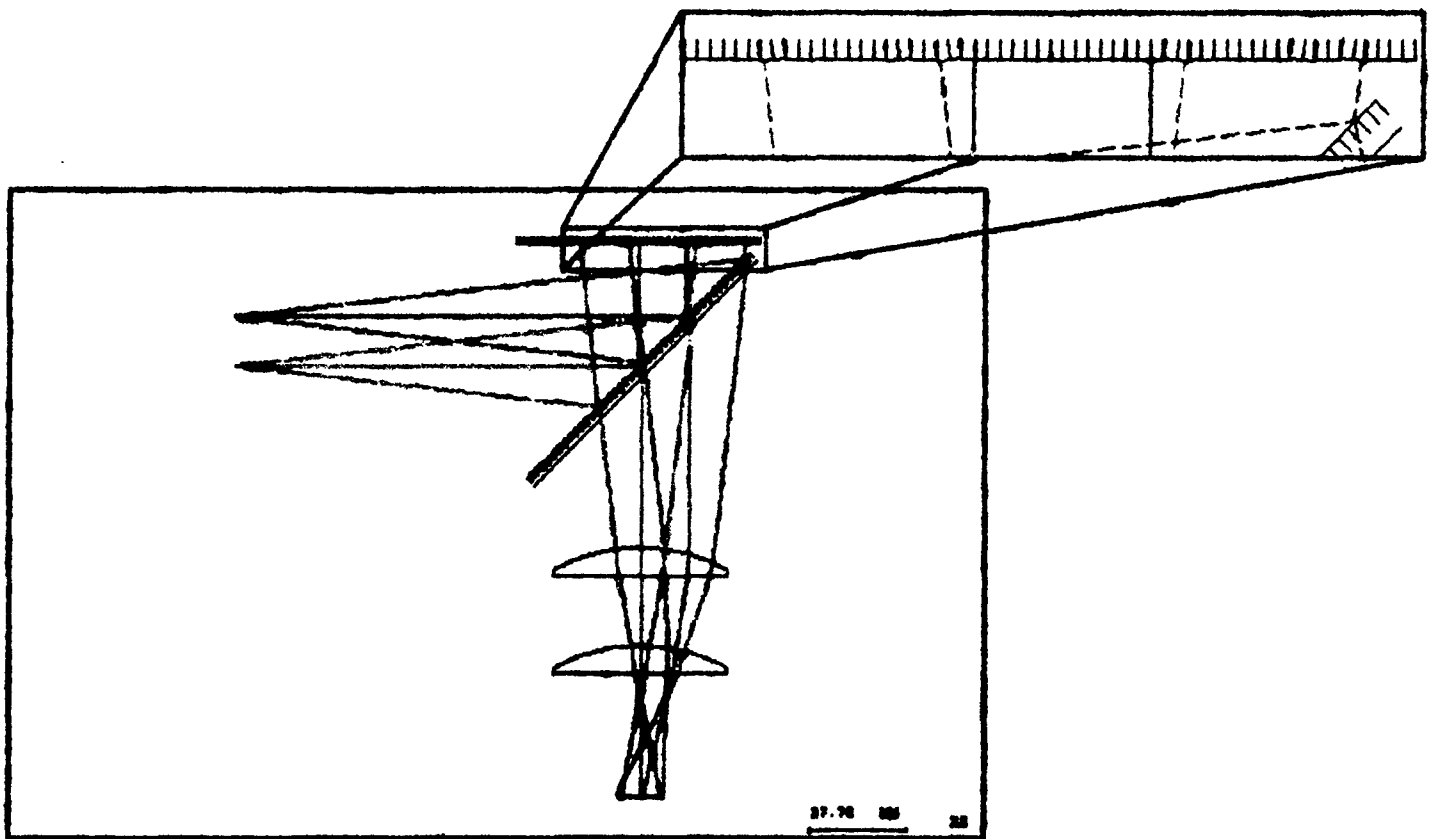


Figure 17a. View of the whole system using NSS

Actually, the figure above is only a view in the X-Z plane and a perspective view (Fig.17b) shows that we built the divided surface only to catch the rays in that plane. In

September 25, 1998

fact, the rays traced by CODE V in the other plane are terminated after touching the front surface of the beamsplitter.

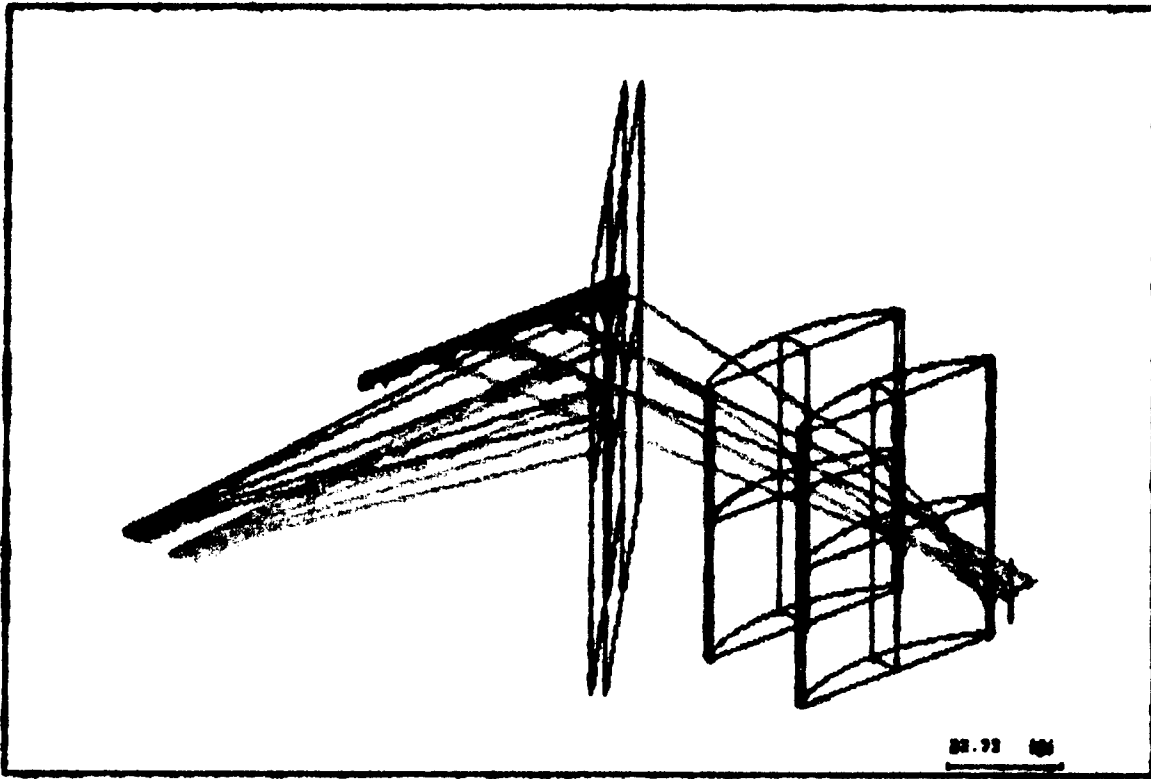
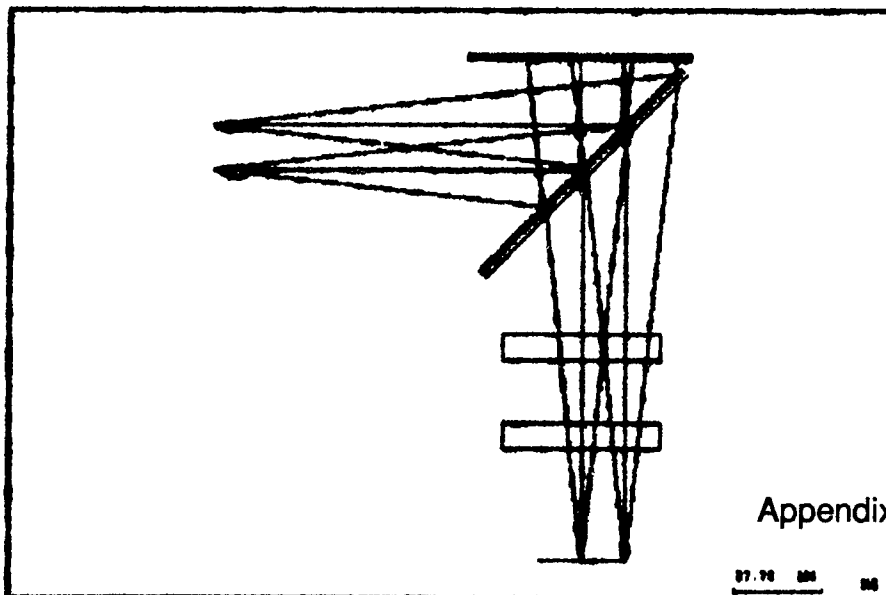


Figure 17b. Perspective view of the whole system using NSS

The next figures (Fig. 18a&18b) show what we get for the other dimension in which we have a one-to-one mapping.

Figure 18a. View of the whole system in the other dimension



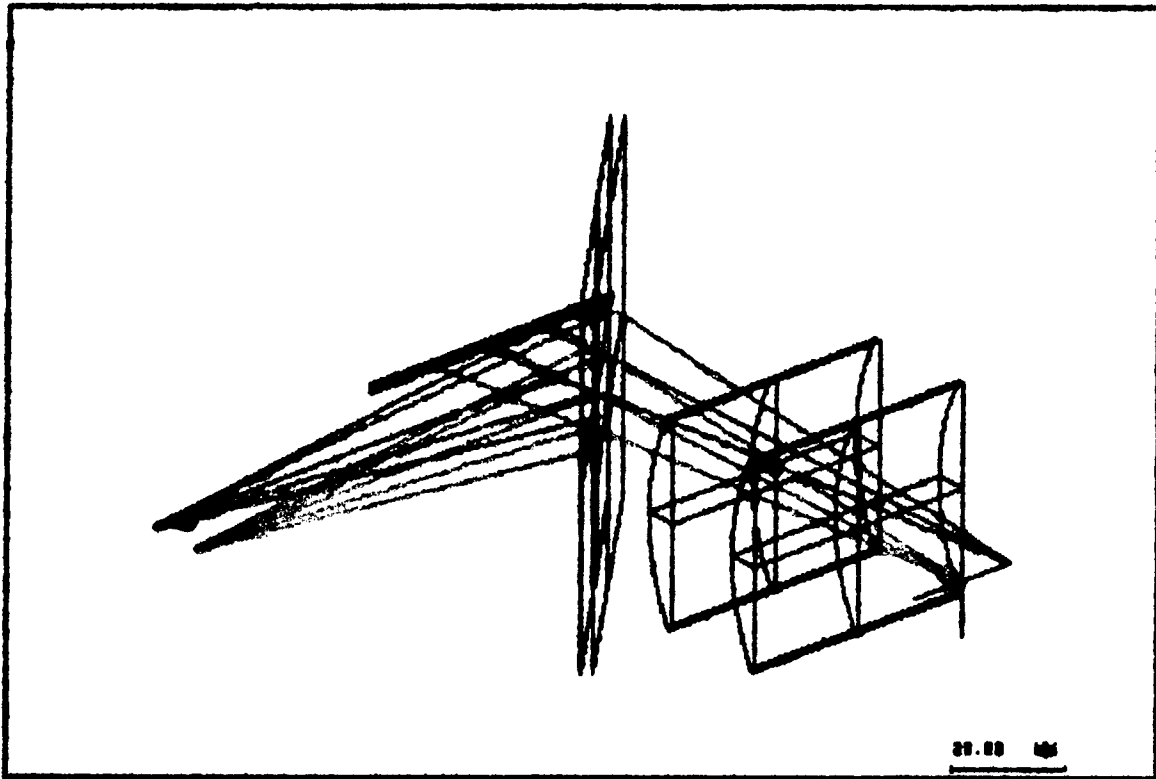


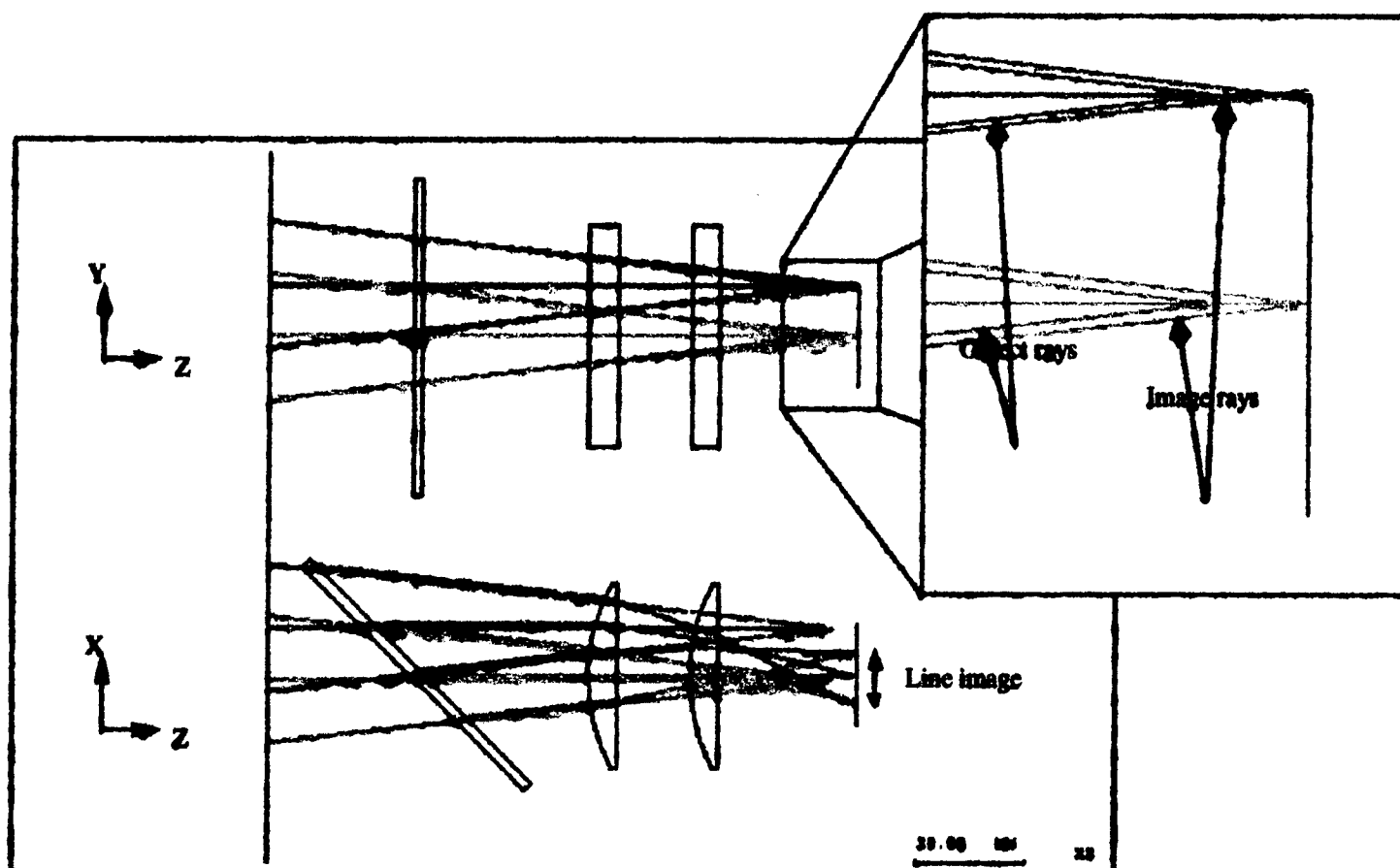
Figure 18a. Perspective view of the whole system rotated to see the modeling in the other dimension

3.3.2. A Macro-based solution.

CODE V also provides the capability to write our own programs in a language called Macro Plus in order to allow us to have user-defined variables, arrays, functions and surfaces in our system. We are especially interested in the fact that CODE V has several user-defined features to supplement the built-in forms. These include the ability of the user to program a user-defined surface (two forms, UDS and UD2).

We then propose to write a short macro using this USERSUR2 function which can program a surface that has the property to send a ray of light back on itself. Basically, we have to model a surface in a way that any ray hitting it encounters a surface exactly perpendicular to it. Thus, if the surface is a reflector, all rays will reflect back onto themselves.

Unfortunately, this macro does not work with the entire system. I manage to make it perfectly work with the unfolded system but apparently, this macro is not compatible with NSS ranges. The problem was not clearly identifiable but when we add some NS surfaces in the system, the macro doesn't work properly and only two rays are computed entirely. Nevertheless it works quite well with the unfolded system that we first designed. Figures 19a&b show that rays coming from the object are sent back on themselves to form the line image. This time, instead of having the rays aiming at the virtual object, we make them start from this object and they are sent back thanks to the UD2 surface.



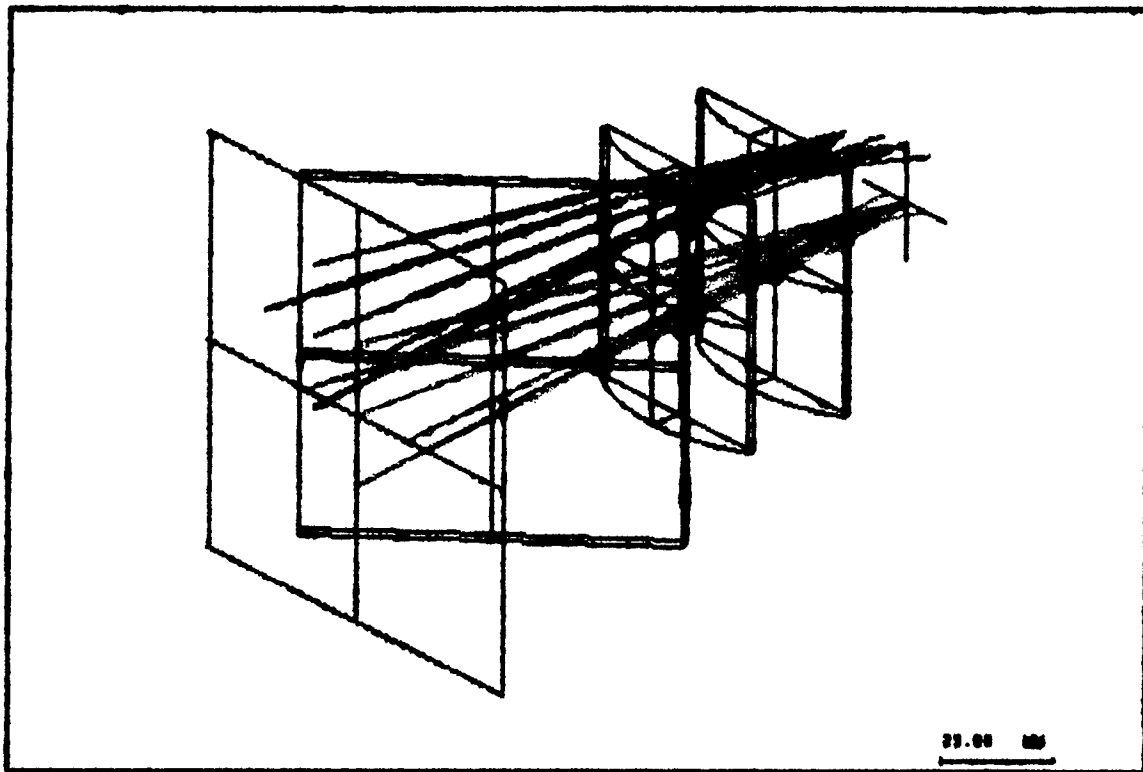


Fig. 19a&b Bidimensional and perspective view of the use of the UD2 surface

Now that we have our entire system designed under CODE V we would like to concretely verify its functioning. We need to determine all the optical and mechanical elements that are going to make this experiment possible.

4. Optical and mechanical hardware.

4.1. Optical elements.

In this paragraph, we are going to describe all the optical elements involved in the experiment. We shall also include the characteristics of the LED here.

4.1.1. The beamsplitter.

When we designed the system under CODE V we realized that the beamsplitter would have to be bigger than what we found usually in the catalogs. We could have asked for a customized beamsplitter but cost was an issue at this prototype stage. The material used

for them is the Soda Lime glass which does not have a precise index. Edmund Scientific told us that it has a floating index that varies between 1.51 and 1.57. They can guarantee a value between these two values but they can't know it in advance. The model we have chosen is a 40R/60T model D61,260.

4.1.2. The Light Emitting Diode.

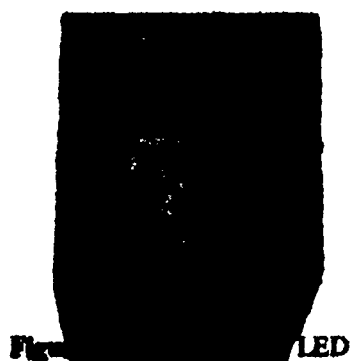


Figure 21. The LED

The LED used fits the specific requirements of the system. It has a peak emission wavelength at 880nm, the maximum value for a continuous forward current is 500mA and with such a current the output power is 100mW. This LED has a very wide angle of emission and insofar to match the first stage specification for an angle of aperture of 0.11 radians, we added in front of the LED a little aperture that would only let pass a cone with the desired angle. The calculation for the diameter of this small aperture is shown in Fig. 22:

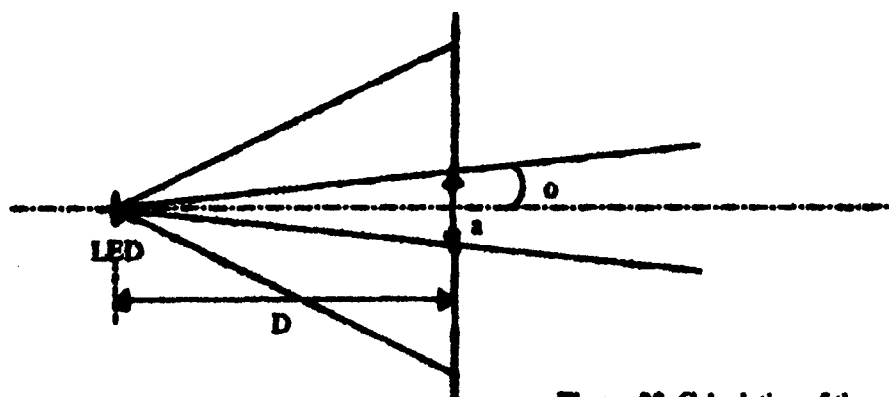


Figure 22. Calculation of the aperture diameter

$$\tan \alpha = \frac{a}{D}; \text{ knowing } \alpha = 0.11 = \tan \alpha: \boxed{a = 0.22d}$$

4.2. Mechanical Assembly

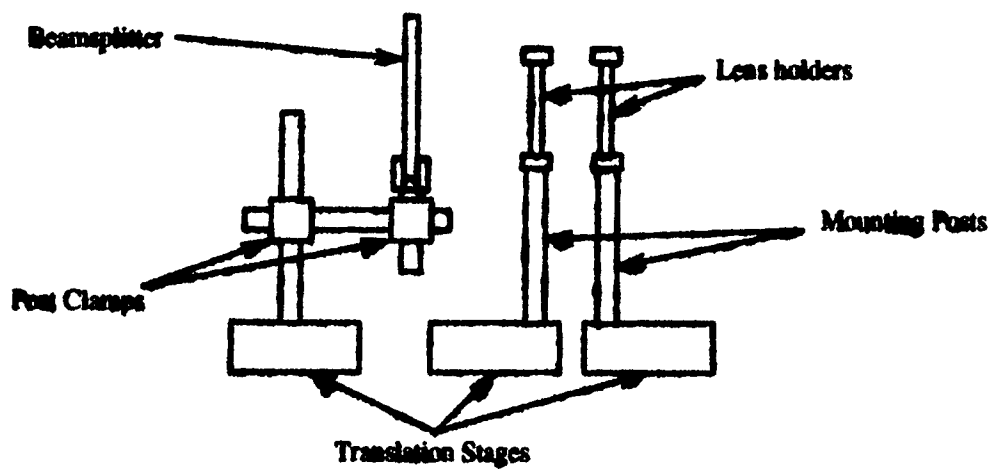
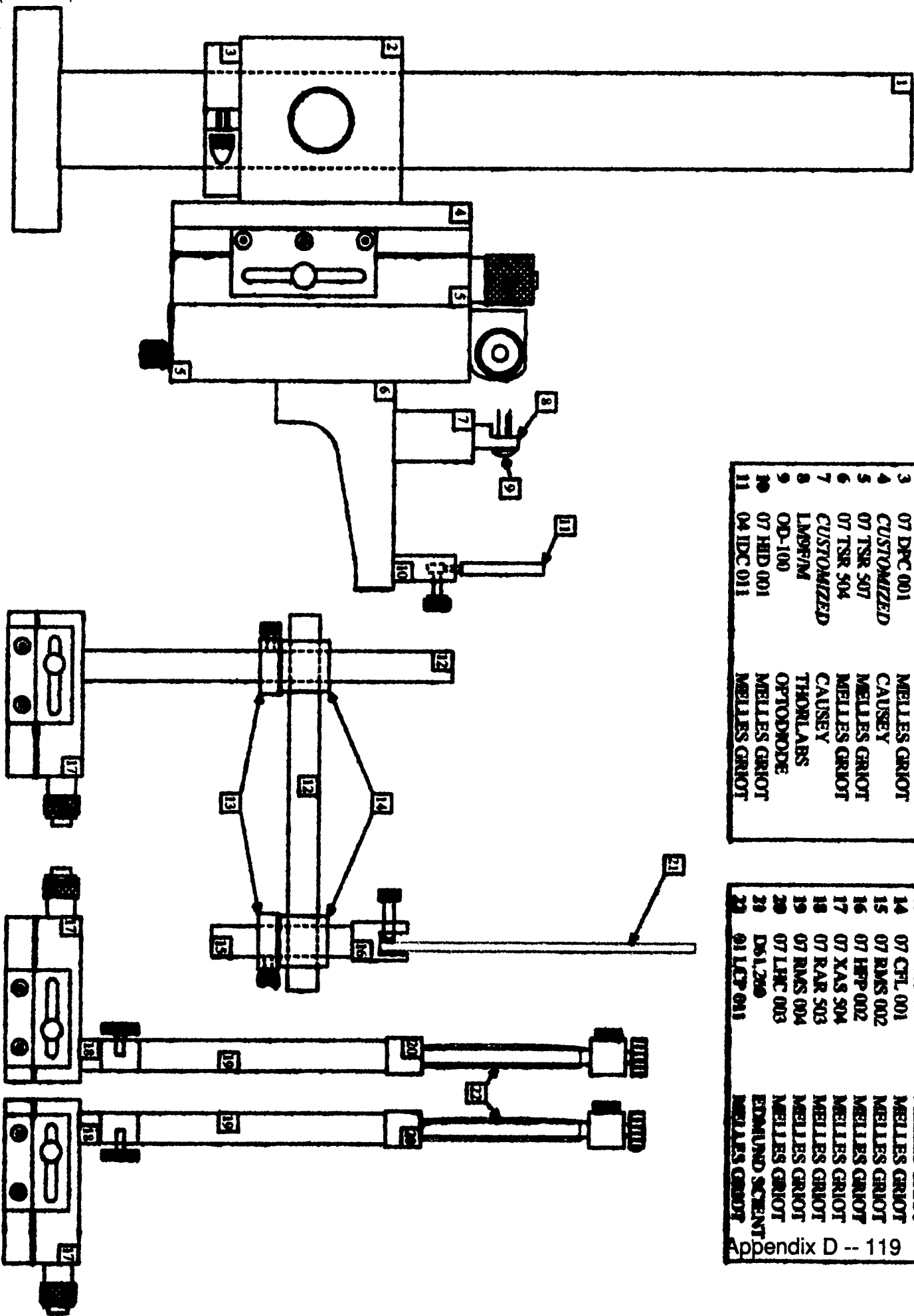


Figure 23. The mounting systems



#	Product Number	Manufacturer
1	07 DUP 512	MELLES GRLOT
2	07 DSQ 503	MELLES GRLOT
3	07 DPC 001	MELLES GRLOT
4	CUSTOMIZED	CAUSEY
5	07 TSR 507	MELLES GRLOT
6	07 TSR 504	MELLES GRLOT
7	CUSTOMIZED	CAUSEY
8	LM9FM	THORLABS
9	OD-100	OPTODODE
10	07 HD 001	MELLES GRLOT
11	04 IDC 011	MELLES GRLOT

#	Product Number	Manufacturer
12	07 RMS 005	MELLES GRLOT
13	07 PHC 001	MELLES GRLOT
14	07 CHL 001	MELLES GRLOT
15	07 RMS 002	MELLES GRLOT
16	07 HRP 002	MELLES GRLOT
17	07 XAS 504	MELLES GRLOT
18	07 RAR 503	MELLES GRLOT
19	07 RMS 004	MELLES GRLOT
20	07 LHC 003	MELLES GRLOT
21	DS1.200	EDMUND SCIENT
22	01 LCP 001	MELLES GRLOT

4.2. The retroreflective surface.

The sheeting is covered with many thousands of micro corner cubes – precisely 47,000 per square inch. Such sheeting material is commonly available from 3M⁽⁵⁾ or Reflexite⁽⁶⁾, Inc. and is routinely used in photoelectric process control. Several samples were sent to us, and the first thing I did was to test their behavior by sending a simple laser beam on them (Fig. 25):

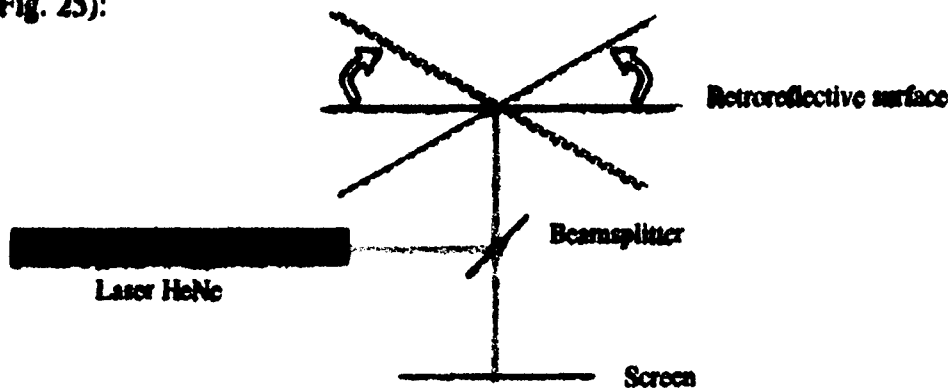


Figure 25. Testing the retroreflective sheet with a LASER

When we tested the sheet, it had indeed a retroreflective behavior: if the retroreflective surface was tilted or bent, the image of the beam was still at the same place on the screen. But what we could immediately notice is that the image spot of the beam on the screen is spread and that leads to think that the retroreflective surface induces scattering in one way or another. And that might have critical consequences when we will put this surface in our system. Moreover we could observe a ghost image coming from the surface and this particular image could be assimilate to a parasite reflection because it follows the movements of the surface. In the meanwhile, we measured what amount of energy we could collect back from the surface, and the results were:

For a 100% amount of incident energy:

Retroreflection: 45%

Ghost image: 7%

The missing amount of energy is apparently lost through the surface.

4.4. The CCD camera.

We used an infrared CCD camera provided by Artificial Reality Corp. The software we used to acquire the images on the computer is XCAP Imaging (limited featured version) that allowed us to capture the images and do basic analysis on them.

5. Measurements and Results.

While waiting for the last parts of the purchase to hold the LED in the right position, we decided to use a LASER as a light source with the setup to really "see" how the system was behaving and to make some observation that could be useful for the usage of the LED.

5.1. Testing the system with a LASER.

Using a laser, we aligned the elements according to CODE V's specifications and we put the CCD camera in the image plane. Then we ran XCAP Imaging and we acquired the image of the LASER. The image we get is shown below (Fig. 26a), with the corresponding energy distribution (Fig. 26b).

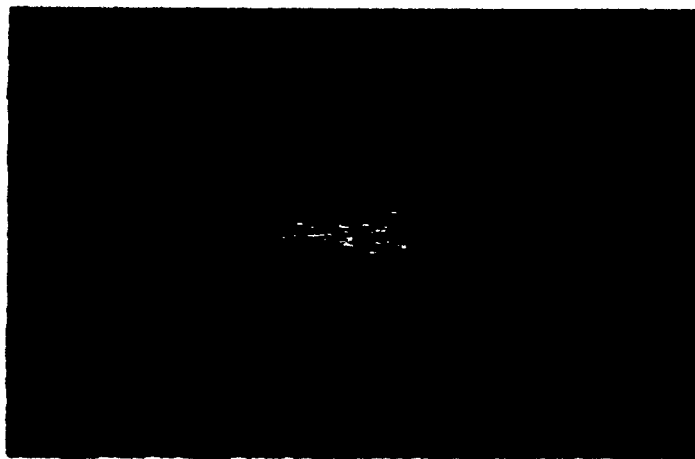


Figure 26a. Image of the LASER through the system

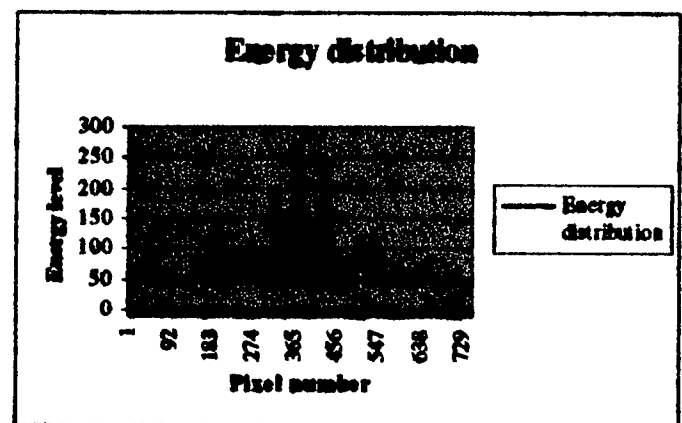


Figure 26b. Corresponding energy distribution

The energy distribution above is obtained thanks to the software by selecting a row in the image; then the software shows the energy along that line with respect to the pixel

involved. That's why, because of the speckle induced by the LASER, the curve is noisy. After smooting, it is shown in Figure 27.

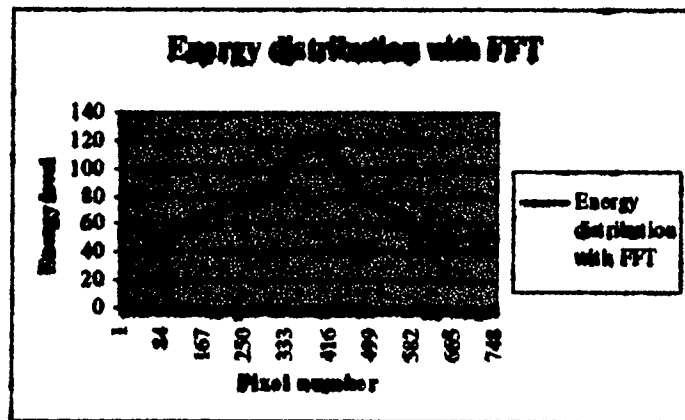


Figure 27. Usage of a FFT filter to smooth the former energy distribution

The LASER can show us two different things:

- The image shape: As we feared it when we analyze the behavior of the retroreflective sheet, the image was spread along one direction, and unfortunately this was the direction of the future 1D CCD line. Actually, we should get a vertical line, but as the lenses have no power along the horizontal direction, we have a big blur around the vertical line.
- The mapping: We can verify if the mapping of the intermediary image plane is correctly done. In fact the system must be invariant in one direction and in the other direction, the image should follow the object. Indeed, the system behaves as expected.

3.2. Using the LED as a light source.

The first thing we should specify is that we use the LED as a point source, but we must keep in mind that in the real system the source of the second stage is not a LED, it is already an intermediary image of that LED obtained by the first stage of the tracking system. So in order to match the specifications of that intermediary image/object, we put an aperture in front of the LED. This LED was a very wide angle LED, so we had to put a black box around the LED to prevent it from directly illuminating the whole system.

Then we positioned the LED in the correct position and we acquired the image given. We will only show in this report the energy distribution of the image because the black and white image we obtained was not very representative. Immediately we notice that it will be difficult to exploit the results. In fact we need to detect very small displacements (about 10 μ m), and the curve appears too flat to get correct detection.

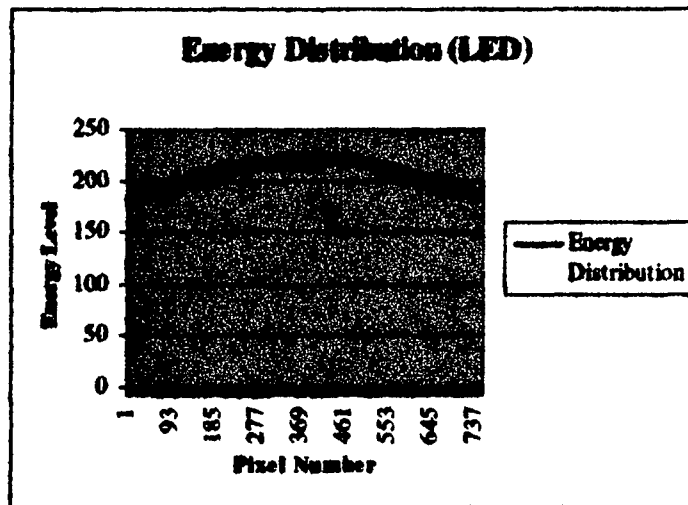


Figure 28. Energy in the image plane using the LED

We computed the position of the maximum of the energy on the image plane to determine where the LED is on the image line. We attempted two methods: the detection of the centroid of the energy distribution, and the detection of the peak of this energy distribution.

Conclusion.

These measurements and tests have shown that the quality of the retroreflective sheet critically affects the performances of our system. The mapping of the image plane is as we expected, but the scattering that is produced by the sheet doesn't allow us to perform a precise detection of the LED position in the square intermediary image plane. We are currently investigating a new line of products with 3M.

Design of an anamorphic fisheye lens

Jannick .P. Rolland, Alexandra Rapaport, and Myron W. Krueger *

Center for Research and Education in Optics and Lasers (CREOL), Orlando, FL 32816

*Artificial Reality Corporation, Vernon, CT 06066

Address: Jannick Rolland, University of Central Florida

CREOL, 4000 Central Florida blvd., Orlando, FL 32816

Phone: (407) 823-6870; FAX: (407) 823-6880; E-mail:rolland@creol.ucf.edu

Abstract: The design of a 90 x 30 degrees FOV anamorphic fisheye lens is presented.

The F/4.5 lens maps on a 60 mm square detector array.

Summary

This lens was designed as an investigation for the first stage of a larger optical system. The first stage images infrared light emitting diodes that can be localized within a 90 degree (x-dimension) x 30 degree (y-dimension) on a 60 mm square array. The spectral bandwidth of the sources is 150nm, with 20% spectral output at 810nm and 960nm. The layout, rayfans, spot diagrams, and the modulation transfer function are presented for performance assessment. Distortion is constrained to achieve a linear mapping. Achromatization of the lens is addressed. Finally, some cost issues associated with fabrication are discussed.

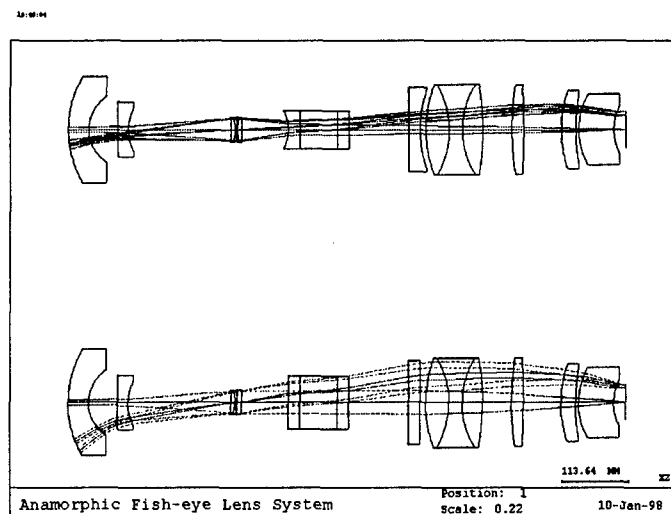


Figure 1. Layout of the anamorphic fisheye lens in the y (top) and x (bottom) dimensions.

Methods: Anamorphic fisheye lenses are most commonly designed by placing an afocal attachment in front of an existing symmetrical fisheye lens. This leads to sub-elegant solutions due to the bulkiness of such a front-end attachment. The solution we propose utilizes an internal afocal sub-system located near the aperture stop. The system aims to satisfy 30 micron RMS spot size over the FOV. The F/# is 4.5 in the x-dimension and 13.5 in the y-dimension. Distortion was constrained using a chief ray in the merit function to achieve a linear mapping. We have chosen the lens to be telecentric in image space to facilitate the mapping requirements of the following optical system. The telecentricity condition was constrained using two chief rays in the FOV, one in each dimension. This constraint could be released for other requirements.

The starting point of the design was chosen to be a symmetrical fisheye lens designed by Edwards et al., (1993) for video see-through head-mounted display technology (Rolland et al., 1994). This lens consisted of two meniscus negative lenses typically encountered in fisheye optics and two doublet lenses, one on each side of the aperture stop. This lens was first scaled to satisfy the focal length requirement in the x-dimension. An afocal lens made of four y-cylindrical lenses was positioned after the aperture stop between the two

doublets. We constrained in the early design stage the light to be collimated, entering as well as exiting the afocal assembly. The required power of the lenses for the afocal assembly were computed to satisfy a reduction ratio of three in FOV between the x and y dimensions. Most importantly for cylindrical optics, the afocal constraint should be satisfied over the entire FOV. Because such a constraint cannot be reached with afocal optics (Wetherell, 1992), the afocal condition was released to balance performance over the FOV. The focal lengths in each dimension were constrained in the merit function.

Results: The layout of the lens, the rayfan plots and spot diagrams, as well as the modulation transfer function are shown in Figs. 1, 2, and 3, respectively

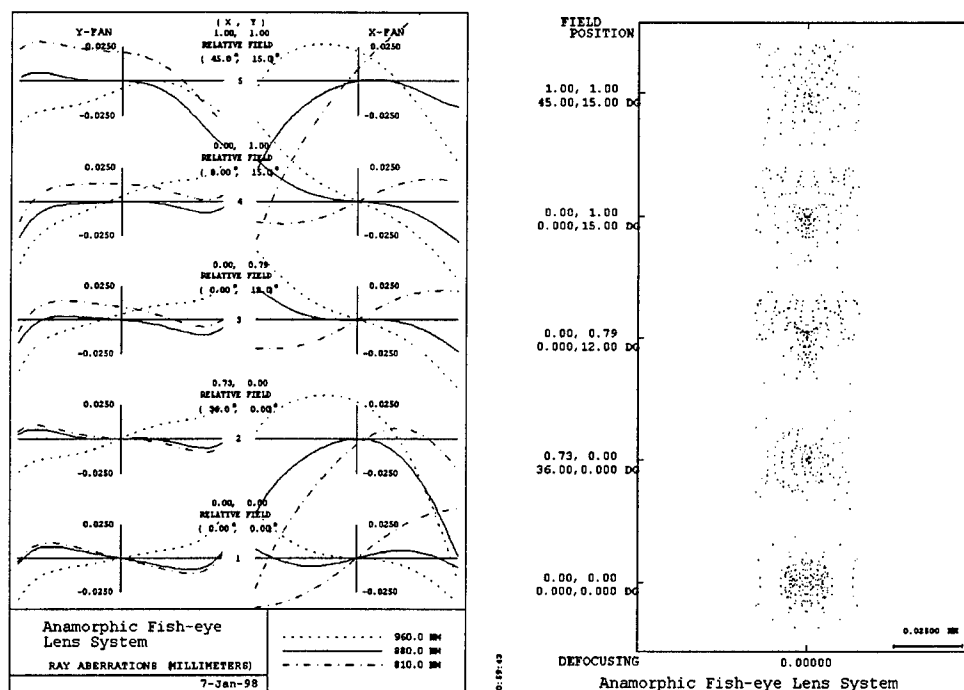


Figure 2. Rayfan plots (left) and spot diagrams (right) of the anamorphic fisheye lens.

The RMS spot size is less than 30 micron across 80% of the FOV. Looking at the rayfans, it can be observed that the lens is essentially limited by chromatic aberrations. This result is presented after optimization with varying indexes and dispersion glasses. Some boundaries were set to limit the choice of glasses to second grade glasses for cost consideration (Thompson, 1994). Further achromatization of the lens using conventional optics did not yield much improvement of the rayfan plots. The addition of a binary optical component located on the flat surface of the smallest cylindrical lens in the afocal assembly was investigated. Performance was significantly improved and will be detailed in the final paper. Typical cost of fabricating a cylindrical lens with a binary optics component is 5K-10K. For cost effective optics, we may use a spectral filter located close to the detector array to further reduce the effective spectral range of the overall system, which is a viable solution in our case.

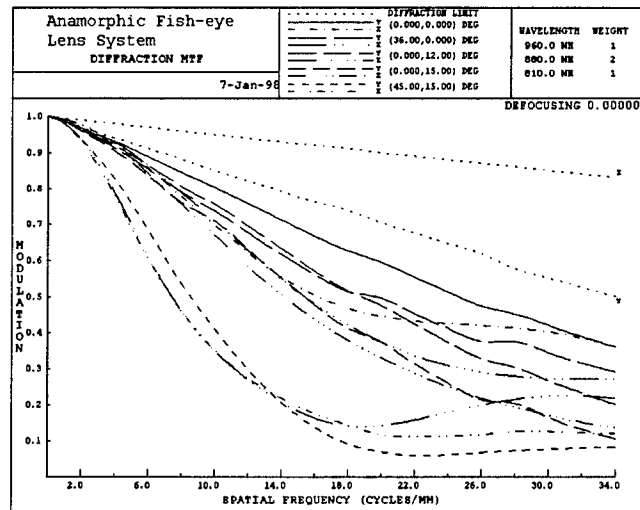
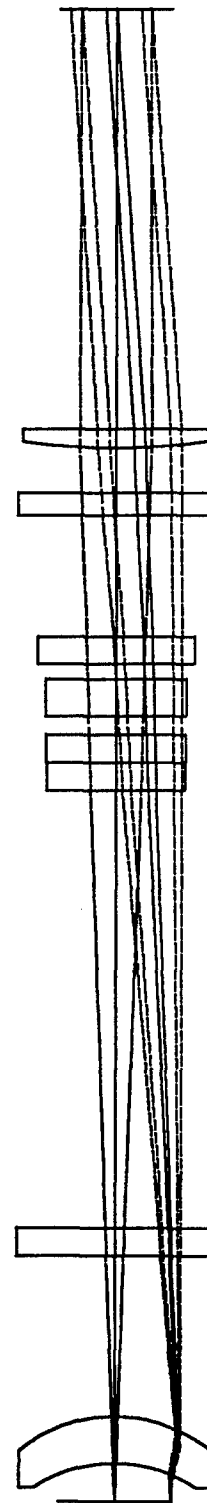
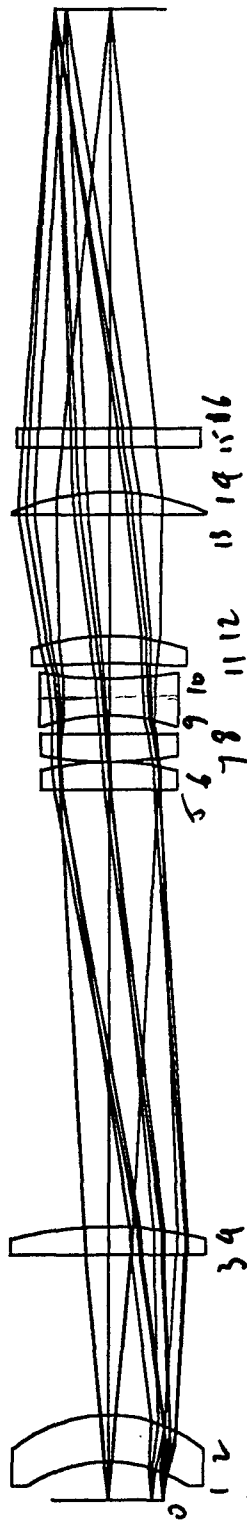


Figure 3. Modulation transfer function (MTF) of the anamorphic fisheye lens. Except at the upper corner point of the FOV that we included in the optimization of the lens to insure acceptable quality on diagonal points as well as on the two main directions, the MTF is greater than 20% for spatial frequencies less than 28 cycles/mm.

If fabrication of such a lens was to be pursued, the glass selection of the first lens should be given special consideration because it is 180mm in diameter and therefore, the cost of fabrication of the first lens can significantly increase by several thousand dollars depending on the selected glass. Because of the overall length of the system (950 mm), a folding prism with 64 millimeter on one side was inserted within the afocal assembly as shown in the layout in Fig. 1.

References

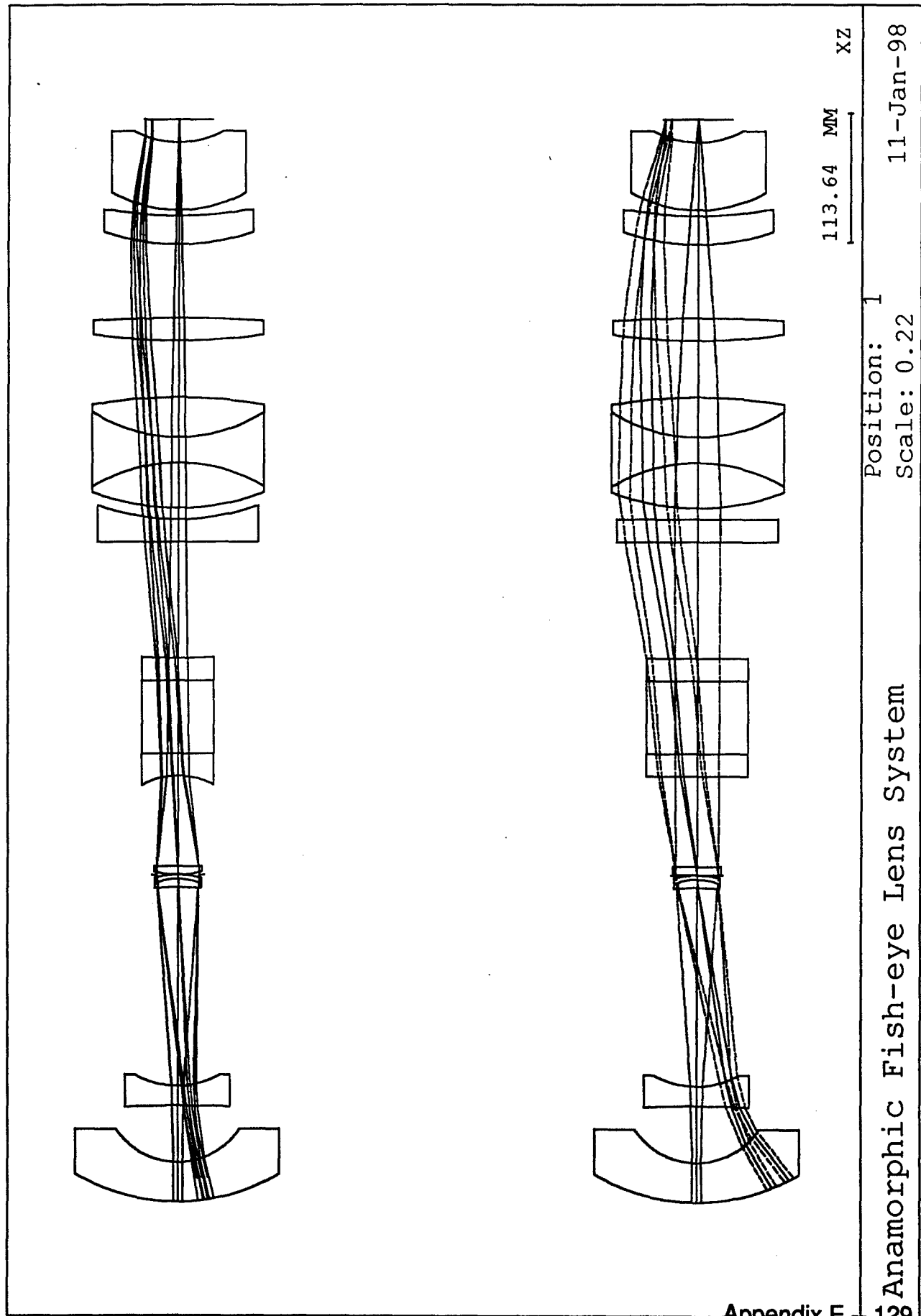
- Wetherell, W.B., "Afocal optics," Chap. 3 in Applied Optics and Optical Engineering. Vol. 10, 109-192, Academic Press, NY.
- Thompson, K.P., "Key to cost effective optical systems: maximize the number of qualifier fabricators," Proc. OSA 22. International Optical Design Conference (1994).
- Edwards, E., J.P. Rolland, and K. Keller, "Video see-through design for merging of real and virtual environments," Proc. IEEE VRAIS'93, 223-233 (1993).
- Rolland, J.P., R.L. Holloway, and H. Fuchs, "A comparison of optical and video see-through head-mounted displays," Proc. SPIE 2351, 293-307 (1994).



96.15 MM XZ

Scale: 0.26

13-Jan-98



RADIUS		RAD TOL		POW/IRR		C.A. DIA		CENTRAL			WEDGE		
S1		S2		CX		CC		EDGE DIA		THI TOL		T.I.R.	
177.819		65.660		+0.2000		+0.0500		180.656		35.000		+0.2000	
174.999		108.744		8.0 / 2.0		8.0 / 2.0						0.1000	

NOTES :

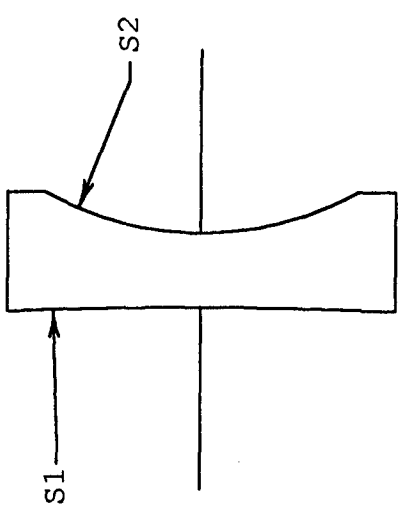
- ALL DIMENSIONS ARE IN MILLIMETERS.
- MATERIAL: OPTICAL GLASS PER MIL-G-174
TYPE: LAK10 SCHOTT NO. 720504
N_d 1.7200 ± 0.0003 V 50.4 ± 0.8%
STRIAE GRADE , ANNEAL
MELT NO.
- 'P' PITCH POLISH TO TEST PLATE WITHIN POWER AND IRREGULARITY INDICATED.
- MANUFACTURE PER MIL-O-13830
- SURFACE QUALITY
- 'C' MAGNESIUM FLUORIDE COATING PER MIL-C-675 FOR MAX TRANSMISSION AT MILLIMICRONS.
- 'G' FINE GROUND & BLACKENED PER MAX FACE WIDTH
- BEVEL EDGES AT 45 DEG TO (REF)
- DIAMETER TO FLAT IS ON SURFACE S2 WITH SURFACE SAG OF

DR		CHK		APPD		SCALE		REL BY		REL DATE	
						0.59:1					

Anamorphic Fish-eye Lens System -J.P. Ro ELEMENT 1		-	
--	--	---	--

RADIUS		RAD TOL POW/IRR		C.A. DIA		CENTRAL			WEDGE		
S1		S2		THI		TOL		TOL		T.I.R.	
1121.405 CC		+3.0000		8.0 / 2.0		88.773		17.500		+0.0750	
77.471 CC		+0.0100		5.0 / 2.0		73.949		92.803		0.0500	

NOTES :
 1. ALL DIMENSIONS ARE IN MILLIMETERS.
 2. MATERIAL: OPTICAL GLASS PER MIL-G-174
 TYPE: SK16 SCHOTT NO. 620603
 N_d 1.6204 \pm 0.0000 V 60.3 \pm 0.8%
 STRIAE GRADE , ANNEAL
 MELT NO.
 3. 'P' PITCH POLISH TO TEST PLATE WITHIN
 POWER AND IRREGULARITY INDICATED.
 4. MANUFACTURE PER MIL-O-13830
 5. SURFACE QUALITY
 6. 'C' MAGNESIUM FLUORIDE COATING PER MIL-C-675
 FOR MAX TRANSMISSION AT MILLIMICRONS.
 7. 'G' FINE GROUND & BLACKENED PER
 MAX FACE WIDTH
 8. BEVEL EDGES AT 45 DEG TO (REF)
 9. DIAMETER TO FLAT IS ON SURFACE S1
 WITH SURFACE SAG OF (REF)
 DIAMETER TO FLAT IS ON SURFACE S2
 WITH SURFACE SAG OF



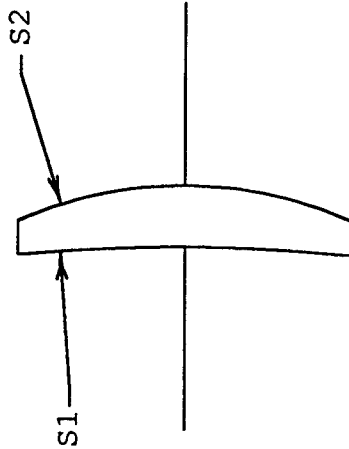
DR		CHK		APPD		SCALE		REL BY		REL DATE	
						0.59:1					

Anamorphic Fish-eye Lens System -J.P. Ro ELEMENT 2		-	
--	--	---	--

RADIUS					RAD TOL POW/IRR		C.A. DIA		CENTRAL					—	
									EDGE DIA	DIA TOL	THICKNESS	THI TOL	WEDGE		
S1	211.360 CC	+0.0050	.50 / .03	38.619				41.277			7.500	+0.0125	0.0160 T.I.R.		
S2	51.001 CX	+0.0020	1.0 / .50	38.403											

NOTES :

- ALL DIMENSIONS ARE IN MILLIMETERS.
- MATERIAL: OPTICAL GLASS PER MIL-G-174
TYPE: SSKN5 SCHOTT NO. 658509
 N_d 1.6584 \pm 0.0000 V 50.9 \pm 0.4%
STRIAE GRADE , ANNEAL
MELT NO.
- 'P' PITCH POLISH TO TEST PLATE WITHIN POWER AND IRREGULARITY INDICATED.
- MANUFACTURE PER MIL-O-13830
- SURFACE QUALITY
- 'C' MAGNESIUM FLUORIDE COATING PER MIL-C-675 FOR MAX TRANSMISSION AT MILLIMICRONS.
- 'G' FINE GROUND & BLACKENED PER
- BEVEL EDGES AT 45 DEG TO MAX FACE WIDTH (REF)
- DIAMETER TO FLAT IS ON SURFACE S1 WITH SURFACE SAG OF



DR			
CHK			
APPD			
SCALE	1.15:1	REL BY	REL DATE
Anamorphic Fish-eye Lens System -J.P. Ro			
ELEMENT 3			
—			

RADIUS				RAD TOL				POW/IRR				C.A. DIA				EDGE DIA				DIA TOL				THICKNESS				THI TOL				WEDGE			
S1	51.001	CC	+0.0020	1.0	/	.50	38.403																												
S2	86.936	CX	+0.0010	.50	/	.03	38.496																												

NOTES :

- ALL DIMENSIONS ARE IN MILLIMETERS.
- MATERIAL: OPTICAL GLASS PER MIL-G-174
TYPE: SF6 SCHOTT NO. 805254
N_d 1.8052 ± 0.0000 V 25.4 ± 0.4%
STRIAE GRADE , ANNEAL
MELT NO.
- 'P' PITCH POLISH TO TEST PLATE WITHIN POWER AND IRREGULARITY INDICATED.
- MANUFACTURE PER MIL-O-13830
- SURFACE QUALITY
- 'C' MAGNESIUM FLUORIDE COATING PER MIL-C-675 FOR MAX TRANSMISSION AT MILLIMICRONS.
- 'G' FINE GROUND & BLACKENED PER MAX FACE WIDTH
- BEVEL EDGES AT 45 DEG TO (REF)
- DIAMETER TO FLAT IS ON SURFACE S1 WITH SURFACE SAG OF

DR				CHK				APPD				SCALE				REL BY				REL DATE			
												2.58:1											

Anamorphic Fish-eye Lens System -J.P. Ro																ELEMENT 4			
--	--	--	--	--	--	--	--	--	--	--	--	--	--	--	--	-----------	--	--	--

RADIUS		RAD TOL		POW/IRR		C.A. DIA		CENTRAL			WEDGE	
EDGE DIA		DIA TOL		THICKNESS		THI TOL						
S1	85.330 CX	+0.0010	.50 / .03	38.136				42.156	7.500	+0.0125	0.0100 T.I.R.	
S2	INF	+*****	.50 / .25	39.469								

NOTES :

- ALL DIMENSIONS ARE IN MILLIMETERS.
- MATERIAL: OPTICAL GLASS PER MIL-G-174
TYPE: BK7 SCHOTT NO. 517642
N_d 1.5168 ± 0.0000 V 64.2 ± 0.8%
STRIAE GRADE , ANNEAL
MELT NO.
- 'P' PITCH POLISH TO TEST PLATE WITHIN POWER AND IRREGULARITY INDICATED.
- MANUFACTURE PER MIL-O-13830
- SURFACE QUALITY
- 'C' MAGNESIUM FLUORIDE COATING PER MIL-C-675 FOR MAX TRANSMISSION AT MILLIMICRONS.
- 'G' FINE GROUND & BLACKENED PER
- BEVEL EDGES AT 45 DEG TO MAX FACE WIDTH

DR		CHK		APPD		SCALE		REL BY		REL DATE	
						2.53:1					
Anamorphic Fish-eye Lens System -J.P. Ro										ELEMENT 5	

RADIUS				RAD TOL		POW/IRR		C.A. DIA		CENTRAL							
										EDGE DIA		DIA TOL THICKNESS		THI TOL		WEDGE	
S1	67.086 CC	+0.0040	2.0 / 1.0	68.499						64.000		20.000	+0.1000	0.0200	T.I.R.		
S2	INF	TPF	8.0 / 2.0	73.219													

NOTES :

- ALL DIMENSIONS ARE IN MILLIMETERS.
- MATERIAL: OPTICAL GLASS PER MIL-G-174
TYPE: F5 SCHOTT NO. 603380
N_d 1.6034 ± 0.0000 V 38.0 ± 0.8%
STRIAE GRADE , ANNEAL
MELT NO.
- 'P' PITCH POLISH TO TEST PLATE WITHIN
POWER AND IRREGULARITY INDICATED.
- MANUFACTURE PER MIL-O-13830
- SURFACE QUALITY
- 'C' MAGNESIUM FLUORIDE COATING PER MIL-C-675
FOR MAX TRANSMISSION AT MILLIMICRONS.
- 'G' FINE GROUND & BLACKENED PER
MAX FACE WIDTH
- BEVEL EDGES AT 45 DEG TO (REF)
- DIAMETER TO FLAT IS ON SURFACE S1
WITH SURFACE SAG OF

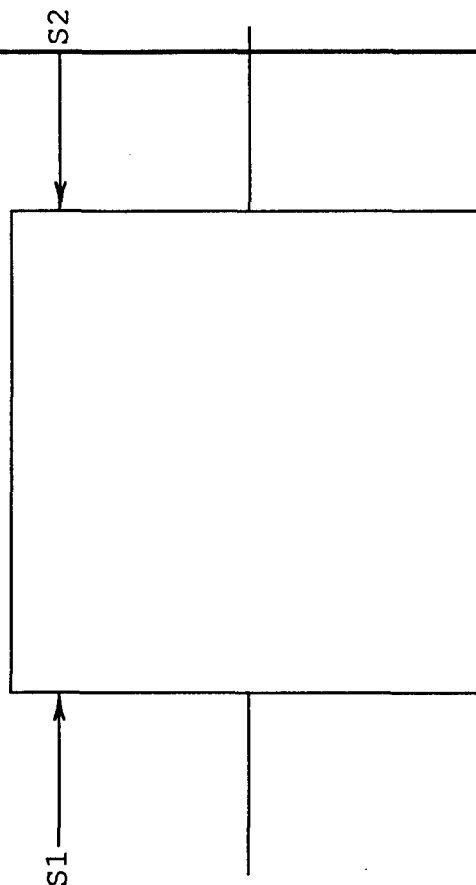
DR			
CHK			
APPD			
SCALE		REL BY REL DATE	
1.67:1			

Anamorphic Fish-eye Lens System -J.P. Ro	
ELEMENT 6	

RADIUS										RAD TOL		POW/IRR		C.A. DIA		EDGE DIA		DIA TOL		CENTRAL THICKNESS		THI TOL		WEDGE				
S1	INF		TPF	8.0 / 2.0	73.219											64.000				64.000			+0.1300			0.0800	T.I.R.	
S2	INF		TPF	8.0 / 2.0	86.798																							
																									—			

NOTES :

1. ALL DIMENSIONS ARE IN MILLIMETERS.
2. MATERIAL: OPTICAL GLASS PER MIL-G-174
TYPE: SF6 SCHOTT NO. 805254
 N_d 1.8052 \pm 0.0020 V 25.4 \pm 0.8%
STRIAE GRADE , ANNEAL
MELT NO.
3. 'P' PITCH POLISH TO TEST PLATE WITHIN
POWER AND IRREGULARITY INDICATED.
4. MANUFACTURE PER MIL-O-13830
5. SURFACE QUALITY
6. 'C' MAGNESIUM FLUORIDE COATING PER MIL-C-675
FOR MAX TRANSMISSION AT MILLIMICRONS.
7. 'G' FINE GROUND & BLACKENED PER
8. BEVEL EDGES AT 45 DEG TO MAX FACE WIDTH

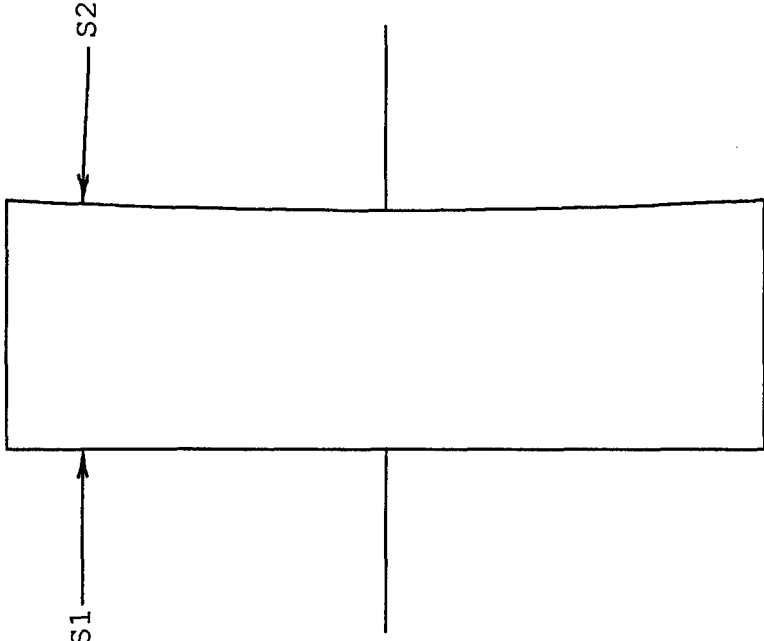


DR			
CHK			
APPD			
SCALE		REL BY REL DATE	
1.05:1			
Anamorphic Fish-eye			
Lens System -J.P. Ro			
ELEMENT 7			

RADIUS				RAD TOL		POW/IRR		C.A. DIA		EDGE DIA			DIA TOL		CENTRAL THICKNESS		THI TOL		WEDGE	
S1	INF	TPF	8.0 / 2.0	86.798						64.000			20.000	+0.1000	0.0800	T.I.R.				
S2	615.950 CC	+0.8900	8.0 / 2.0	91.874																

NOTES :

- ALL DIMENSIONS ARE IN MILLIMETERS.
- MATERIAL: OPTICAL GLASS PER MIL-G-174
TYPE: BK7 SCHOTT NO. 517642
N_d 1.5168 ± 0.0003 V 64.2 ± 0.8%
STRIAE GRADE , ANNEAL
MELT NO.
- 'P' PITCH POLISH TO TEST PLATE WITHIN
POWER AND IRREGULARITY INDICATED.
- MANUFACTURE PER MIL-O-13830
- SURFACE QUALITY
- 'C' MAGNESIUM FLUORIDE COATING PER MIL-C-675
FOR MAX TRANSMISSION AT MILLIMICRONS.
- 'G' FINE GROUND & BLACKENED PER
MAX FACE WIDTH
- BEVEL EDGES AT 45 DEG TO (REF)
- DIAMETER TO FLAT IS ON SURFACE S2
WITH SURFACE SAG OF



DR			
CHK			
APPD			
SCALE		REL BY REL DATE	
1.67:1			
Anamorphic Fish-eye Lens System -J.P. Ro ELEMENT 8			

RADIUS				RAD TOL		POW/IRR		C.A. DIA		CENTRAL					
S1	INF	TPF	8.0 / 2.0	132.267	EDGE DIA	DIA TOL	THICKNESS	THI TOL	WEDGE						
S2	208.667 CC	+0.7600	8.0 / 2.0	137.713	142.732		20.000	+0.2000	0.0900 T.I.R.						

NOTES :

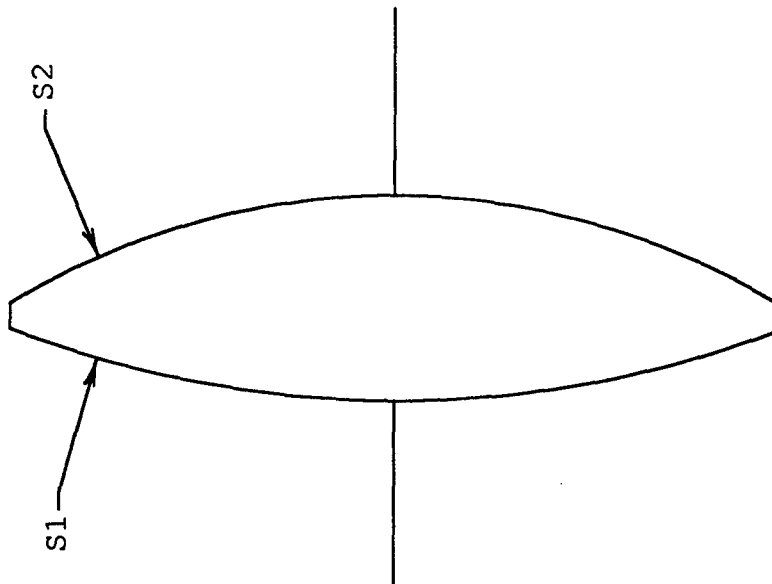
- ALL DIMENSIONS ARE IN MILLIMETERS.
- MATERIAL: OPTICAL GLASS PER MIL-G-174
TYPE: BK7 SCHOTT NO. 517642
 N_d 1.5168 \pm 0.0002 V 64.2 \pm 0.8%
STRIAE GRADE , ANNEAL
MELT NO.
- 'P' PITCH POLISH TO TEST PLATE WITHIN
POWER AND IRREGULARITY INDICATED.
- MANUFACTURE PER MIL-O-13830
- SURFACE QUALITY
- 'C' MAGNESIUM FLUORIDE COATING PER MIL-C-675
FOR MAX TRANSMISSION AT MILLIMICRONS.
- 'G' FINE GROUND & BLACKENED PER
MAX FACE WIDTH
- BEVEL EDGES AT 45 DEG TO (REF)
- DIAMETER TO FLAT IS
WITH SURFACE SAG OF ON SURFACE S2

DR							
CHK							
APPD							
SCALE				REL BY REL DATE			
0.75:1							
Anamorphic Fish-eye Lens System -J.P. Ro ELEMENT 9							

RADIUS		RAD TOL POW/IRR		C.A. DIA		EDGE DIA		DIA TOL THICKNESS		THI TOL		WEDGE	
S1	213.690 CX	+0.2000	8.0 / 2.0	147.272		152.462		40.000	+0.2000	0.0400	T.I.R.		
S2	149.001 CX	+0.1600	8.0 / 2.0	146.763									

NOTES :

- ALL DIMENSIONS ARE IN MILLIMETERS.
- MATERIAL: OPTICAL GLASS PER MIL-G-174
TYPE: LAK10 SCHOTT NO. 720504
 N_d 1.7200 \pm 0.0001 V 50.4 \pm 0.3%
STRIAE GRADE , ANNEAL
MELT NO.
- 'P' PITCH POLISH TO TEST PLATE WITHIN POWER AND IRREGULARITY INDICATED.
- MANUFACTURE PER MIL-O-13830
- SURFACE QUALITY
- 'C' MAGNESIUM FLUORIDE COATING PER MIL-C-675 FOR MAX TRANSMISSION AT MILLIMICRONS.
- 'G' FINE GROUND & BLACKENED PER
- BEVEL EDGES AT 45 DEG TO MAX FACE WIDTH

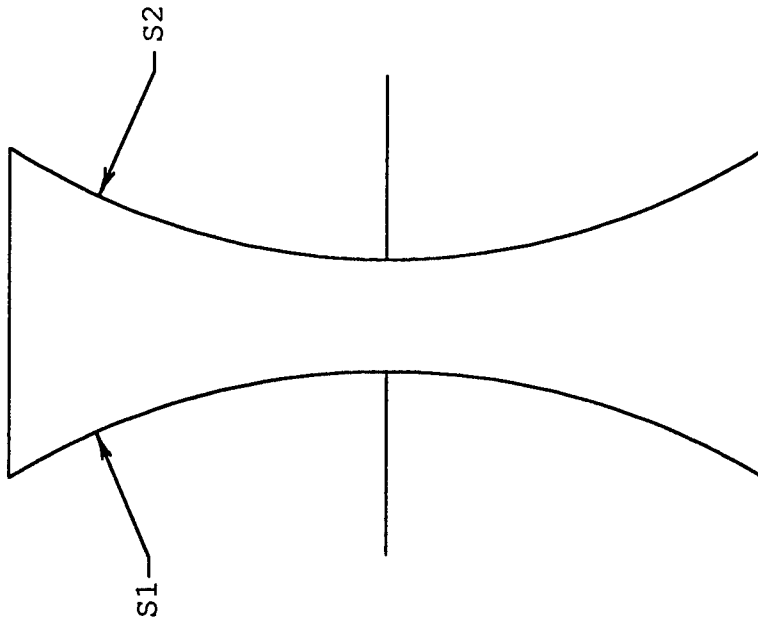


DR					
CHK					
APPD					
SCALE	0.70:1	REL BY	REL DATE		
Anamorphic Fish-eye Lens System -J.P. Ro ELEMENT 10					

RADIUS				RAD TOL		POW/IRR		C.A. DIA		CENTRAL				WEDGE	
S1	149.001 CC	+0.1600	8.0 / 2.0	146.763	EDGE DIA	DIA TOL	THICKNESS	THI	TOL	THI	TOL	THI	TOL	WEDGE	
S2	142.485 CC	+0.0850	8.0 / 2.0	145.801	152.462		22.500	+0.2000	0.0300	T.I.R.					

NOTES :

- ALL DIMENSIONS ARE IN MILLIMETERS.
- MATERIAL: OPTICAL GLASS PER MIL-G-174
TYPE: SF6 SCHOTT NO. 805254
N_d 1.8052 ± 0.0001 V 25.4 ± 0.2%
STRAIE GRADE , ANNEAL
MELT NO.
- 'P' PITCH POLISH TO TEST PLATE WITHIN
POWER AND IRREGULARITY INDICATED.
- MANUFACTURE PER MIL-O-13830
- SURFACE QUALITY
- 'C' MAGNESIUM FLUORIDE COATING PER MIL-C-675
FOR MAX TRANSMISSION AT MILLIMICRONS.
- 'G' FINE GROUND & BLACKENED PER
MAX FACE WIDTH
- BEVEL EDGES AT 45 DEG TO (REF)
ON SURFACE S1
- DIAMETER TO FLAT IS (REF)
ON SURFACE S2

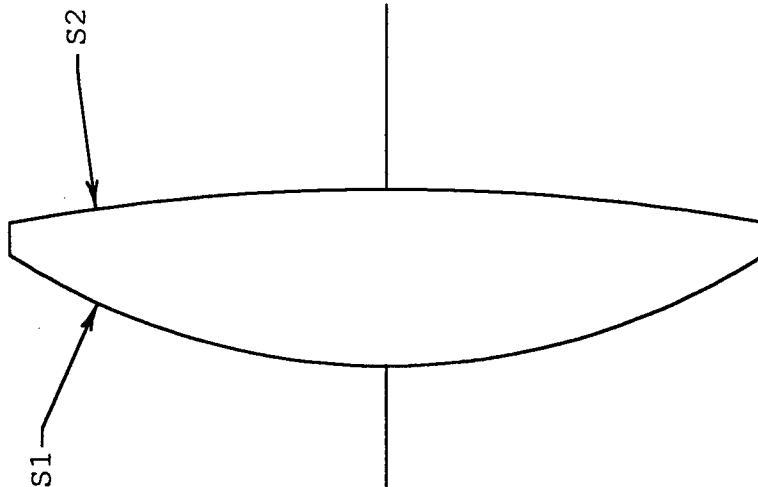


DR			
CHK			
APPD			
SCALE 0.70:1		REL BY	REL DATE
Anamorphic Fish-eye Lens System -J.P. Ro		ELEMENT 11	

RADIUS				RAD TOL POW/IRR		C.A. DIA		CENTRAL				—		
								EDGE DIA	DIA TOL	THICKNESS	THI TOL			WEDGE
S1	142.485 CX	+0.0850	8.0 / 2.0	145.801				151.959		35.000	+0.2000			0.0300 T.I.R.
S2	435.093 CX	+1.0000	8.0 / 2.0	146.778										

NOTES :

- ALL DIMENSIONS ARE IN MILLIMETERS.
- MATERIAL: OPTICAL GLASS PER MIL-G-174
TYPE: SK16 SCHOTT NO. 620603
N_d 1.6204 ± 0.0003 V 60.3 ± 0.5%
STRIAE GRADE , ANNEAL
MELT NO.
- 'P' PITCH POLISH TO TEST PLATE WITHIN
POWER AND IRREGULARITY INDICATED.
- MANUFACTURE PER MIL-O-13830
- SURFACE QUALITY
- 'C' MAGNESIUM FLUORIDE COATING PER MIL-C-675
FOR MAX TRANSMISSION AT MILLIMICRONS.
- 'G' FINE GROUND & BLACKENED PER
- BEVEL EDGES AT 45 DEG TO MAX FACE WIDTH

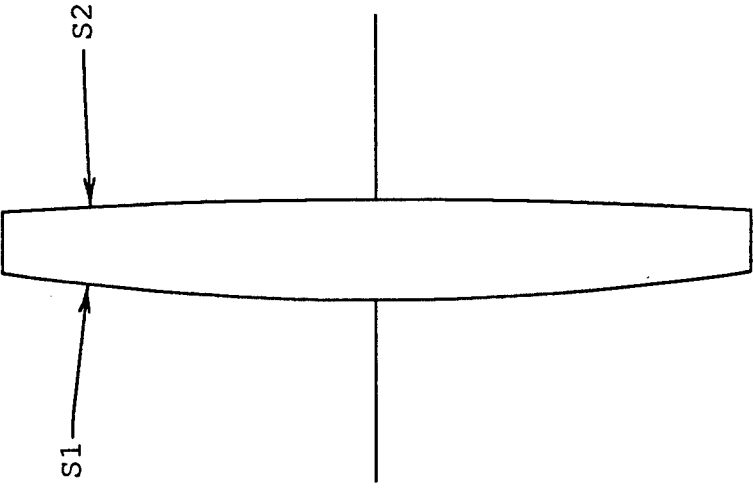


DR					
CHK					
APPD					
SCALE	0.70:1	REL BY	REL DATE		
Anamorphic Fish-eye Lens System -J.P. Ro					—
ELEMENT 12					

RADIUS				RAD TOL		POW/IRR		C.A. DIA		CENTRAL							
										EDGE DIA		DIA TOL		THI TOL		WEDGE	
S1	515.974	CX	+5.0000	8.0 / 2.0	145.371					150.527		20.000	+0.2000	0.0900	T.I.R.		
S2	1256.927	CX	+*****	8.0 / 2.0	143.997												

NOTES :

- ALL DIMENSIONS ARE IN MILLIMETERS.
- MATERIAL: OPTICAL GLASS PER MIL-G-174
TYPE: BK7 SCHOTT NO. 517642
N_d 1.5168 ± 0.0020 V 64.2 ± 0.8%
STRAIE GRADE , ANNEAL
MELT NO.
- 'P' PITCH POLISH TO TEST PLATE WITHIN POWER AND IRREGULARITY INDICATED.
- MANUFACTURE PER MIL-O-13830
- SURFACE QUALITY
- 'C' MAGNESIUM FLUORIDE COATING PER MIL-C-675 FOR MAX TRANSMISSION AT MILLIMICRONS.
- 'G' FINE GROUND & BLACKENED PER
- BEVEL EDGES AT 45 DEG TO MAX FACE WIDTH

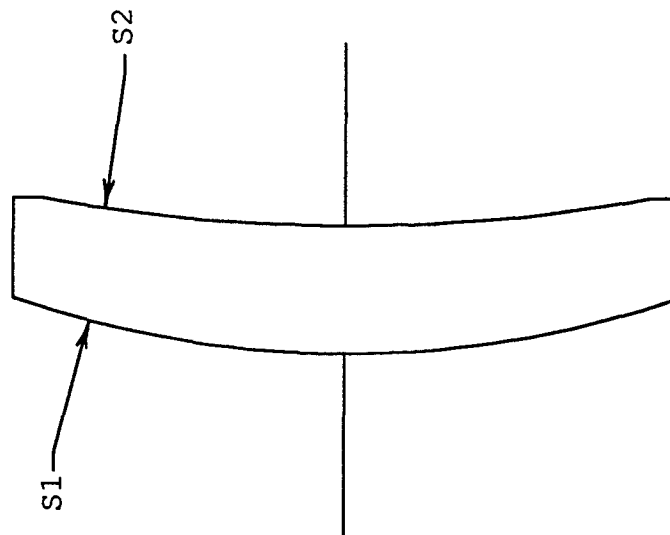


DR			
CHK			
APPD			
SCALE		REL BY	REL DATE
0.70:1			
Anamorphic Fish-eye Lens System -J.P. Ro		ELEMENT 13	

RADIUS		RAD TOL		POW/IRR		C.A. DIA		EDGE DIA		DIA TOL		CENTRAL THICKNESS		THI TOL		WEDGE	
S1	203.117 CX	+1.0000	8.0 / 2.0	127.576				132.406				25.000	+0.2000	0.1000	T.I.R.		
S2	343.960 CC	+3.3000	8.0 / 2.0	120.078													

NOTES :

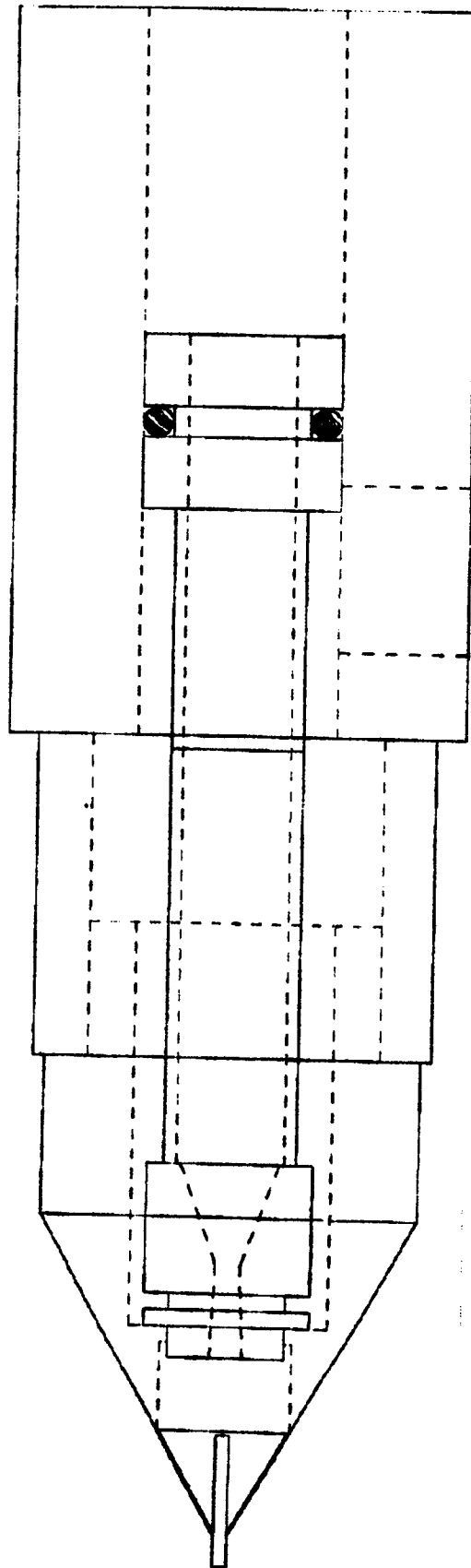
- ALL DIMENSIONS ARE IN MILLIMETERS.
- MATERIAL: OPTICAL GLASS PER MIL-G-174
TYPE: SK16 SCHOTT NO. 620603
 N_d 1.6204 \pm 0.0020 V 60.3 \pm 0.8%
STRIAE GRADE , ANNEAL
MELT NO.
- 'P' PITCH POLISH TO TEST PLATE WITHIN POWER AND IRREGULARITY INDICATED.
- MANUFACTURE PER MIL-O-13830
- SURFACE QUALITY
- 'C' MAGNESIUM FLUORIDE COATING PER MIL-C-675 FOR MAX TRANSMISSION AT MILLIMICRONS.
- 'G' FINE GROUND & BLACKENED PER
- BEVEL EDGES AT 45 DEG TO MAX FACE WIDTH
- DIAMETER TO FLAT IS (REF)
WITH SURFACE SAG OF ON SURFACE S2

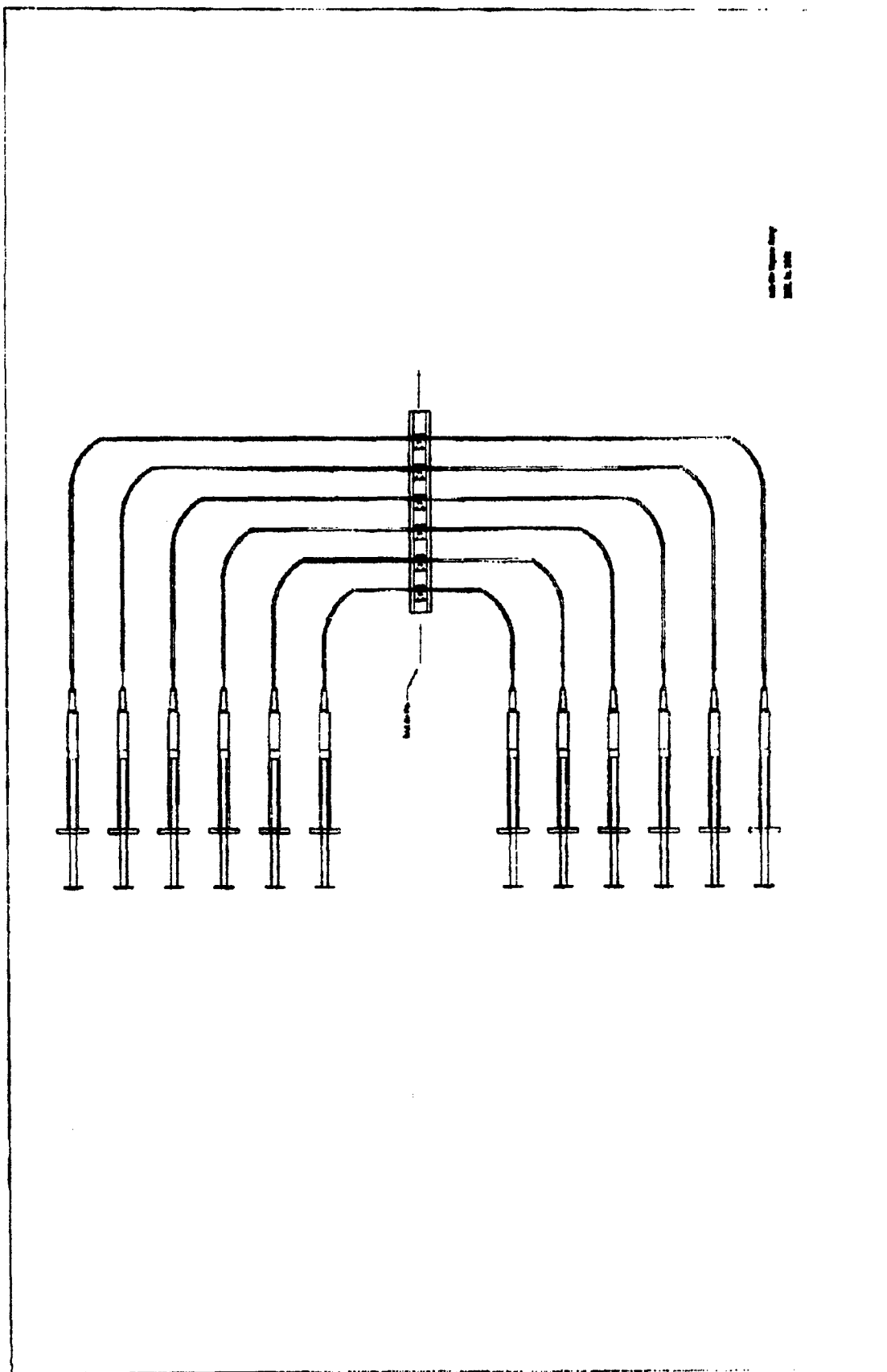


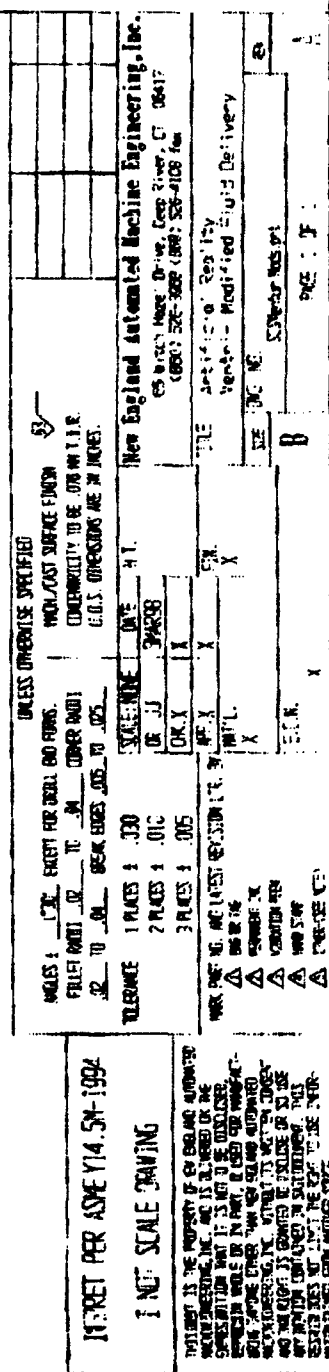
DR																	
CHK																	
APPD																	
SCALE	0.71:1	REL BY	REL DATE														
Anamorphic Fish-eye Lens System -J.P. Ro																	
ELEMENT 14																	

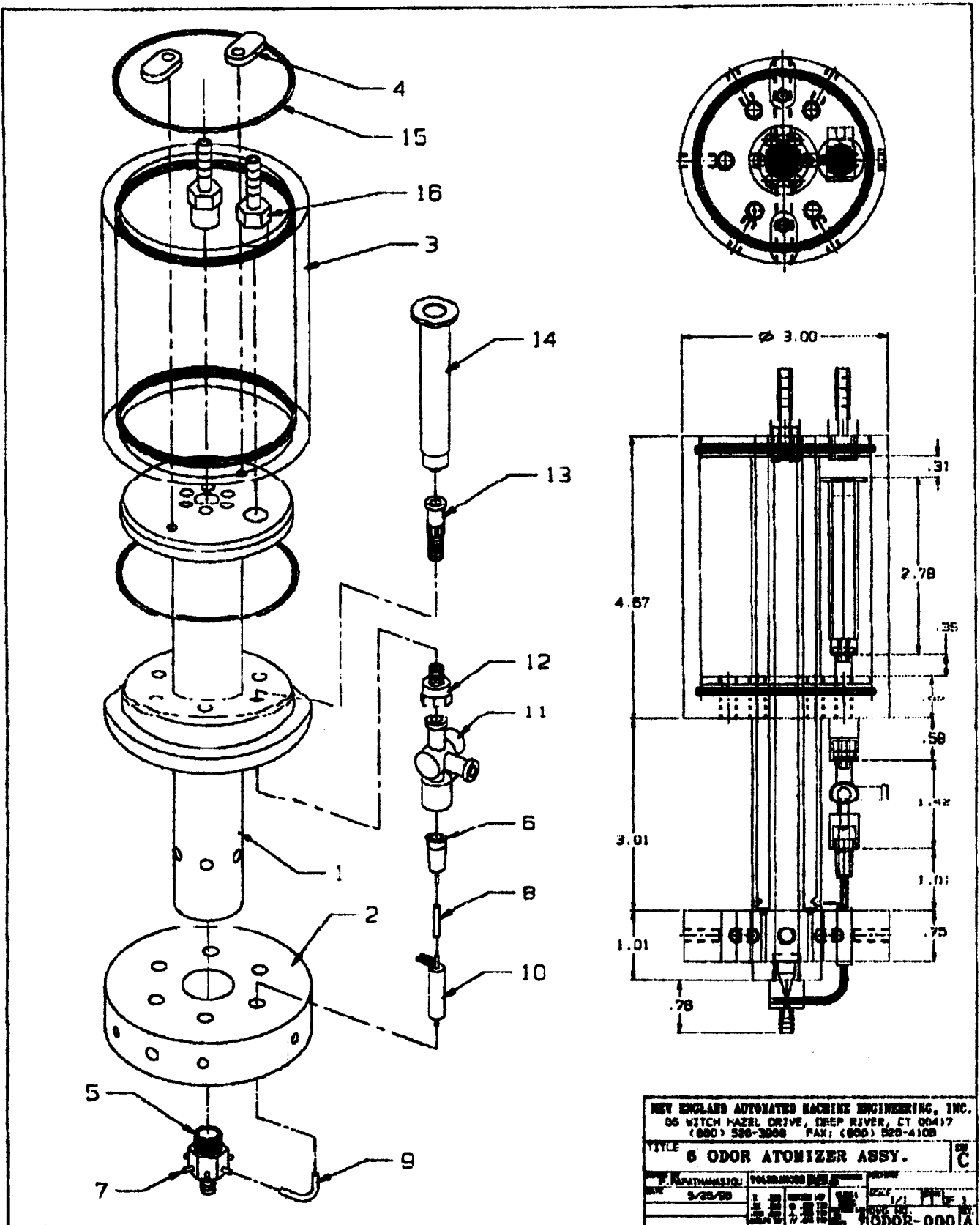
RADIUS		RAD TOL		POW/IRR		C.A. DIA		CENTRAL				WEDGE	
S1		120.583 CX		+0.2000		8.0 / 2.0		114.633		EDGE DIA		THI TOL	
S2		87.401 CC		+0.3900		8.0 / 2.0		78.802		119.212		+0.2000	
										60.000		+0.0900 T.I.R.	
<p>NOTES :</p> <p>1. ALL DIMENSIONS ARE IN MILLIMETERS.</p> <p>2. MATERIAL: OPTICAL GLASS PER MIL-G-174 TYPE: LAK10 SCHOTT NO. 720504 N_d 1.7200 \pm 0.0020 V 50.4 \pm 0.8% STRIAE GRADE , ANNEAL MELT NO.</p> <p>3. 'P' PITCH POLISH TO TEST PLATE WITHIN POWER AND IRREGULARITY INDICATED.</p> <p>4. MANUFACTURE PER MIL-O-13830</p> <p>5. SURFACE QUALITY</p> <p>6. 'C' MAGNESIUM FLUORIDE COATING PER MIL-C-675 FOR MAX TRANSMISSION AT MILLIMICRONS.</p> <p>7. 'G' FINE GROUND & BLACKENED PER MAX FACE WIDTH</p> <p>8. BEVEL EDGES AT 45 DEG TO (REF)</p> <p>9. DIAMETER TO FLAT IS ON SURFACE S2 WITH SURFACE SAG OF</p>													
<p>DR</p> <p>CHK</p> <p>APPD</p> <p>SCALE 0.81:1</p> <p>REL BY REL DATE</p> <p>Anamorphic Fish-eye Lens System -J.P. Ro ELEMENT 15</p>													

Appendix F -- 145











DEPARTMENT OF THE ARMY

US ARMY MEDICAL RESEARCH AND MATERIEL COMMAND
504 SCOTT STREET
FORT DETRICK, MARYLAND 21702-5012

REPLY TO
ATTENTION OF:

MCMR-RMI-S (70-1y)

2 Feb 01

MEMORANDUM FOR Administrator, Defense Technical Information
Center, ATTN: DTIC-OCA, 8725 John J. Kingman
Road, Fort Belvoir, VA 22060-6218

SUBJECT: Request Change in Distribution Statements

1. The U.S. Army Medical Research and Materiel Command has reexamined the need for the limitation assigned to technical reports written for the following grant numbers:

96-C-6117


94-J-4113

ADB233743, ADB243030, ADB259960,
ADB251394, ADB241076, ADB220530

Request the limited distribution statement for Accession Document Numbers listed be changed to "Approved for public release; distribution unlimited." These reports should be released to the National Technical Information Service.

2. Point of contact for this request is Ms. Judy Pawlus at DSN 343-7322 or by email at judy.pawlus@det.amedd.army.mil.

FOR THE COMMANDER:


PHYLIS M. RINEHART
Deputy Chief of Staff for
Information Management